INVESTIGATION OF MECHANICAL PROPERTY CHANGES AFTER MIG WELDING OF (7XXX) SERIES ALUMINUM ALLOYS

A THESIS SUBMITTED TO
THE GRADUATE SCHOOL OF NATURAL AND APPLIED SCIENCES
OF
MIDDLE EAST TECHNICAL UNIVERSITY

BY

SENA OKAY

IN PARTIAL FULFILLMENT OF THE REQUIREMENTS
FOR
THE DEGREE OF MASTER OF SCIENCE
IN
METALLURGICAL AND MATERIALS ENGINEERING

SEPTEMBER 2016

Approval of the thesis:

INVESTIGATION OF MECHANICAL PROPERTY CHANGES AFTER MIG WELDING OF (7XXX) SERIES ALUMINUM ALLOYS

submitted by **SENA OKAY** in partial fulfillment of the requirements for the degree of **Master of Science in Metallurgical and Materials Engineering Department, Middle East Technical University** by,

Prof. Dr. Gülbin Dural Ünver _____
Dean, Graduate School of **Natural and Applied Sciences**

Prof. Dr. Cemil Hakan Gür _____
Head of Department, **Metallurgical and Materials Engineering**

Prof. Dr. Bilgehan Ögel _____
Supervisor, **Metallurgical and Materials Engineering Dept., METU**

Dr. Caner Batıgün _____
Co-Supervisor, **Weld. Tech. and NDT Res./App. C., METU**

Examining Committee Members:

Prof. Dr. Rıza GÜRBÜZ _____
Metallurgical and Materials Engineering Dept., METU

Prof. Dr. Bilgehan ÖGEL _____
Metallurgical and Materials Engineering Dept., METU

Prof. Dr. Caner DURUCAN _____
Metallurgical and Materials Engineering Dept., METU

Assist. Prof. Dr. Kazım TUR _____
Materials Engineering Dept., Atılım University

Assist. Prof. Dr. Mert EFE _____
Metallurgical and Materials Engineering Dept., METU

Date: 09.09.2016

I hereby declare that all information in this document has been obtained and presented accordance with the academic rules and ethical conduct. I also declare that, as required by these rules and conduct, I have fully cited and referenced all material and results that are not original to this work.

Name, Last name : Sena OKAY

Signature :

ABSTRACT

INVESTIGATION OF MECHANICAL PROPERTY CHANGES AFTER MIG WELDING OF (7XXX) SERIES ALUMINUM ALLOYS

Okay, Sena
M.Sc., Department of Metallurgical and Materials Engineering
Supervisor: Prof. Dr. Bilgehan Ögel
Co-Supervisor: Dr. Caner Batıgün
September 2016, 115 pages

There is an increasing demand for aluminum alloys not only in aerospace industry but also in automotive industry due to its low density. Welding is the most effective and commonly used joining technique in those industries, therefore, aluminum welding plays an important role. 7039 aluminum alloy, is a high strength alloy and it is suitable for armor applications. Like other aluminum alloys, after MIG welding, remarkable decrease in strength is observed and therefore applications are restricted. The aim of this study is to investigate the mechanical property changes after welding for different weld groove shapes of 7039 alloy and to recover the strength in HAZ by performing post weld heat treatment.

Different weld groove shapes affected the heat input since the area subjected to heat changed depending on the angle of the groove. EDX analyses were conducted in order to understand the changes in elemental distribution. By performing post weld heat treatments, hardness for each sample increased in HAZ. However UTS and yield strength in several samples were decreased after prolonged solutionizing heat treatments.

On the other hand, welding defects such as lack of fusion affects the mechanical properties negatively. In 45° X shaped weld grooved sample, the most effective results were obtained. After post weld heat treatment the hardness values increased around 10%.

Keywords: 7000 aluminum alloy, MIG welding, post weld heat treatment, aging, tensile test, hardness measurement

ÖZ

(7XXX) SERİSİ ALÜMİNYUM ALAŞIMLARININ MIG KAYNAĞI SONRASI MEKANİK ÖZELLİKLERİNDEKİ DEĞİŞİMİN İNCELENMESİ

Okay, Sena
Y. Lisans, Metalurji ve Malzeme Mühendisliği Bölümü
Tez Yöneticisi: Prof. Dr. Bilgehan Ögel
Ortak Tez Yöneticisi: Dr. Caner Batıgün
Eylül 2016, 115 sayfa

Alüminyum alaşımları, genel özellikleri sebebiyle çeşitli sektörlerde kullanımlarında artan bir eğilim göstermektedir. Kaynak işlemi, endüstride çoğunlukla kullanılan birleştirme yöntemlerinden olup alüminyum alaşımları kaynak işlemlerinde büyük bir rol oynamaktadır. 7039 alüminyum alaşımı, diğer alüminyum alaşımlarının arasında en iyi mukavemete sahip zırh metalidir. Diğer alüminyum alaşımları gibi, MIG kaynağı sonrasında alüminyum alaşımlarında ciddi bir mukavemet kaybı görülmekte, mekanik özelliklerin olumsuz etkilenmesi de alaşımın kullanım durumunu riskli bir hale getirmektedir. Bu çalışmanın amacı, farklı kaynak ağızlarına sahip 7039 alaşımının kaynak işleminden sonra mekanik özelliklerindeki değişimin incelenmesi ve HAZ bölgesinde mukavemetin kaynak sonrası ısıl işlemle kazanılmasının sağlanmasıdır.

Farklı kaynak ağızları her bir numuneyi, farklı ısı girdilerine maruz kalmaları ve farklı açılı ağız yapıları sebebiyle farklı etkilemiştir. Bu da beraberinde kaynak havuz formu ve içyapıda farklılıklara sebep olmuştur. X-ışınları erke dağılım çözümlemesi (EDX) yöntemi ile kaynak sonrası elementlerin dağılımı incelenmiş ve kaynak sonrası uygulanan ısıl işlem yöntemi ile her bir numunenin ısıdan

etkilenen bölgesinde (HAZ) sertlik artışına rastlanmıştır. Ancak fazla yaşlanma sebebiyle, maksimum çekme dayanımı (UTS) ve akma dayanımları bazı numunelerde azalmıştır. Benzer şekilde, yetersiz ergime gibi kaynak hataları da mekanik özellikleri olumsuz yönde etkilemiştir. En etkili sonuçlar, 45° X kaynak ağzında elde edilmiştir. Kaynak sonrası ısıl işlemde sertlik değerlerinin %10 mertebelerinde arttığı görülmüştür.

Anahtar Sözcükler: 7000 serisi alüminyum alaşımları, MIG kaynağı, kaynak sonrası ısıl işlem, yaşlandırma, çekme testi, sertlik ölçümü

To my family.

ACKNOWLEDGEMENTS

I would like to express my gratitude to my supervisor Prof. Dr. Bilgehan Ögel for his permanent encouragement, supervision, and guidance during this study. With his effort and guidance, I also would like to express my gratitude to my co-supervisor Dr. Caner Batıgün.

I am so much thankful to Dr. Süha Tirkeş whom showed me the way I have to follow and helped me to find the answers when I was up against the wall. Without his knowledge, experience and inquiring mind, this study might not proceed that much.

I would like to express my sincere thanks to Mustafacan Kutsal and Bengisu Yaşar from METU Metallurgical and Materials Engineering Department for their dynamic support and help in EDX analysis, SEM analysis and other laboratory issues and measurements. I also must thank to my lab mates for their valuable supports.

I must express my special thanks to Zeynep Öztürk, Gözde Çambel, Baran Güler and Erhan Özen for their invaluable friendships and always being there for me when I felt embattled. Together with, I must thank to my colleagues, especially Mertcan Hacıoğlu and Şeyda Şimşek and heads in ASELSAN for their faith and support on me.

I would like to express my indebted feelings to my mentors, friends and colleagues Ali Erdem Eken, Evren Tan and Berk Seçen for their unlimited friendships, knowledge, belief and support during this study. I learned so many different technical and non-technical things from them whom provided me different visions in the field and life. I hope, we will still be working together in future.

Deeply from my heart, I would like to thank the one, whom did not refrain to support me, make me feel unique and never stopped loving me.

I must thank to Dilara Demir, my bestie, for balancing my emotions when I was down and for her priceless friendship and support. Further, I need to thank Yücel Türegün for great times while writing our thesis together and his fellowship and support.

I must thank to my half-mother, Arzu Sayın Şakul for her endless support and compassion although we are separated with long distances.

Finally, the greatest gratitude is to my mother Yeşim Okay, to my father Mustafa Okay and to my sister Eda for their endless love, support, encouragement, patience and the opportunities they provided me in every second of my life. Thanks to them for always being there and hope they will always be there. Deeply from my heart, I am feeling that I am the luckiest person in the world as long as I have them.

One last thing to universe, always, HAKUNA MATATA.

TABLE OF CONTENTS

ABSTRACT v
ÖZ vii
DEDICATION ix
TABLE OF CONTENTS xii
LIST OF TABLES xv
LIST OF FIGURES xvi
CHAPTERS
1. INTRODUCTION 1
2. THEORY 3
2.1. Aluminum and Aluminum Alloys 3
2.1.1. (7xxx) Series Aluminum Alloys and AA7039 7
2.2. Arc Welding 10
2.2.1. Metal Inert Gas Welding (MIG) 10
2.3. Weld Structure 12
2.3.1. Weld Metal 13
2.3.2. Partially Melted Zone (PMZ) 15
2.3.3. Heat Affected Zone (HAZ) 17
2.4. Aluminum Welding Discontinuities 18
2.5. Heat Treatment of Aluminum Alloys 20
2.5.1. Age Hardening of 7xxx Series Aluminum Welds 24
3. MECHANICAL PROPERTY EXAMINATION OF WELDED 7039 ALUMINUM ALLOY 29
3.1. Effect of Welding Parameters on Mechanical Properties 29
3.2. Post Weld Heat Treatment 31
4. EXPERIMENTAL PROCEDURE 35
4.1. Materials Used 35
4.2. Spectral Analyses and Preliminary Mechanical Tests 38
4.2.1. Spectral Analyses 38

4.2.2. Mechanical Tests 39
4.2.2.1. Mechanical Tests for As-Received 7039 Aluminum Plate 39
4.2.2.2. Mechanical Tests for As-Welded Samples 41
4.3. Weld Parameters 42
4.4. Macrostructural Examinations 45
4.5. Microstructural Examinations 47
4.6. Fracture Surface Examinations 48
4.7. Heat Treatments 48
4.8. Software Calculations 49
5. EXPERIMENTAL RESULTS 51
5.1. Characterization of Aluminum alloy 7039 Plate in As-Received Condition 51
5.1.1. Spectral Analyses and Microstructure 51
5.1.2. Mechanical Testing of 7039 Aluminum Alloy Plate 55
5.2. Welding Results 58
5.2.1. Macrostructural Examinations 58
5.2.2. Microstructural Examinations 59
5.3. Post Weld Heat Treatments 72
5.3.1. Hardness Measurements 72
5.3.2. Microstructures 76
5.4. Mechanical Tests 89
5.4.1. Hardness Measurements 89
5.4.2. Tensile Tests 93
5.5. Results of Software Calculations 97
5.6. Fracture Surface Morphologies 99
6. DISCUSSION 103
6.1. Heat Input Examinations for Different Weld Grooves in As Weld Condition 103
6.2. Microstructure Examinations for Different Weld Grooves in As Weld Condition Subjected to Different Heat Input 104
6.3. Compositional Changes in As Weld Samples in Weld Deposits 106
6.4. Effect of Different Weld Grooves on Mechanical Properties in As Weld Condition 106

6.5. Post Weld Heat Treatment and It's Effect on the Microstructure and Mechanical Properties 107
7. CONCLUSION 111
REFERENCES 113

LIST OF TABLES

TABLES

Table 1 The comparison between pure aluminum and pure iron [5] 4
Table 2 Aluminum alloy groups [8] 6
Table 3 Chemical composition of AA7039[15] 9
Table 4. Typical mechanical Properties of 7039[8] 9
Table 5 Typical Welding Problems in Aluminum Alloys [17] 19
Table 6 Designations [27] 22
Table 7 Basic Designations [27] 23
Table 8 Basic Temper Designations-3 [27] 23
Table 9 The hardness results of Sharma et.al.. [35] 33
Table 10. Identification of the Welded Samples 36
Table 11 Chemical composition of 7039 alloy literally [15] 38
Table 12 The nominal composition of filler material. [36] 39
Table 13 Welding Parameters 44
Table 14 The composition of Flick solution 46
Table 15 The composition of Keller's solution 47
Table 16 Post weld heat treatments performed 48
Table 17 The spectral analysis of 7039 by optical spectroscopy 52
Table 18 The weight percentages of primary phases of Type 1 and Type 2 54
Table 19 The spectral analysis of 5356 and the comparison of the results 55
Table 20 Preliminary tensile test results for 7039 56
Table 21 The measured values of base metal hardness 57
Table 22 Hardness values of 45V.1 in as weld and post weld heat treated (HT.550.4HR) condition 74
Table 23 Hardness values of 45V.1 in as weld, HT.480.2HR and HT.480.20HR condition 75
Table 24 Mechanical property summary of samples 94

LIST OF FIGURES

FIGURES

Figure 1 Hall Heroult Flow Chart [7]..... 5
Figure 2 Semi-schematic processing schedule for high-strength Al−Zn−Mg−Cu plate (Some commercial and experimental variations are indicated by dashed lines) [11] 8
Figure 3 MIG welding: (a) overall process; (b) welding area enlarged [17] 11
Figure 4 MIG welds in 5083 aluminum alloy by argon gas (left) and 75% He–25% Ar (right). Reprinted from Gibbs [18] Courtesy of American Welding Society. 12
Figure 5 Weld metal solidification affected by cooling rate and growth rate. [17] 14
Figure 6 a) Growth Rate b) Temperature Gradient c) Solidification mode along the weld pool. [17] 15
Figure 7 Liquation mechanisms solid solubility limit and above the solid solubility limit respectively. [17] 17
Figure 8 Finely distributed porosity in a weld groove [24]..... 18
Figure 9 Representative binary phase diagram for solution strengthening mechanism. [17] 21
Figure 10 Aging characteristics of heat-treatable aluminum alloys: (*a*) 2014 quenched from 500°C; (*b*) 7005 quenched from 450°C [28]. 25
Figure 11 HAZ hardness profiles in 7005 alloy: (*a*) naturally aged before welding (1: 3 hour, 2: 4 days, 3: 30 days, 4: 90 days); (*b*) artificially aged at 130°C for 1 h before welding. [29]. 26
Figure 12 Hardness profiles in HAZ of aged 7039 aluminum: (a) 4 passes, continuous welding; (b) 16 passes, 150°C interpass temperature. [30]. Courtesy of American Welding Society. 27
Figure 13 HAZ hardness profiles in alloy 7146 welded in annealed condition. [31] 28
Figure 14 3D drawings for the base metal plates (Siemens NX Drawing for Design) 36

Figure 15 3D drawings of the weld grooved sample (a) 45° V Weld Groove, (b) 30° V Weld Groove, (c) 45° X Weld Groove, (d) 30° X Weld Groove (Siemens NX Drawing for Design) 37
Figure 16 Shimadzu Micro Hardness Indenter 40
Figure 17 Preliminary tensile test specimens for the base metal (7039 as obtained) in accordance with ASTM B557 41
Figure 18 Welding machine used in experiments. Lincoln Electric Powertec 425C MIG Welder. Retrieved from http://www.lincolnelectric.com/en-gb/equipment/Pages/product.aspx?product=K14062-1A(LincolnElectric_EU_Base) 43
Figure 19 The macroscopic view of the samples after MIG welding 45
Figure 20 Schematic representation of samples 46
Figure 21 The microstructure of 7039 aluminum plate (a) rolling direction and (b) transverse direction. (Keller's reagent.) 53
Figure 22 SEM graph of 7039 base metal showing primary phases and intermetallics 54
Figure 23 The representative sample of the 7039 plate and the location of the hardness measurements 57
Figure 24 Macrographs of the samples 58
Figure 25 Macrographs of new (second set) welded samples 59
Figure 26 45V.1 weld and parent metal. Keller's reagent. (PMZ: Partially melted zone, HAZ: Heat affected zone) 60
Figure 27 30V.1 weld and parent metal. Keller's reagent. (PMZ: Partially melted zone, HAZ: Heat affected zone) 61
Figure 28 45V.1. The microstructure of the weld metal. Dendritic structure. Keller's reagent. 62
Figure 29 30V.1. The microstructure of the weld metal. Dendritic structure. Keller's reagent. 62
Figure 30 45V.1. The microstructure of the base metal. Keller's reagent. 63
Figure 31 30V.1.The microstructure of the base metal. Keller's reagent. 64
Figure 32 45V.1. The SEM image of fusion line. 65

Figure 33 SEM image of HAZ, 8000x magnification, 45V.1 (45° V Weld Groove)..... 66
Figure 34 45X.1. The microstructure of weld and parent metal. First set. Keller's reagent. (PMZ: Partially melted zone, HAZ: Heat affected zone)..... 67
Figure 35 30X.1. The microstructure of weld and parent metal. First set. Keller's reagent. (PMZ: Partially melted zone, HAZ: Heat affected zone)..... 68
Figure 36 45X.1. The microstructure of weld metal. Dendritic structure. First set. 68
Figure 37 30X.1. The microstructure of weld metal. Dendritic structure. First set. 69
Figure 38 45X.2. The microstructure of weld and parent metal. Second set. Keller's reagent. (PMZ: Partially melted zone, HAZ: Heat affected zone)..... 70
Figure 39 30X.2. The microstructure of weld and base metal. Second set. Keller's reagent. (PMZ: Partially melted zone, HAZ: Heat affected zone)..... 71
Figure 40 30X.2. The microstructure of weld metal. Second set. Keller's reagent. 71
Figure 41 Hardness distribution in 45V.1 after post weld and post weld heat treatment. (HT.550.4HR). 73
Figure 42 Changes in hardness values after HT.480.2HR and HT.480.20HR 74
Figure 43 Comparison of microstructures (a) As weld (b) HT.480.2HR (c) HT.480.20HR. Keller's reagent. 77
Figure 44 Comparison of weld metal microstructures (a) As weld (b) HT.480.2HR (c) HT.480.20HR. Keller's reagent. 79
Figure 45 EDX analysis of precipitates in HT.480.2HR heat treated sample, fusion zone and HAZ 81
Figure 46 SEM. Elemental mapping of HT.480.2HR..... 82
Figure 47 EDX analysis of precipitates in HT.480.20HR heat treated sample, fusion zone and HAZ 82
Figure 48 SEM. Elemental mapping of HT.480.20HR..... 84
Figure 49 45V.1. Comparison of microstructures (a) As weld (b) HT.480.2HR. Keller's reagent. 85

Figure 50 45V.1. Comparison of weld metal microstructures (a) As weld (b) HT.480.2HR. Keller's reagent. 86
Figure 51 45X.2. Comparison of microstructures (a) As weld (b) HT.480.2HR. Keller's reagent. 87
Figure 52 45X.2. Comparison of weld metal microstructures (a) As weld (b) HT.480.2HR. Keller's reagent. 88
Figure 53 Comparison of the hardness distributions of V-formed and X-formed weld grooved samples in as weld and post weld heat treated (HT.480.2HR) conditions. 89
Figure 54 Comparison of the hardness distributions of V-formed and X-formed weld grooved samples in as weld conditions. 92
Figure 55 Comparison of the hardness distributions of V-formed and X-formed weld grooved samples in heat treated (HT.480.2HR) conditions. 93
Figure 56 The comparison of average yield strength and UTS of samples in as weld and heat treated conditions 96
Figure 57 Weight fraction of the phases for 7039 aluminum alloy with respect to temperature. JMat Pro. 97
Figure 58 CCT diagram for 7039 aluminum alloy. JMat Pro. 98
Figure 59 TTT diagram for 7039 aluminum alloy. JMat Pro. 98
Figure 60 Phase diagram for Al-Zn aluminum alloy. ThermoCalc. 99
Figure 61 45V.1. The section for weld metal from fracture surface. Keller's reagent. 100
Figure 62 45V.1. The section from the fracture surface (edge-fusion line). Keller's reagent. 100
Figure 63 45V.1. The image of fracture surface under SEM. 101
Figure 64 30V.1. The image of fracture surface under SEM. 101

CHAPTER 1

INTRODUCTION

Steel parts in several applications are now replaced with aluminum alloys due to their lightweight, easy fabrication and machinability, good corrosion resistance and other superior properties compared with steel and other metals. Especially, in aerospace, defense, automotive, food industries, strength with high toughness are reasons for preference of aluminum alloys.

Considering the joining mechanism in those industrial fields, welding is the most suitable and easy application. When the welding of aluminum alloys are taken into consideration costs are playing an important role, therefore, gas tungsten arc welding (GTAW) and gas metal arc welding (GMAW) techniques are widely used. GMAW technique, which metal inert gas welding (MIG) is the subsystem, is the cost effective method used in industry. Therefore, in most of the applications, MIG welding is used for joining aluminum alloys. Although, several defects can be seen during welding such as porosities, hot cracking and so, related with some properties of particularly heat treatable aluminum alloys, they can be eliminated by controlling welding parameters and choosing correct fillers. However, arising from the nature of welding, strength losses can be seen after welding. After welding, the main strength loss is seen in the heat affected zone (HAZ) and in vicinity. According to EN ISO 15614-2, the strength at least in annealed condition can be enough after welding, barely, the places of use are not always allow this situation.

Based on this necessity, several post weld treatments are used in order to recover the strength after welding. The main advantage of aluminum alloys is the ability to be heat treated. With heating and cooling routes, strength can be increased in aluminum alloys even after welding. There are also many studies performed on this topic to recover the strength losses after welding in literature.

In this study, one of the members of 7xxx series aluminum alloy, 7039 was used. In this alloy, zinc (3.5-4.5%) is the main alloying element, but also, magnesium (2.3-3.3%) has a significant amount. The 7039 alloy is widely used for the applications that require high strength and good weldability. Further, resulting from its superior ballistic properties, this series of aluminum alloy is also used for armor applications in defense industry. Consequently, preventing the strength losses after welding is very important in these alloys.

Several studies discussed the optimum welding techniques, parameters and optimum filler material for 7039 alloy. However, these studies are not focused on MIG welding, which is extensively used in industry. Hence, the aim of this study is to improve the strength by applying a suitable heat treatment and related the changes to microstructural variables.

During this study, 7039 alloy samples were MIG welded by using filler material 5356. After deciding the optimum welding parameters, various heat treatments were performed. In addition to heat treatments, different weld grooves were created in order to understand the effect of heat input on mechanical properties and microstructure. After each process, hardness tests, tensile tests and metallographic examinations were carried out in order to observe the relations of different heat inputs, different pass geometries, and the recovery of the mechanical properties.

CHAPTER 2

THEORY

2.1. Aluminum and Aluminum Alloys

In today's technology, aluminum plays an important role for variety of industries. Starting mainly from the automotive and aerospace industry, it can also be used in food, aeronautical and even chemical industries. Aluminum and its alloys are the most attractive engineering materials due to their good combination of mechanical properties with low density and excellent resistance to degradation in some corrosive environments. [1]

Aluminum, itself, is the second rife metallic element on earth. It generates about 8% by mass of the Earth's crust and according to common knowledge, it is the most widely used non-ferrous metal. Based upon the Ancient Greeks and Romans, it is known that aluminum salts were used for dyeing mordant and as styptic. [2] However, the very first production of aluminum dates back to 1825 by Danish physicist and chemist Hans Christian Ørsted. As far as known, he reacted anhydrous aluminum chloride with potassium amalgam, and surprisingly yielded a lump of metal with similar spectrum of tin. [3] Following years, the importance of aluminum and its alloys increased drastically and as for the end of the 19th century, it became an economical competitor comparing with other metals, especially steel in engineering applications. As a result of to its light weight and other mechanical properties, aluminum is far more favorable than steel in this day and time. The

thermal conductivity of aluminum, that has 2.7 gr/cm^3 density, is approximately about six times and thermal expansion is about twice that of steel. [4] Also, without any surface protection, it shows excellent corrosion resistance. Comparison of the mechanical properties of pure aluminum and iron can be seen in Table 1.

Table 1 The comparison between pure aluminum and pure iron [5]

Properties	**Aluminum**	**Steel**
Atomic Weight [g/mol]	26,98	55,84
Density [g/cm^3]	2,7	7,87
Elastic Modulus [MPa]	67x10^3	210x10^3
Expansion Coefficient [1/K]	24x10^{-6}	12x10^{-6}
Heat of Fusion [J/g]	≈390	≈272
Melting Temperature [°C]	660	1536
Heat Conductivity [W/m.K]	235	75

Aluminum is extracted by the process named as Hall-Heroult by smelting from bauxite ore. This process embraces electrolyzing a bath to extract alumina. First the bauxite is dissolved in a cryolite bath, with additional fluoride salts to be able to control the temperature. While the electrical current is passed through all over the bath, the alumina that is dissolved is electrolyzed. Following this step oxygen comes into existence which reacts with the carbon anode, and finally aluminum as the metal collects at the cathode. [6] The Hall-Heroult process can be seen as a flow chart in Figure 1.

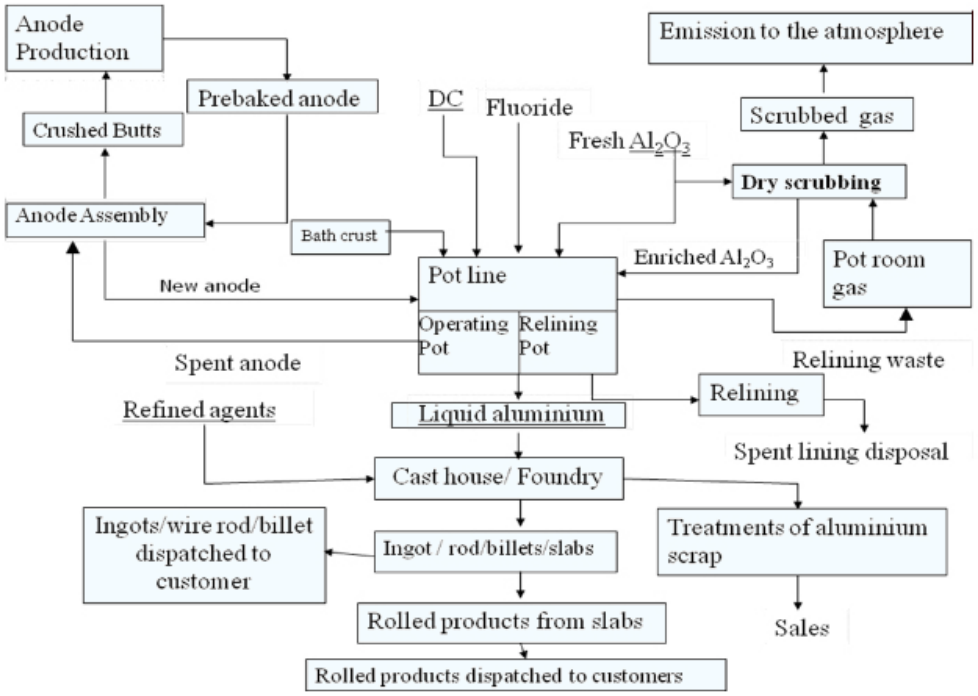

Figure 1 Hall Heroult Flow Chart [7]

Like most of other metals, aluminum is used in alloyed condition, which means aluminum element is the predominant ingredient and zinc, copper, magnesium, silicon and so are the remaining alloying elements. However, the true division is to group aluminum alloys into two major categories: as casting and wrought alloys. Wrought alloy groups are given in Table 2 below.

Table 2 Aluminum alloy groups [8]

Designation	Main Alloying Element	Properties
1xxx	-	NHT**, used primarily in electrical and chemical industries
2xxx	Copper (Cu)	HT*, majority use in aircraft industry
3xxx	Manganese (Mn)	NHT, good corrosion resistance, formability and weldability. Useful for architectural and general purpose applications
4xxx	Silicon (Si)	NHT, excellent castability and corrosion resistance. Useful for making brazing and welding consumables
5xxx	Magnesium (Mg)	NHT, good weldability, corrosion resistance, useful for boat hulls, gangplanks and other things exposed to marine environments
6xxx	Silicon-Magnesium (Si-Mg)	HT, used in structural applications due to excellent corrosion resistance and workability
7xxx	Zinc (Zn)	HT, high tensile strength but poor corrosion resistance and susceptible for stress corrosion cracking. Useful in aircraft applications

*HT: Heat Treatable **NHT: Not Heat Treatable

Considering the properties of the aluminum alloys, mostly the alloying elements play an important role. Each element addition affects a specific property and

changes the microstructure together with mechanical properties somehow. The main effects of alloying elements on aluminum can be seen below.

Copper: During solidification, copper forms chemical recombination with aluminum and iron in two different phases. Then following heat treatment cannot dissolve these phases, however can transform them from one another.

Manganese: Manganese drives excellent formability to the aluminum. During the solidification process some of the manganese forms Al-Mn-Fe and Al-Mn-Si compounds along the rest of it remains in the solution as dispersoids to strengthen and provides to control the recrystallized grain size.

Silicon: Silicon can both be seen as an impurity or two different phases in the aluminum alloy. At such low silicon contents almost all Al exists as a compound with Fe, and while Si content increases the compound becomes Al-Fe-Si and in larger amounts of silicon in the alloy improves the castability and fluidity.

Zinc: If strength is the main consideration, zinc and aluminum do not offer considerable strength to the alloy. However, Al-Zn-Mg precipitates provide two phases that result in high strength values that can be seen in 7xxx alloys.

Magnesium: It has a direct effect in increasing the solidification range of aluminum alloys. Considering welding, as solidification range increases mushy zone becomes larger and the strain zone under applied strain becomes more prone to liquation cracking.

2.1.1. (7xxx) Series Aluminum Alloys and AA7039

As mentioned earlier, 7xxx series, Al-Zn-Mg aluminum alloys are widely used for aircraft structures due to their high strength, low density and cost. [9, 10] Considering the operation conditions the most important properties necessary are strength, ductility, elastic modulus, corrosion and damage tolerance, which are fracture toughness and fatigue resistance. The mentioned properties can be overhauled by appropriate alloying, processing or a combination of these. Since, 7xxx series are age-hardenable, when structural applications are taken into account

they are mostly processed in the form of plates, extrusions or forgings. As an example, for a thick plate product, typical processing schedule involves casting, homogenizing, hot rolling, solution treating, quenching, and stress relieving by stretching and age hardening, as shown in Figure 2. [11] Considering the strengthening mechanism in 7xxx series (Al-Zn-Mg-Cu alloys) zinc plays an important role. It is also known that greater than 3% Zn and additionally, Zn to Mg ratio greater than two, the hardening mechanism occurs as a result of $MgZn_2$ (η). [12, 13] Therefore, precipitates in these alloys starts as GP zones then becomes η' coherent platelets then with time, transforms into η. [13]

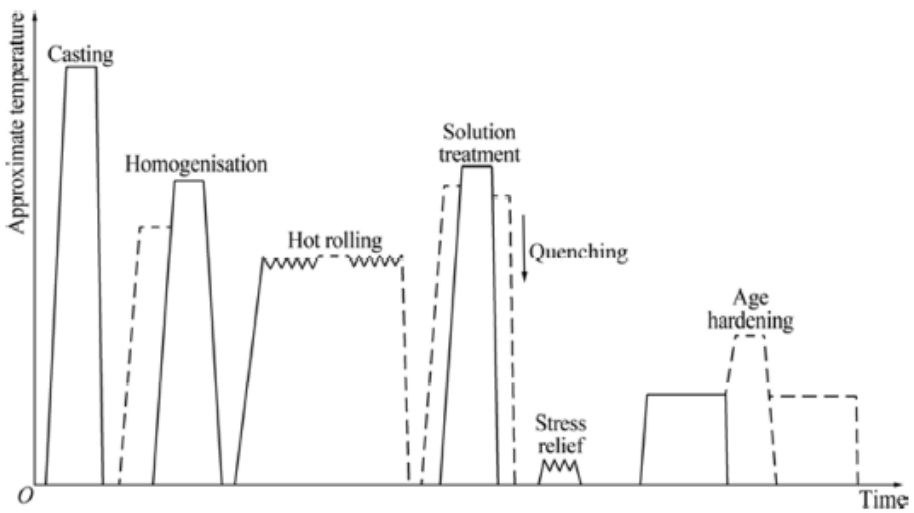

Figure 2 Semi-schematic processing schedule for high-strength Al−Zn−Mg−Cu plate (Some commercial and experimental variations are indicated by dashed lines) [11]

Considering AA7039 aluminum alloy, it is mainly an Al-Zn(%4)-Mg(%2.8) alloy that is a medium strength armor grade. It also has important ballistic properties that makes AA7039 useful for military applications. [8] Addition to military applications like military vehicles, this alloy can also be used for automobile industry, innumerous applications such as transportable bridges, girders, railway transportation. [14] Since AA7039 is widely used in military industry, there are also military standard to specify AA7039 such as MIL-DTL-46063H (Table 3).

Table 3 Chemical composition of AA7039[15]

	%Zn	%Mg	%Mn	%Cu	%Fe	%Si	%Cr	%Ti	%Al
MIL-DTL-46063H	**3.5-4.5**	**2.3-3.3**	**0.10-0.40**	**0.10 (max)**	**0.40 (max)**	**0.30 (max)**	**0.15-0.25**	**0.10 (max)**	**Reminder**

AA7039 alloys shows great machinability in annealed state and readily weldable by fusion welding methods, such as metal-arc-inert gas (MIG) process. Compared with 5083 which is most commonly used structural aluminum alloy in welded condition, AA7039 has better weld strength and ductility. It has a nominal weld strength of around 360 MPa. Moreover, during welding, there is no need for special pre-weld or post-weld heat treatments. [16] Together with its mechanical properties, the corrosion resistance of 7039 is much superior that of other heat treatable alloys. The mechanical properties is summarized in Table 4 depending on the condition of the material.

Table 4. Typical mechanical Properties of 7039[8]

Property	**Property value* at temper:**		
	T64	**T61**	**O**
Tensile Strength (MPa)			
Longitudinal	450	400	227
Transverse	450	400	227
0.2% Tensile Yield Strength (MPa)			
Longitudinal	380	330	103
Transverse	380	330	103
Brinell Hardness (1500kg), HB	133	123	61

*Property values for 6 to 75 mm thick plate

Since major alloying element is Zinc, the strengthening mechanism occurs with heterogeneous η' and then transforms into η ($MgZn_2$) precipitates.

2.2. Arc Welding

Arc welding process, is a welding process with a formation of an electric arc between an electrode and the metal workpiece by heating of the workpiece metal and cause to melt the filler and base metal together and join. This method was originally developed by aluminum and aluminum alloys but soon, is now also used for steels. In this study a subtype of arc welding method called, “Metal Inert Gas” (MIG) welding will be used for welding of 7039 alloy.

2.2.1. Metal Inert Gas Welding (MIG)

Metal-inert gas welding (MIG) is a joining process by melting with the heat input caused by an arc established between a continuously fed filler wire electrode and the metal workpiece that can be seen in Figure 3.

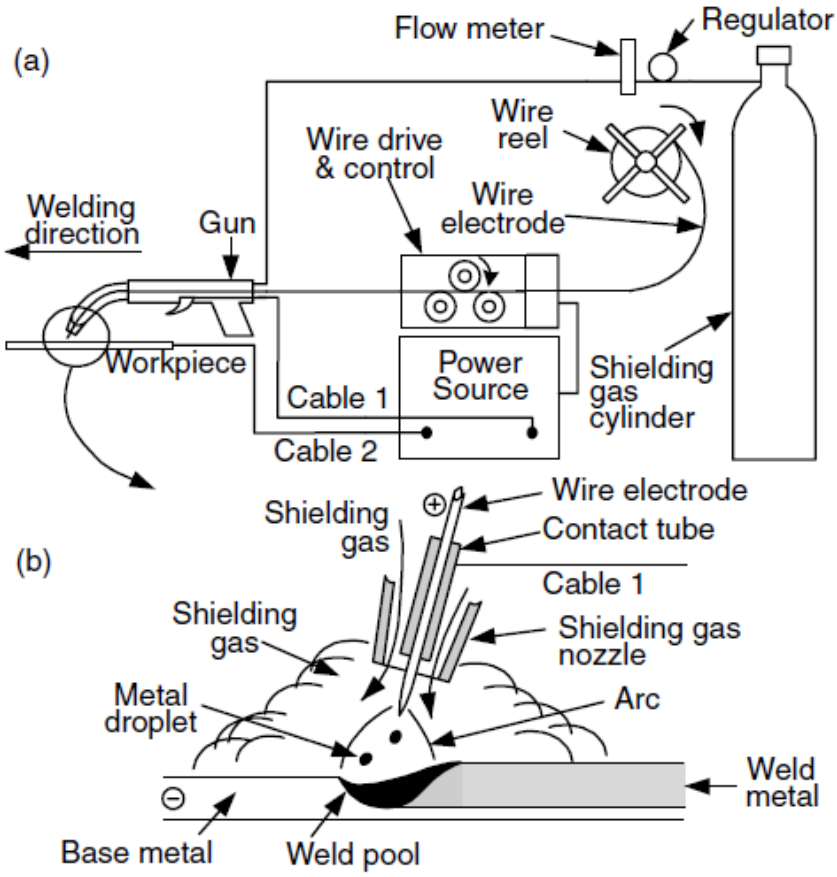

Figure 3 MIG welding: (a) overall process; (b) welding area enlarged [17]

The molten weld pool and the arc zone is shielded by inert gases like argon or helium. Metal inert gas (MIG) is also known as Gas Metal Arc Welding (GMAW) and this technique is the most commonly used technique for aluminum alloys and a smooth metal transfer with low spatter loss and good weld penetrations can be obtained by a stable arc. [17]

Considering the shielding gases, argon, helium and their mixtures are used for nonferrous metals as well as stainless and alloy steels. However, comparing the arc energies, in argon arc, the energy is less uniformly dispersed than the helium arc due to the lower heat conductivity of argon gas. Therefore, as a result of this phenomena, argon arc plasma has a very high energy core and an outer mantle of lesser thermal energy and by this, a stable, axial transfer of metal droplets through

argon arc plasma can be obtained. An example of the shapes of the droplets can be seen in Figure 4.

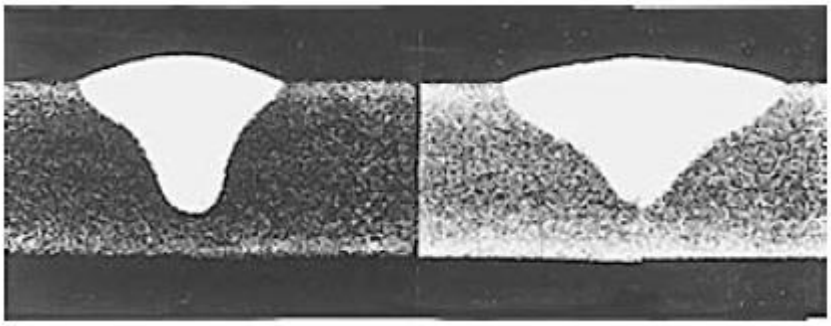

Figure 4 MIG welds in 5083 aluminum alloy by argon gas (left) and 75% He–25% Ar (right). Reprinted from Gibbs [18] Courtesy of American Welding Society.

2.3. Weld Structure

In the welding process, as a result of the arc, heat is generated on the weld pool and some regions are directly affected by this heat generation and some other regions are yet less affected. On this respect, there are three main regions in the weldment that can be distinguished either with naked eye or with chemical etching. The weldment regions are named as Weld Metal (WM), Partially Melted Zone (PMZ) and Heat Affected Zone (HAZ). Besides these main regions, the remaining part of the metal can be named as parent metal (PM) or base metal (BM) which is less affected by heat during welding.

Weld Metal (WM), is region where is completely melted and solidified, therefore consists of base metal and filler materials. By increasing the number of weld passes, the chemical composition of the weld metal starts to reach to the chemical composition of the filler metal. The boundary that separates the weld metal and the base metal is called the fusion line (FL) where the temperature reaches the liquidus temperature (T_L). The region which is affected by the heat evolved during welding and between the weld metal and base metal is called Heat Affected Zone (HAZ). The region in HAZ that starts from fusion line and ends at the point where solidus

temperature (T_S) is reached is called Partially Melted Zone (PMZ) where the heat is too low to melt tough high enough to alter the microstructure. [19, 20]

2.3.1. Weld Metal

As mentioned in Chapter 2.2.1, heat required for melting is generated by the arc burning between welding torch and base metal. Since the solution of weld metal, composition, heat distribution, and microstructure of weld metal are in direct relation with weld parameters like welding current, welding speed and so, base metal grains around the weld pool act as nucleation sites during solidification of the weld metal. Accordingly, solidification mode together with microstructure of the WM basically depends on the solute distribution, chemical composition, cooling rate and growth rate.

In Figure 5, the effect of temperature gradient and growth rate on solidification mode can be seen. Growth rate (R) and temperature gradient (G) maps the solidification mode and the microstructure size also described in Figure 5 and G/R determines the solidification mode and GxR represents the size of the solidification microstructure. Considering the solidification mode indirectly that is G/R ratio, it is affected by heat input and welding speed, meaning, increasing line energy with constant weld speed, in other words, only an increment in heat input, results with decrease in temperature gradient, thus G/R ratio decreases. Decline of the G/R ratio changes the solidification mode (microstructure) from cellular to dendritic. [17]

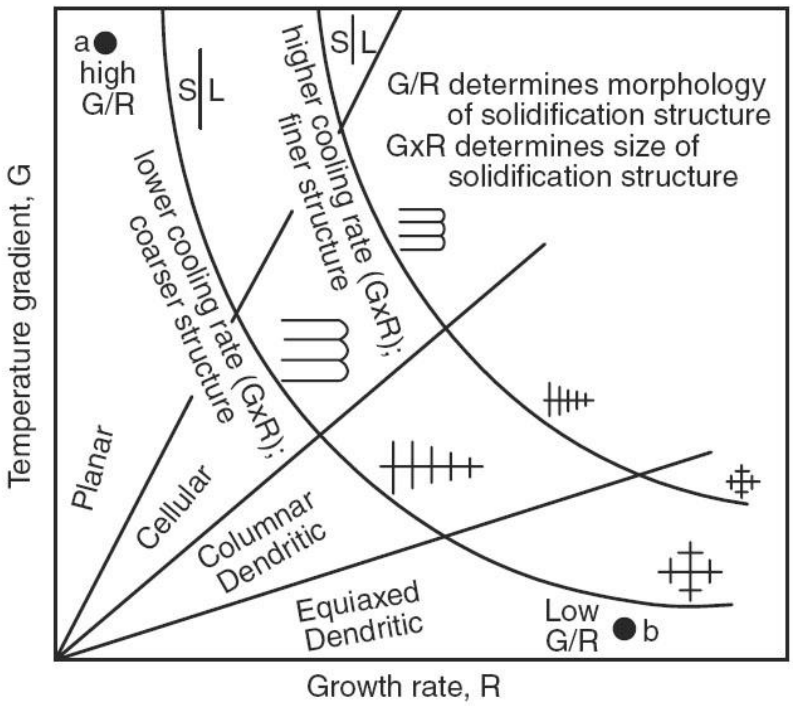

Figure 5 Weld metal solidification affected by cooling rate and growth rate. [17]

Further, the size of the microstructure is also affected by heat input and welding speed such as increasing cooling rate decreases the dendrite arm spacing. The cooling rate can also be altered by dropping the line energy (Q/V) where Q represents the heat input and V represents the welding speed. Therefore, decreasing the line energy results with finer microstructure.

When it comes to discuss the growth rate and temperature gradient, they both change along the weld pool boundary starting from the center line and ended in fusion line. For this reason, weld pool boundary plays an important role for changing the solidification mode and welding speed affects the growth rate, so it changes from V to zero from centerline to fusion line that can be seen in Figure 6.

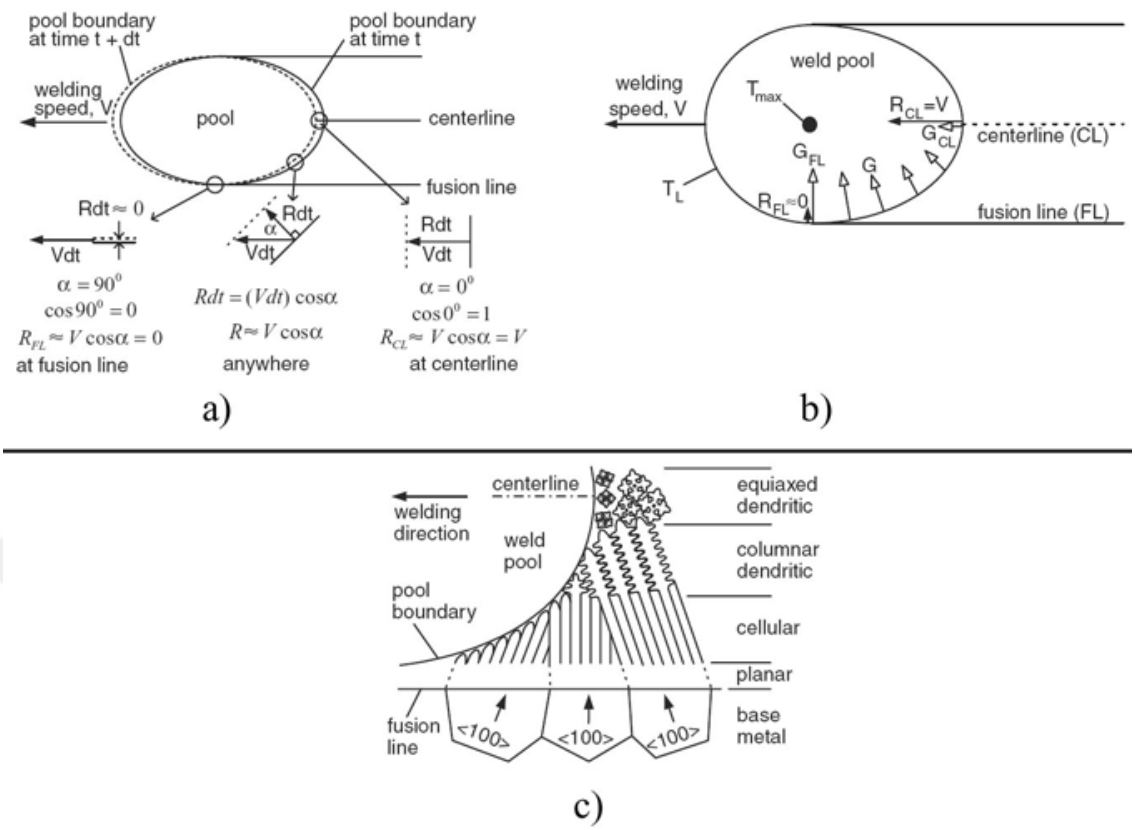

Figure 6 a) Growth Rate b) Temperature Gradient c) Solidification mode along the weld pool. [17]

Weld pool shape is also affected by welding parameters. Low weld speeds together with low heat input results more elliptical weld pool whereas high weld speeds with high heat input results tear dropped shape weld pool which yields heterogeneous nucleation at the center of weld.

2.3.2. Partially Melted Zone (PMZ)

The region in HAZ that starts from fusion line and ends at the point where solidus temperature (T_S) is reached is called Partially Melted Zone (PMZ) where the heat is too low to melt tough high enough to alter the microstructure. [19, 20] PMZ is a detectable region in aluminum alloys due to the wide solidification range.

As far as it is known that, welding harms the strength of the metals, especially aluminum alloys. Strengthening mechanism of aluminum alloys can occur with age hardening, work hardening and other different methods. These methods help to recover the strength of the alloys. 7xxx series aluminum alloys, that are heat treatable, loose their strength after welding, therefore, by post weld heat treatment processes, recovery of mechanical properties can be derivable.

Since heating rate is very fast during welding, various liquation mechanism results from equilibrium condition. Researches state approximately five different mechanism depending on the alloy composition.[20-22] First mechanism can be applicable for an alloy having composition of C_2 that can be seen in Figure 7a. The second mechanism that can be seen in Figure 7b, at room temperature A_xB_y and α phases are present but during the welding procedure the eutectic reaction occurs at eutectic temperature (T_E) between these phases therefore C_2 also contains α+ A_xB_y. The third mechanism is named as constitutional liquation. [20, 23] In this mechanism, C_1 contains A_xB_y particles and in equilibrium condition when temperature is T_s, A_xB_y dissolves in α phase, hence, no liquation is seen up to solidus line. On the other hand, if high heating rates is seen, A_xB_y particles can remain without dissolution in α phase during welding and for this reason at T_E liquation occurs between A_xB_y particles and α phase as a result of eutectic reaction. In the fourth mechanism represented in Figure 7c, solute segregation at grain boundaries may be a pioneer for formation of eutectics in C_1 alloy. Therefore, during welding process, as a result of the high heating rate, they remain undissolved up to T_E. Consequently, at T_E, some residual eutectic melts remains at the grain boundary. The fifth and last liquation mechanism is the melting of C_1 alloy consisting of solely α phase. By virtue of this, melting does not occur before reaching T_S. (See Figure 7c)

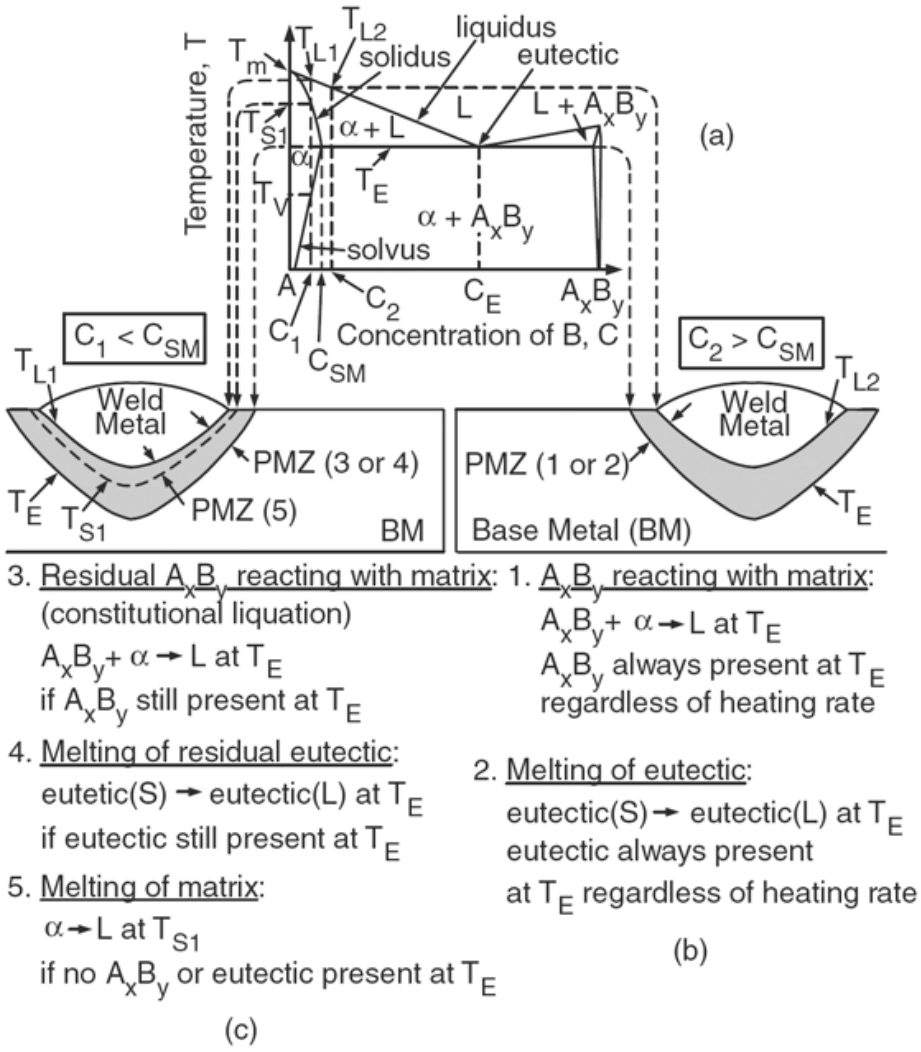

Figure 7 Liquation mechanisms solid solubility limit and above the solid solubility limit respectively. [17]

2.3.3. Heat Affected Zone (HAZ)

Heat Affected Zone (HAZ), as mentioned in Chapter 2.3, is the region between partially melted zone and the base metal. Hence, it is affected by the high temperatures during welding but there occurs no melting across HAZ. However, as a result of the heat input, the base metal microstructure changes and previously gained good mechanical properties are affected negatively. Therefore, in order to

recover the mechanical properties in HAZ, post weld heat treatments are necessary. The recovery mechanism will be mentioned in detail in Chapter 2.5.1.

2.4.Aluminum Welding Discontinuities

Although aluminum alloys have wide range of application areas, considering the welding of aluminum alloys, it is known that it is a limited process. The reason for these limitations stems mainly from the intrinsic defects (hot tearing, inclusions, and hydrogen cracking) associated with fusion and solidification. Discontinuities coming from welding process itself such as undercut, porosities, lack of penetration, arc strike, incomplete fusion, overlaps, melt-through shrinkage voids, oxide inclusions and so can be seen. [8, 17] The summary of problems with solutions can be seen in Table 5.

Discussing the porosity as a discontinuity in aluminum alloy welds, which was seen during this study, it is mainly a problem confined to the weld metal, and occurs as a result of the dissolved gas in the molten weld metal becoming trapped as it solidifies thus, forms gas cavities can be seen in Figure 8. [24]

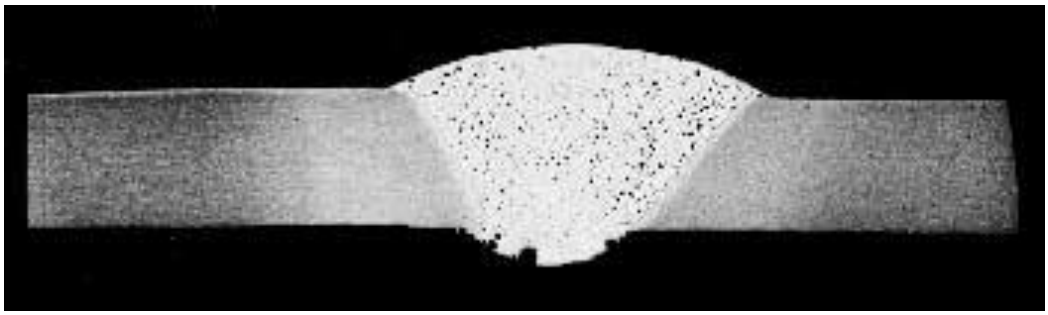

Figure 8 Finely distributed porosity in a weld groove [24]

Table 5 Typical Welding Problems in Aluminum Alloys [17]

TYPICAL PROBLEMS	ALLOY TYPE SOLUTIONS	ALLOY TYPE SOLUTIONS
Porosity	Al-Li alloys (severe)	Surface scraping or milling Thermovacuum treatment Variable-polarity keyhole PAW
	Powder-metallurgy alloys (severe)	Thermovacuum treatment Minimize powder oxidation and hydration during atomization and consolidation
	Other types (less severe)	Clean workpiece and wire surface Variable-polarity keyhole PAW
Solidification cracking in FZ	Higher-strength alloys (e.g., 2014, 6061, 7075)	Use proper filler wires and dilution In autogenous GTA welding, use arc oscillation or less susceptible alloys (2219)
Hot cracking and low ductility in PMZ	Higher-strength alloys	Use low heat input, Use proper filler wires Low-frequency arc oscillation
Softening in HAZ	Work-hardened materials Heat-treatable alloys	Use low-heat input Post weld heat treating

Therefore, porosity in welds can range from being extremely fine micro-porosity, up to coarse pores. It is known that, increasing the arc current increases the temperature, herewith increases the temperature of the weld pool, thereby, increases the rate of absorption of hydrogen in the molten metal, as a result, amount of porosity increases. Conversely, changing the weld position to flat position again heat input increases but porosity may decrease. If the rate of gas evolution from the weld exceeds the rate of absorption, similar to say that, slowing the rate at which the weld freezes allows hydrogen to bubble out of the weld metal. [24]

2.5.Heat Treatment of Aluminum Alloys

"Heat Treatment" as a definition, is basically a heating and a cooling route in order to increase the strength of the alloys. The improvement can be seen as a result of a second phase that precipitates of a supersaturated solid solution ends up with an increment in strength due to the reasons of coherent interface between the matrix and the precipitate up to precipitate are coarsening and becoming incoherent. Further, following by solutionizing, hardness is decreased in order to have an opportunity for easy forming and shaping. The main advantage of this route is its repeatability therefore, it is mostly possible to reheat and harden the heat-treatable alloys over non-heat treatable ones. [8, 25, 26]

Precipitation from solid solution is the main attribute in precipitation hardening and plays an important role in strengthening mechanism by heat treatment. Therefore, discussing the precipitation from solid solution, is the temperature-dependent equilibrium solid solubility that is characterized by increasing solubility with increasing temperature. Since this mechanism is already seen in most of the binary aluminum alloy systems, some exhibit negligible precipitation hardening which makes them non-heat treatable. However, alloys of the binary aluminum-silicon and aluminum-manganese, aluminum-zinc systems shows substantial precipitation, therefore grouped as heat treatable. Therefore, in aluminum-zinc-manganese systems, in other words in 7xxx series, the main strengthening mechanism occurs as

a result of $MgZn_2$ precipitation. A schematic representation of solution treatment procedure in a binary phase diagram can be seen in Figure 9.

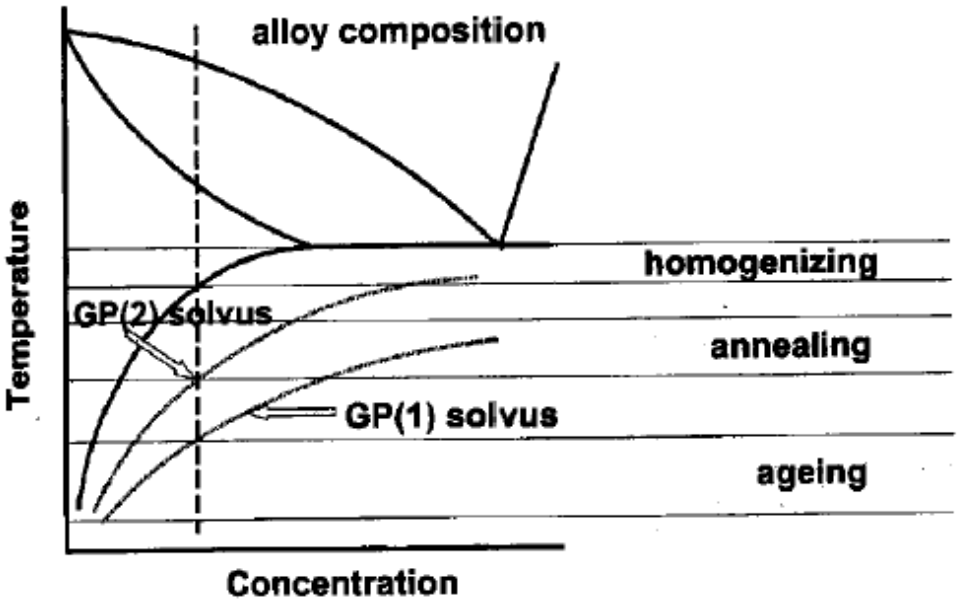

Figure 9 Representative binary phase diagram for solution strengthening mechanism. [17]

The general demand for precipitation strengthening of supersaturated solid solutions involves mainly formation of finely dispersed precipitates during aging. After solution treatment, followed by quenching, hardening is achieved either at room temperature (natural aging) or with a precipitation heat treatment (artificial aging). As a very simple explanation, ageing by heating is known as artificial aging, and aging without heating is natural aging. Aging, must be achieved not only below the equilibrium solvus temperature, but also below a metastable miscibility gap, GP zones. (Figure 9) Strengthening mechanism, from the formation of these GP zones involves the coherent cluster of the solute atoms that have the same crystal structure with the solvent phase. Therefore, as a result of the mismatch between the solvent and solute atoms, strain is generated. The generated strain field in matrix herewith, acts as an obstacle and retards the dislocation movements, hence an increase in strength is observed. [26] As in Chapter 2.1.1 already discussed, in the

strengthening mechanism of 7xxx series (Al-Zn-Mg-Cu alloys) zinc plays an important role and the hardening mechanism occurs as a result of $MgZn_2$ (η) precipitation. [12, 13] Therefore, precipitates in these alloys starts as GP zones then becomes η' coherent platelets then with time, transforms into η as mentioned previously. [13]

Aluminum alloys in general, are strengthened by heat treatments which is a three-step process. The first step is so far mentioned dissolution of soluble phases named as solution treatment, the second step is to develop supersaturation called as quenching and the last step is to precipitate of the solute atoms either in an artificial or a natural way called age hardening. The explanations of several designations are given in Tables 6-8.

Table 6 Designations [27]

Letter	Description
F	As fabricated and no mechanical properties specified
O	Annealed to obtain lowest strength temper
W	Strain-hardened wrought products with or without additional thermal treatment
H	Solution heat treatment
T	Thermally heat-treatment to produce stable tempers other than F, O or H

Table 7 Basic Designations [27]

Temper	Description
H1	Strain hardened only
H111	Annealed and cold worked by small amount
H112	Slightly strain hardened
H116	Specially fabricated, controlled strain, corrosion resistant temper
H11	Strain hardened by 1/8
H12	Strain hardened by 1/4
H3	Strain hardened and stabilized to improve ductility
H4	Strain hardened and lacquered or paint

Table 8 Basic Temper Designations-3 [27]

Temper	Description
T1	Cooled from an elevated temperature shaping process and naturally aged
T2	Cooled from an elevated temperature shaping process, cold worked and naturally aged
T3	Solution heat treatment, cold worked and naturally aged.
T4	Solution heat treatment, and naturally aged.
T5	Cooled from an elevated temperature shaping process, and artificially aged
T6	Solution heat treatment, and artificially aged.
T7	Solution heat treatment, and artificially overaged.
T8	Solution heat treatment, cold worked and artificially aged.
T9	Solution heat treatment, artificially aged and cold worked.
T10	Cooled from an elevated temperature shaping process, cold worked and artificially aged

After solution treatment followed by quenching, hardening is achieved either with natural aging or with artificial aging. Several alloys, at room temperature, show precipitation in order to yield stable products, however, several others, exhibit very slow reactions therefore they are always artificially aged before being used. [26]

When natural aging of aluminum alloy groups are discussed, highly alloyed 6xxx series, 7xxx series containing copper and all of the 2xxx series are almost always used in solution heat treated and quenched condition.

The 7xxx alloys show less stability at room temperature and the mechanical property changes proceed for years. As a result of this relative instability, the naturally aged 7xxx series, after solution treatment and quenching), are shown with a suffix, W. (For example 7075-W, 1 month), but in 2xxx series, (Table 8) natural ageing is designated with a suffix T3.

When artificially aging is considered, the major designations are T6 and T7 tempers. In T6 type of temper, which contributes the highest strength without giving sacrifice of the other properties, the part is solution treated and quenched. Then a precipitation heat treatment is applied at a temperature than room temperature. Further, T7 type of temper, the part is overaged, meaning that some of the strength is sacrificed in order to develop other properties. For 7xxx series, there are two variations of T7, namely T73 and T76, which is generally applied to alloys containing 1.25% Cu. [26] The application of these tempers are intended to improve the resistance to corrosion and stress—corrosion cracking. However, as overaging is seen, the fracture toughness increases together with a higher resistance to fatigue crack propagation.

2.5.1. Age Hardening of 7xxx Series Aluminum Welds

7xxx series show different age hardening behavior than 6xxx and 2xxx series. For example, comparing 2014 and 7005 series, in Figure 10, 7005 ages much more slowly than 2014. In general, 7039 alloys age more slowly than either 6xxx or 2xxx series. Therefore, these alloy groups have much smaller tendency to overage during welding than other alloys. Additionally, unlike 6xxx and 2xxx series, 7xxx series have ability to recover strength slowly but rather significantly by natural aging. Addition to natural aging after welding procedure in order to recover the strength in

HAZ, post weld heat treatment is also a useful tool to increase the strength in HAZ. An example of hardness distribution of a 7xxx series alloy, the behavior of 7005 alloy, can be seen according to Figure 11.

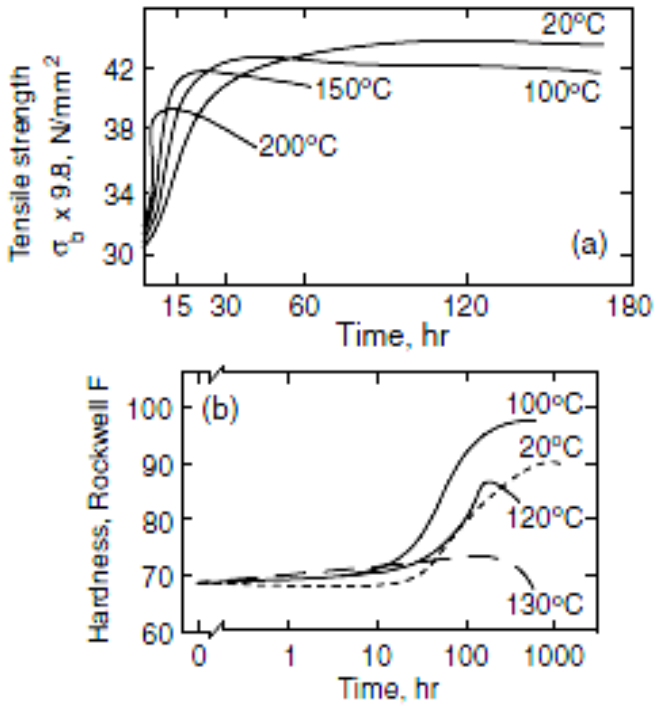

Figure 10 Aging characteristics of heat-treatable aluminum alloys: (*a*) 2014 quenched from 500°C; (*b*) 7005 quenched from 450°C [28].

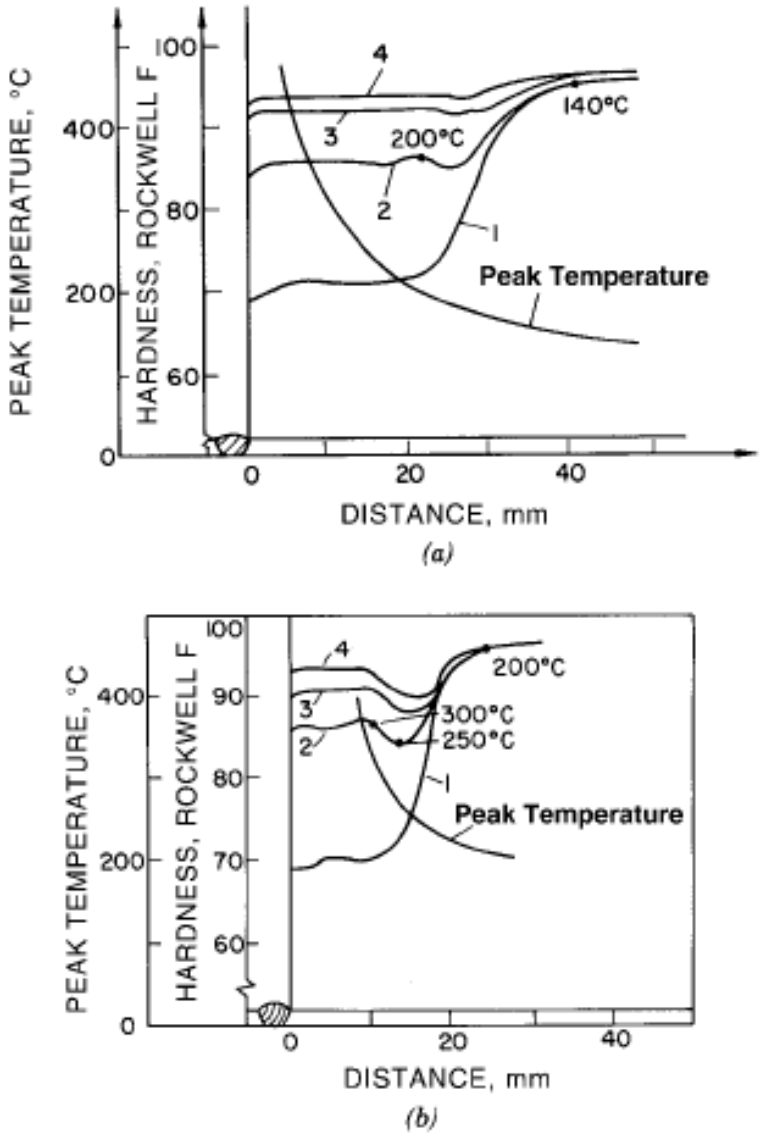

Figure 11 HAZ hardness profiles in 7005 alloy: (*a*) naturally aged before welding (1: 3 hour, 2: 4 days, 3: 30 days, 4: 90 days); (*b*) artificially aged at 130°C for 1 h before welding. [29].

When the artificial aging of 7xxx series is discussed in the previous section, it is mentioned that, excessive heat inputs must be avoided, especially in aged condition. Figure 12 shows the hardness profile in the HAZ of 7039 alloy in artificially aged condition after welding, which can shed light on this thesis study.

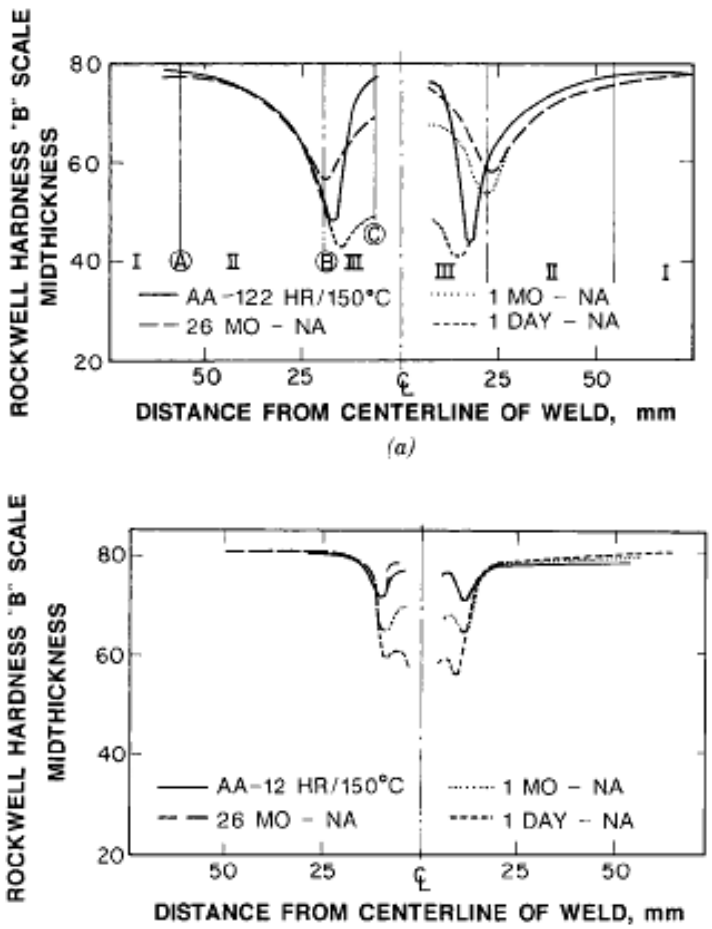

Figure 12 Hardness profiles in HAZ of aged 7039 aluminum: (a) 4 passes, continuous welding; (b) 16 passes, 150°C interpass temperature. [30]. Courtesy of American Welding Society.

As shown in Figure 12, it is possible to reduce the strength significantly while increasing the number of passes (thus decreasing the heat input in each pass) and keeping the process at a low interpass temperature.

Undoubtedly, heat-treatable aluminum alloy in annealed condition behave different. The parent metal is relatively soft in annealed condition, therefore, HAZ is solutionized during welding and thus is getting stronger by solution strengthening which results an increase in hardness in HAZ (Figure 13 is given as an example and represents alloy 7146). [31]

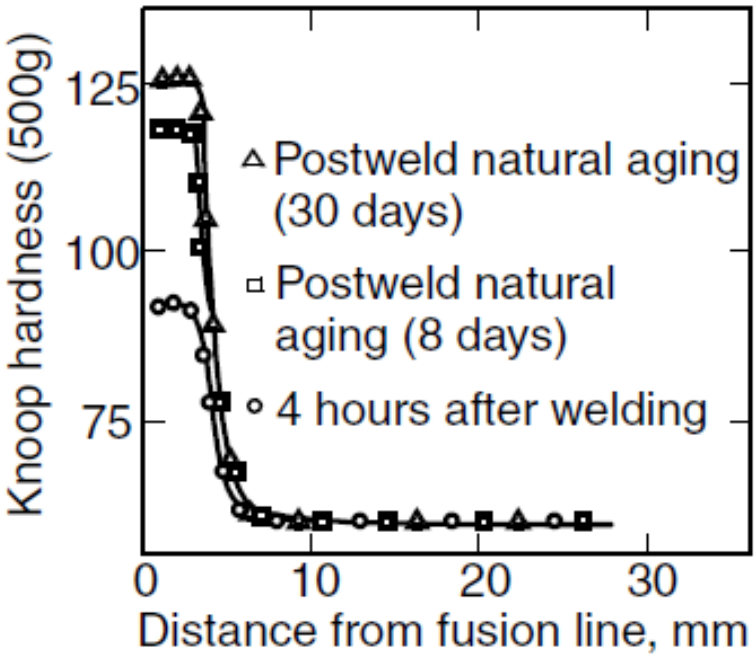

Figure 13 HAZ hardness profiles in alloy 7146 welded in annealed condition. [31]

CHAPTER 3

MECHANICAL PROPERTY EXAMINATION OF WELDED 7039 ALUMINUM ALLOY

3.1. Effect of Welding Parameters on Mechanical Properties

Improving the mechanical properties after welding of aluminum alloys in an important concern for most of the studies. Of course, together with the development of welding technology, new welding techniques have been developed. With an enhancement in the strength of Al-Zn-Mg alloys, recent investigations are concentrated on welding parameters, like heat input, filler material and welding speed.

7039 aluminum alloy, itself, plays and important role in defense industry due to its ballistic and other mechanical properties. Since it is sometimes difficult to weld this alloy by arc welding techniques some research studies were performed on the technique called friction stir welding (FSW). However, this technique is very costly, therefore, for industry it is not preferable. As a result, this technique will be briefed shortly.

In 2012, Sharma et.al. [32] investigated the microstructure and mechanical properties of 7039 alloy after FSW. According to their study, traditional fusion arc welding techniques impose some difficulties such as porosity, solidification cracking which results with a respectable strength loss. Hence, as an alternative way of joining, FSW was performed to a 7039-T6 alloy by varying welding and rotary speed of the tool in

order to investigate the effect of the changes in welding parameters on microstructure and mechanical properties. Results have shown that, low welding speed brings more homogeneous weld nugget than high weld speed as a result of high heat input per unit weld length. High heat input per unit length, consequently, results in a more homogeneous temperature distribution and more effective recrystallization. Further, after FSW, tensile strength is decreased similar with the fusion arc welding techniques. Lower values of yield and UTS of FSW of 7039 compared with the base metal is achieved, but percent elongation and toughness are superior.

Further studies were performed in order to investigate the effect of using different welding techniques on mechanical properties. Sharma et.al., [14] aimed to reveal the differences between the FSW and TIG weld joints on hardness and tensile behavior of 7039-T6 alloy. When the microstructures were compared with each other, FSW, results with a weld nugget zone (WNZ), thermomechanically affected zone (TMAZ) and similar with TIG, heat affected zone (HAZ), but, TIG welded joints includes a fusion zone (FL), partially melted zone (PMZ) and HAZ. The WNZ is the central region that lies beneath the tool shoulder therefore, the highest peak temperatures are seen here as a result of the maximum frictional and deformational heating during FSW. Consequently, dynamic recrystallization became more favorable and coarse grain structure of parent metal turned into recrystallized grain structure in this region. [14, 32] TMAZ, on the other hand, showed unrecrystallized deformed grains and contrary to WNZ; HAZ showed similar grain structure with the parent metal but more coarsened. In TIG welds, partially melted grains of the parent metal and fusion line could be seen in PMZ. If compared both weld techniques, transformation of grain structure in FSW is gradual to the extent that TIG welding results with weld thermal cycle. Thus, the grain structure is finer and grain coarsening is less in FSW than TIG weld joint. As for tensile strength, the results were showing lower values than parent metal. However, comparing the results with each other, TIG weld joints had lower tensile strength than FSW weld joints.

According to the fusion welding of 7039 alloy, heat input was examined by Kumar et.al., [33] by GTA welding. By applying various pulse combinations the microstructure, HAZ width and mechanical properties were examined. This work shed light on this subject. Four different heat inputs were provided to the samples, hence, the grains in weld zone are found to be coarser as a result of the as cast nature of the weld and in fusion line, fine equiaxed grains were seen. Further, in HAZ, large columnar grains just near the fusion boundary and the size reduces towards the unaffected parent metal. Increasing the heat input as expected increases the HAZ width and grain size. Since it is known that, the heat input per inch of weld in arc welding is proportional to the welding voltage, current and inversely proportional to the welding speed, although some of the heat is dissipated by conduction through the adjacent metal, and some amount is also get lost by radiation and convection to the surrounding. When heat-treatable aluminum alloys are taken into account, 7039 for example, HAZ shows a complicated distribution as a result of the temperature variations. According to the results of the study of Kumar et.al., base metal properties were seem to be unaffected in the locations where temperature during welding did not exceed 205°C. [33] It was shown that if samples were heated to the temperature range 205-315°C, the hardness reduction is seen drastically in HAZ, and could not be restored by natural or artificial post weld aging. However, if heating to 315°C and above, the greatest reduction in hardness immediately after welding, but can be nearly fully recovered by post-weld natural or artificial aging. On the other hand, wider HAZ, due to coarse grains, is also unfavorable for the mechanical properties.

3.2. Post Weld Heat Treatment

The post-weld heat treatment receives considerable attention by many other research groups. Since FSW is the alternative way of fusion welding, same mechanical strength loss is also seen in this method too. Therefore, some of the post-weld heat treatment studies will be mentioned here to create a general perspective.

Singh and his group [34] studied the microstructure and mechanical properties of FSW welded 7039 alloy as in welded and heat treated conditions. As a standard method, the 7039 plates were FSW welded with same rotary speed. Then one batch is subjected to a solution treatment at 550°C for 4 hours, followed by water quenching at room temperature and then artificial aging at 190°C for 6 hours. Results have shown that, in TMAZ, the grains were coarser than that of the weld nugget but in HAZ, the grains were finer. Further, the decrease in yield strength of the FSW welds is more than the decrease in UTS, and results have proven that by post-weld heat treatment percent elongation can be increased.

Another study performed by same group, in order to study different post weld heat treatments. [35] Five different post weld heat treatments were performed on 7039 alloys and the microstructure alterations and their relation to mechanical property changes have investigated. The need for different post-weld treatments came up as a result of the Singh's study results, in which there is a decrease in UTS and yield strength. These five heat treatments include natural aging (NA, at room temperature, aging more than one year after FSW), artificial aging (AA, at 120°C for a soaking period for 18 hours), step aging (pre aging at 100°C for 8 hours and followed by final aging at 150°C for 24 hours), solution treatment (ST, solutionizing at 480°C for 30 minutes followed by water quenching to room temperature) and finally solution treatment and artificial aging (STA, solutionizing at 480°C for 30 minutes followed by water quenching to room temperature and subsequent artificial aging at 165°C for 6 hours). The results have proven that, post-weld heat treatments had a radical effect on microhardness distribution depending on the heat treatment type. The hardness results can be seen in Table 9.

Table 9 The hardness results of Sharma et.al.. [35]

Material/Joint Condition	Microhardness (HV)			
	WNZ	**HAZ**	**Maximum**	**Minimum**
Base Metal	135			
As Welded	115.3	107.6	139	89
NA	131.7	128.3	159	112
AA	125.5	121.6	148	106
Step Aging	109.7	123	137	102
ST	101.2	92.7	99	82
STA	102.8	104.9	109	92

As can be seen in Table 9, natural aging results with the highest hardness values than others in HAZ. However, considering the industry conditions, waiting more than one year may not be applicable, therefore, step aging or STA seemed to be a good option.

The studies mentioned above, were also the starting point of the thesis. However, as far as gathered from the literature, the number of studies on fusion welding technique is a few. In this thesis study, GMA welding was performed with different passes to 7039 alloy samples and the mechanical properties on welding conditions were studied. Also, the effect of artificial ageing on the mechanical properties of the welded specimens was studied.

CHAPTER 4

EXPERIMENTAL PROCEDURE

The first step in the experimental work was the base and filler material characterization. For this purpose, mechanical tests and metallographic examinations were conducted. The material characterization of the raw plate was carried out in order to be sure that the selected material ensures the expected results, and preliminary tensile tests were done to compare the changes in the mechanical behavior of the material after the welding application. Afterwards, the weld joints were prepared with different angles and forms. The major weld grooves were V-Weld Groove and X-Weld Groove with angles 30° and 45° in each.

After deciding the suitable welding parameters, the samples were prepared for welding. Further, tensile tests were performed to the welded samples after macro and microexaminations.

4.1. Materials Used

In this thesis, 7039 Aluminum alloy plates were used as base material and 5356 wire as filler material. They were both obtained from METU Welding Technology and NDT Center. The composition and mechanical properties of 7039 alloy can be obtained from the literature. Therefore, in order to characterize the raw material mechanical tests and spectral analysis were performed.

To perform the welding procedure, 7039 base metal plates were machined in the form of 160x160x10 mm sized samples. Then for welding 45° and 30° Single V and

X weld grooves were trimmed perpendicular to the rolling direction in one edge. The schematic representation of the parent metal itself and the weld grooves belonging to the samples were drawn by using Siemens NX for Design and can also be seen in Figure 14 and Figure 15.

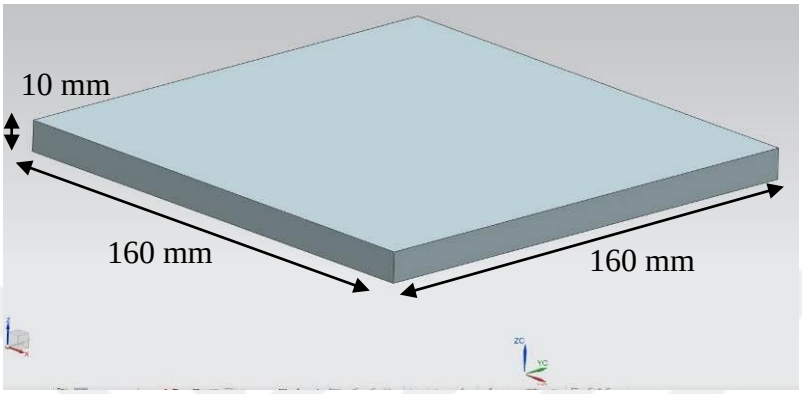

Figure 14 3D drawings for the base metal plates (Siemens NX Drawing for Design)

In the light of Figure 15, the identification of the samples can be seen in Table 10. The nomenclature in Table 10 will be used throughout the thesis.

Table 10. Identification of the Welded Samples

45V.1	45° V Weld Groove (Single V butt)
30V.1	30° V Weld Groove (Single V butt)
45X.1	45° X Weld Groove (First Set)
30X.1	30° X Weld Groove (First Set)
45X.2	45° X Weld Groove (Second Set)
30X.2	30° X Weld Groove (Second Set)

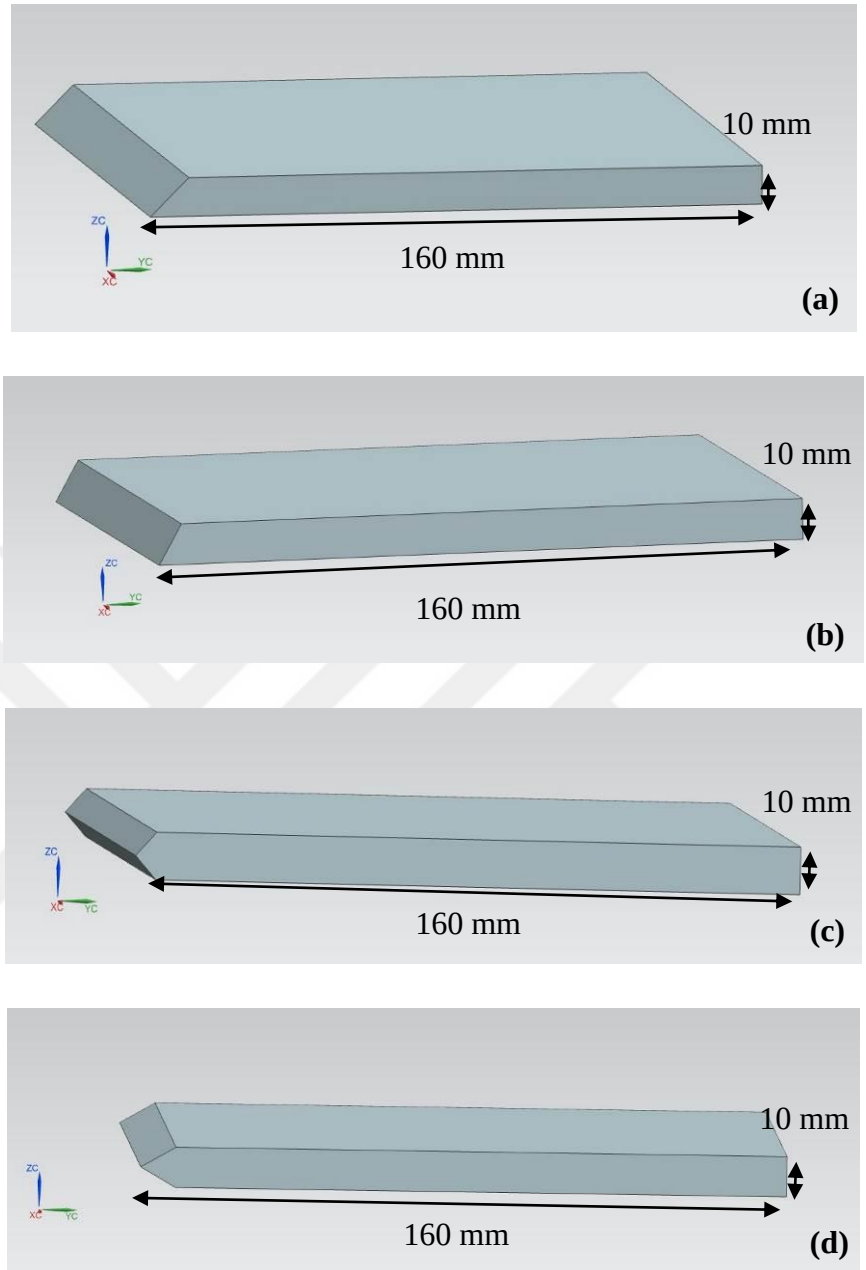

Figure 15 3D drawings of the weld grooved sample (a) 45° V Weld Groove, (b) 30° V Weld Groove, (c) 45° X Weld Groove, (d) 30° X Weld Groove (Siemens NX Drawing for Design)

4.2. Spectral Analyses and Preliminary Mechanical Tests

In order to verify the raw plate, tensile test and hardness measurements were performed to the base metal, 7039.

4.2.1. Spectral Analyses

The spectral analyses were performed by the Optical Emission Spectrometer located in Radar and Electronic Warfare Systems Business Sector at ASELSAN. Since 7039 alloy is one of the most important armor alloy in defense industry, the comparison was done in accordance with the military standard MIL-DTL-46063H. [15] Table 11 represents the composition range of 7039 given in the standard.

Table 11 Chemical composition of 7039 alloy literally [15]

	%Zn	**%Mg**	**%Mn**	**%Cu**	**%Fe**	**%Si**	**%Cr**	**%Ti**	**%Al**
MIL-DTL-46063H	3.5-4.5	2.3-3.3	0.10-0.40	0.10 (max)	0.40 (max)	0.30 (max)	0.15-0.25	0.10 (max)	Reminder

Further, choosing the right filler material is also an important issue for welding. The filler material was obtained in the form of wires. In accordance with the ASM Handbook and the studies, to minimize the crack tendency during welding the most suitable filler material for 7039 is given as 5356. [8, 24] The composition range of 5356 is given in Table 12.

Table 12 The nominal composition of filler material. [36]

	%Zn	%Mg	%Mn	%Cu	%Fe	%Si	%Cr	%Ti	%Al
5356	0.10	4.50-5.50	0.050-0.20	0.10	0.40	0.25	0.050-0.20	0.060-0.20	Reminder

4.2.2. Mechanical Tests

4.2.2.1. Mechanical Tests for As-Received 7039 Aluminum Plate

Hardness tests were performed using Shimadzu Micro Hardness Indenter under a under constant load of 9.807N (HV1) with 10 seconds dwell time and with 2 mm intervals in Vickers hardness scale at Metallography and Image Analysis Laboratory in Metallurgical and Materials Engineering Department (METU) (Figure 16).

Figure 16 Shimadzu Micro Hardness Indenter

After hardness measurements, tensile tests were conducted to the base metal in accordance with ASTM B557 by using Instron Universal Tester and Extensometer machine at Mechanical Testing Laboratory in Metallurgical and Materials Engineering Department (METU). The images of the specimens can be seen in Figure 17.

Figure 17 Preliminary tensile test specimens for the base metal (7039 as obtained) in accordance with ASTM B557

The specimens were prepared in two directions that are transverse and longitudinal to the rolling direction. The mechanical properties of 7039 were given in Part 2.1.1 in Table 4. Further tensile tests and hardness measurements were also conducted by using the equipment mentioned above.

4.2.2.2. Mechanical Tests for As-Welded Samples

In the light of the hardness measurements, around twenty-five to thirty points recorded starting from the base metal from one side to another including HAZ, PMZ and weld deposit for each sample. The hardness measurements were again performed with the Shimadzu Micro Hardness Indenter under a constant load of 9.807N (HV1) and 10s of dwell time in Vickers hardness scale at Metallography and Image Analysis Laboratory in Metallurgical and Materials Engineering Department (METU).

However, in order to compare the tensile test results, this time, the sample sizes were machined in accordance with EN ISO 15614-2. According to the EN ISO 15614-2, the weld deposit was transversely located in the mid sections of the gage and the

gage length were calculated by taking weld nugget width into account. Instron Universal Tester and Extensometer machine at Mechanical Testing Laboratory in Metallurgical and Materials Engineering Department (METU) was used to calculate the tensile strength.

The main procedure was implemented by applying post weld heat treatment to the samples for both microstructure examinations and tensile test specimens. After heat treatment, samples were subjected to metallographic examinations and hardness measurements. The tensile properties of the heat treated samples were also done.

4.3. Weld Parameters

Before deciding to welding parameters several preliminary weldings were done by the MIG welder Lincoln Electric Powertec 425C (Figure 18). By using different voltages and current values the parameters in Table 13 were decided. In Table 13, the number of passes and heat input calculations can also be seen. The heat input, travel speed and arc energy calculations were performed by using the Equations (1), (2) and (3). In those equations, V denotes voltage (potential difference), I denotes current, υ denotes travel speed, L denotes length, t denotes time and η denotes the efficiency factor.

Figure 18 Welding machine used in experiments. Lincoln Electric Powertec 425C MIG Welder. Retrieved from http://www.lincolnelectric.com/en-gb/equipment/Pages/product.aspx?product=K14062-1A(LincolnElectric_EU_Base)

Travel Speed, υ: $\frac{Length\ (L,mm)}{time\ (t,min)}$ (1)

Arc Energy, AE, J/mm: $\frac{6\ V\ I}{1000\ \upsilon}$ $\frac{6\ V\ I}{1000\ \upsilon}$ (2)

Heat Input, HI, J/mm: $\eta(AE)(\#of\ passes)$ η=efficiency factor (MIG) = 0.8

(3)

The heat input calculations were conducted in order to create a relation between different weld grooves and the microstructures together with hardness and tensile tests. The welded samples can be seen in Figure 19.

Table 13 Welding Parameters

PARAMETERS					
		First Set (45V.1,30V.1,45X.1,45X.1)		Second Set (45X.2& 30X.2)	
Filler Wire:		5356 (1.2 mm diameter)		5356 (1.2 mm diameter)	
Current, A:		110 A		207 A	
Voltage, V:		20 V		20 V	
Gas Flow Rate:		Ar (18 lt/min)		Ar (18 lt/min)	
Travel Speed:		320 mm/min		290 mm/min	
Heat Input:		330 J/mm		685 J/mm	
Arc Energy:		412,5 J/mm		856,6 J/mm	
NUMBER OF PASSES					
45V.1	**30V.1**	**30X.1**	**45X.1**	**30X.2**	**45X.2**
7 passes	4 passes	2 passes	4 passes	2 passes	2 passes
HEAT INPUT CALCULATIONS					
30V.1	**45V.1**	**30X.1**	**45X.1**	**30X.2**	**45X.2**
1320 J/mm	2310 J/mm	660 J/mm	1320 J/mm	1370 J/min	1370 J/min
HEAT INPUT PER UNIT LENGTH (Line Energy)					
30V.1	**45V.1**	**30X.1**	**45X.1**	**30X.2**	**45X.2**
8,25 J/mm	14,4 J/mm	4 J/mm	8,25 J/mm	8,6 J/mm	8,6 J/mm

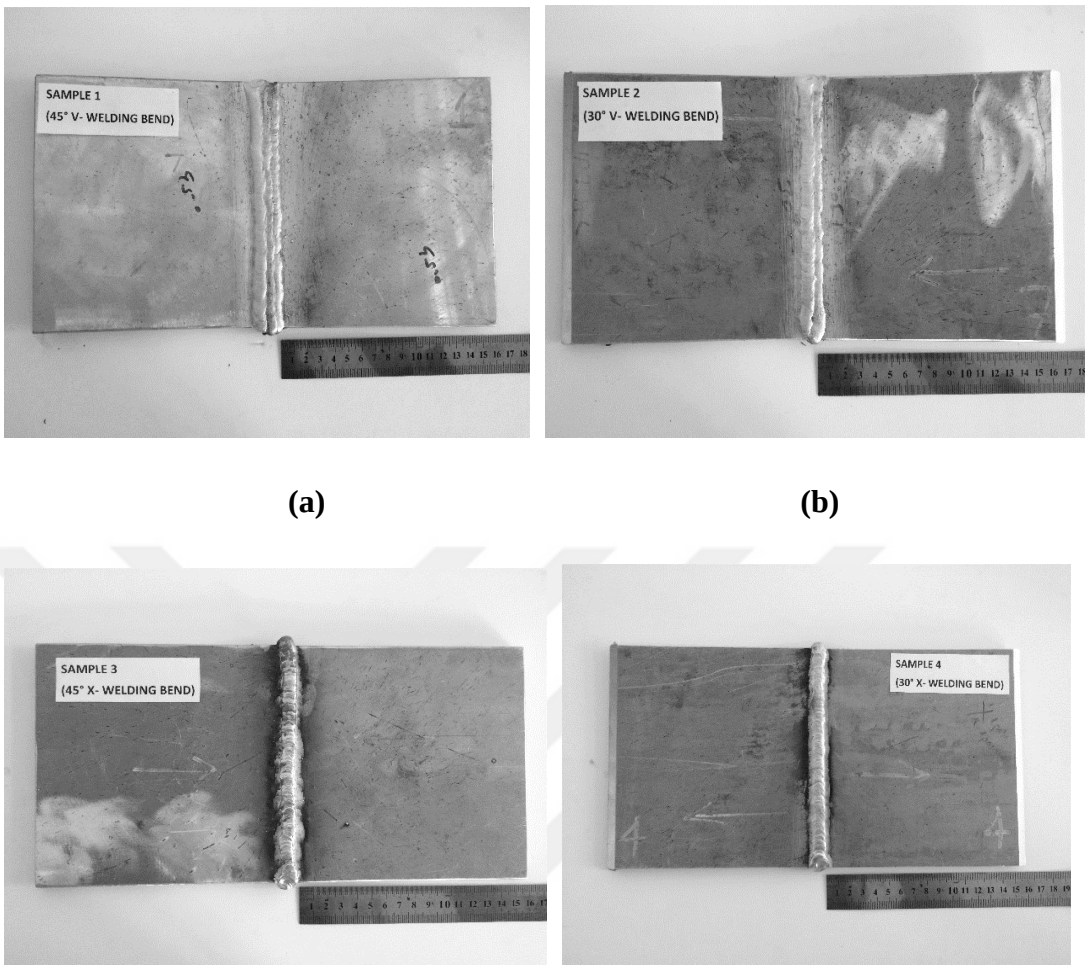

(a) **(b)**

(c) **(d)**

Figure 19 The macroscopic view of the samples after MIG welding

4.4. Macrostructural Examinations

The macrostructural examinations were performed after MIG welding in order to see the quality of the welding procedure and to determine if there was any welding defects. The schematic representation of the samples and the dimensions are given in Figure 20.

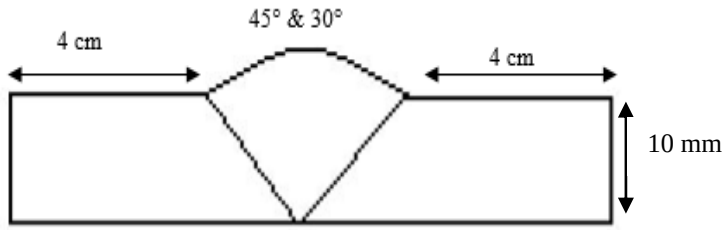

(a)

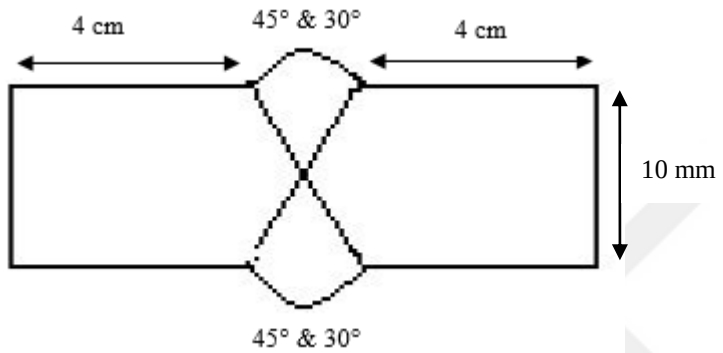

(b)

Figure 20 Schematic representation of samples

The surface of the samples were grinded by using 220, 400, 600, 1200 emery papers and the macrostructural examinations were carried out after etching with Flick solution (Table 14).

Table 14 The composition of Flick solution

ETCHANT	AMOUNT
Flick	90 ml H_2O
	15 ml HCl (Hydrochloric acid)
	10 ml HF (Hydrogen fluoride)

4.5. Microstructural Examinations

Microstructural examinations were performed in order to see the effect of welding on microstructure. Microstructural examinations are also very useful to see the alterations after post weld heat treatments. The examinations were done on the weld region including fusion line, HAZ, weld metal and base metal. The investigations were carried out by using HUVITZ Digital Microscope HDS-5800 at Metallography and Image Analysis Laboratory at Metallurgical and Materials Engineering Department (METU). To be able to examine the microstructure, the surfaces were grinded by using 220, 400, 600, 1200 emery papers and etched with Keller's reagent. (Table 15)

Table 15 The composition of Keller's solution

ETCHANT	AMOUNT
Keller	190 ml H_2O
	3 gr HCl (Hydrochloric acid)
	5 gr NH_3 (Ammonia)
	1 gr HF (Hydrogen fluoride)

In an effort for a clean image, after each emery, all samples were cleaned with ethyl alcohol to avoid contamination from abrasive particles.

4.6. Fracture Surface Examinations

Fracture surface examinations were conducted after tensile tests of the welded specimens. The main aim was to create an understanding about the fracture mechanism and to understand the initiation point of failure. The surfaces were examined under SEM (JEOL-JSM6400) for possible failure initiation sites and for the effect of welding groove.

4.7. Heat Treatments

One of the aims of this thesis is to recover the mechanical properties in HAZ after welding by applying post weld heat treatment. Therefore, choosing the best heat treatment is one of the main issues of this study. In the light of the previous studies in the literature, several heat treatments with different parameters were performed after welding of different weld grooved samples. The major treatments performed can be seen in Table 16.

Table 16 Post weld heat treatments performed

HEAT TREATMENT PROCESSES					
DESIGNATION	**SOLUTIONIZING**		**QUENCHING**	**AGING**	
	Temperature (°C)	**Time (hr)**		**Temperature (°C)**	**Time (hr)**
HT.550.4HR	550°C	4	Water	190°C	6
HT.480.2HR	480°C	2	Water	120°C	20
HT.480.20HR	480°C	20	Water	120°C	20

As can be seen from Table 16, three different heat treatment procedures were applied. The first treatment, HT.550.4HR, is based on Singh and his colleagues study [34].

The second treatment designated HT.480.2HR is created in the light of standard heat treatment procedure given in ASM Handbook for 7039 aluminum alloys which has lower solutionizing temperature. However, in order to see the effect of solutionizing time on microstructure and mechanical properties HT.480.20HR was planned.

4.8. Software Calculations

Parallel to the experimental studies, some simulations were also performed in order to create an idea about the precipitates, the phases and the possible heat treatments. These simulations would give an idea about the phase changes after heat treatments and would help discussing the metallographic approach. Therefore, by suitable simulations, the experimental results would also be supported. Starting this point of view, two main software analyses were done. The computer programs used were JMat Pro Practical Software for Materials Properties and Thermo-Calc (Thermodynamic Software).

JMat Pro, is basically a simulation software that helps to calculate a wide range of materials properties for alloys. These alloys particularly including the multi-components alloys commonly used in industry. This simulation software further provides calculations for solidification behavior and mechanical properties of alloys, the stable/metastable phases in equilibrium, phase transformations, chemical properties and thermo-physical properties. In addition to all that calculations it also creates TTT/CCT diagrams for the alloy composition defined in the software. Therefore, CCT/TTT diagrams of 7039 were obtained by using JMat Pro together with the phases during solidification.

Thermo-Calc, besides, is the most popular software used to calculate the thermodynamic calculations. It is very basically used for calculating the stable/metastable heterogeneous phase equilibria, amounts of the phases and their compositions, binary, ternary and multi component phase diagrams, transformation temperatures like liquidus and solidus and so. In the aim of this study Thermo-Calc was used to obtain the phase diagram of 7039. CALPHAD (CALculation of PHAse Diagrams) Methodology creates the basis for phase diagram calculations in this software. The methodology is used to obtain a steady description of the phase diagram and other thermodynamic properties in order to estimate the stable phases and their thermodynamic properties dependably without any experiment. Together with, it also aspires to predict the metastable states during simulations of phase transformations. Therefore, in Thermo-Calc, in order to simulate the phase diagram of 7039, the TCAL4 Version 4, Al-Alloys database was used.

CHAPTER 5

EXPERIMENTAL RESULTS

The aim of this study is to understand the effects of welding parameters on the mechanical properties of HAZ region with different weld groove angles. The 30 and 45 degrees with X and V groove forms applied since these shapes results in different heat inputs. In addition to this aim, recovering the strength loss in HAZ is another issue discussed during this study. Microstructural relations were also conducted while examining the loss in strength and the alterations in microstructures and mechanical properties, particularly in hardness and tensile strength after post-weld heat treatments. An attempt was made to find a correlation between the microstructure and mechanical properties. Filler material (5356) and the welding parameters were kept constant throughout the study. However, welding grooves with different angles and different welding parameters were applied (Table 13).

5.1. Characterization of Aluminum alloy 7039 Plate in As-Received Condition

5.1.1. Spectral Analyses and Microstructure

The raw plate was subjected to spectral analysis in order to verify the composition. As previously mentioned, the reference composition was the military standard MIL-DTL-46063H. Further, same analysis was conducted for filler material and weld deposits after welding operation. The results of spectral analysis of 7039 can be seen in Table 17 and confirms the predicted elemental composition distribution. For

further examinations, base metal is subjected to EDX analysis in order to determine if there were any inclusions or precipitates.

Table 17 The spectral analysis of 7039 by optical spectroscopy

	%Zn	**%Mg**	**%Mn**	**%Cu**	**%Fe**	**%Si**	**%Cr**	**%Ti**	**%Al**
MIL-DTL-46063H	3.5-4.5	2.3-3.3	0.10-0.40	0.10 (max)	0.40 (max)	0.30 (max)	0.15-0.25	0.10 (max)	bal.
7039 (analysed)	3.74	2.8	0.43	0.0695	0.45	0.14	0.215	0.0445	bal.

Micrographs taken from as received 7039 plates in longitudinal and transverse direction can be seen in Figure 21. The microstructure consists of fine grains, and uniformly distributed non-metallic precipitates and primary phases. (Figure 21).

Following spectral analyses performed on base metal, the microstructure of the 7039 alloy in as received condition was tried to be examined in a detailed way. With this purpose in mind, SEM studies were performed to examine if there were any precipitates or inclusions (Figure 22).

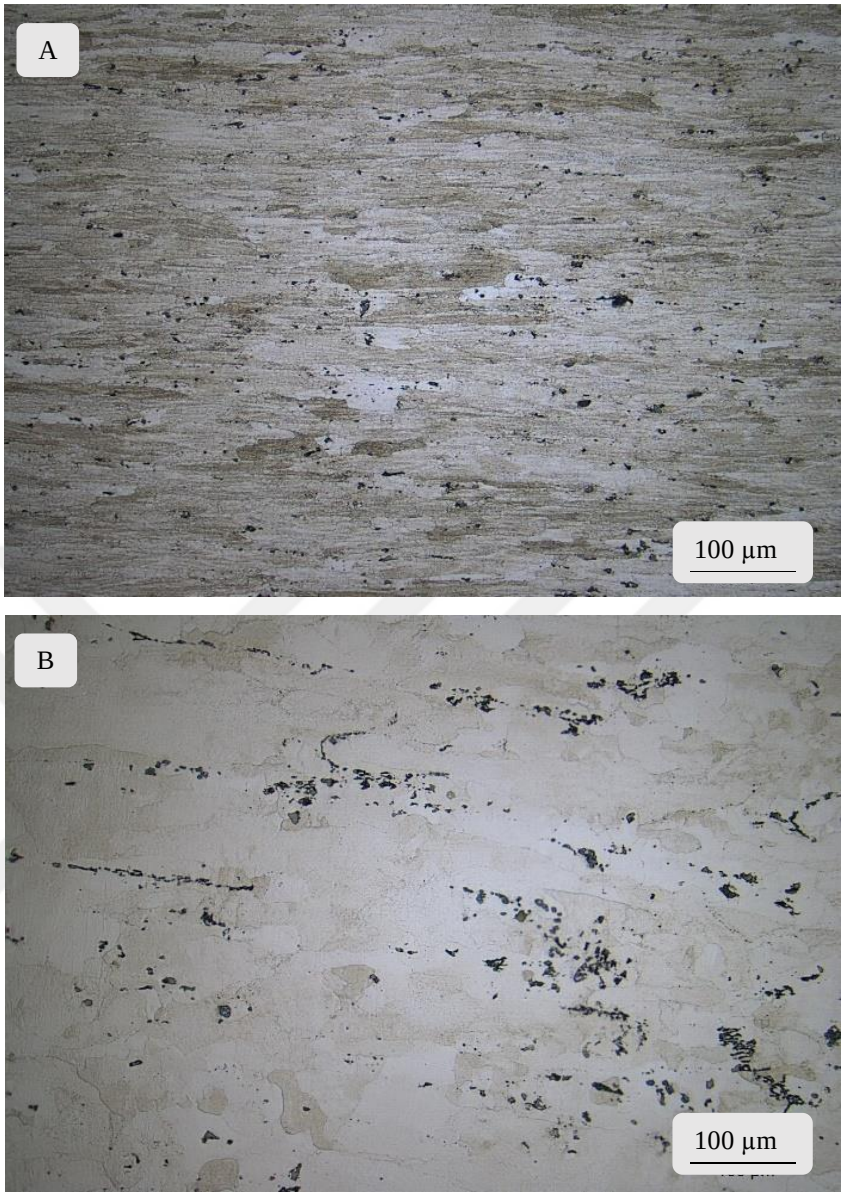

Figure 21 The microstructure of 7039 aluminum plate (a) rolling direction and (b) transverse direction. (Keller's reagent.)

As can be seen in Figure 22, there are two types of phases that are symbolized as white (Type 1) and black (Type 2). In order to understand the elemental distribution of the precipitates, Line and Point Analyses were performed together with EDX analysis. (Table 18).

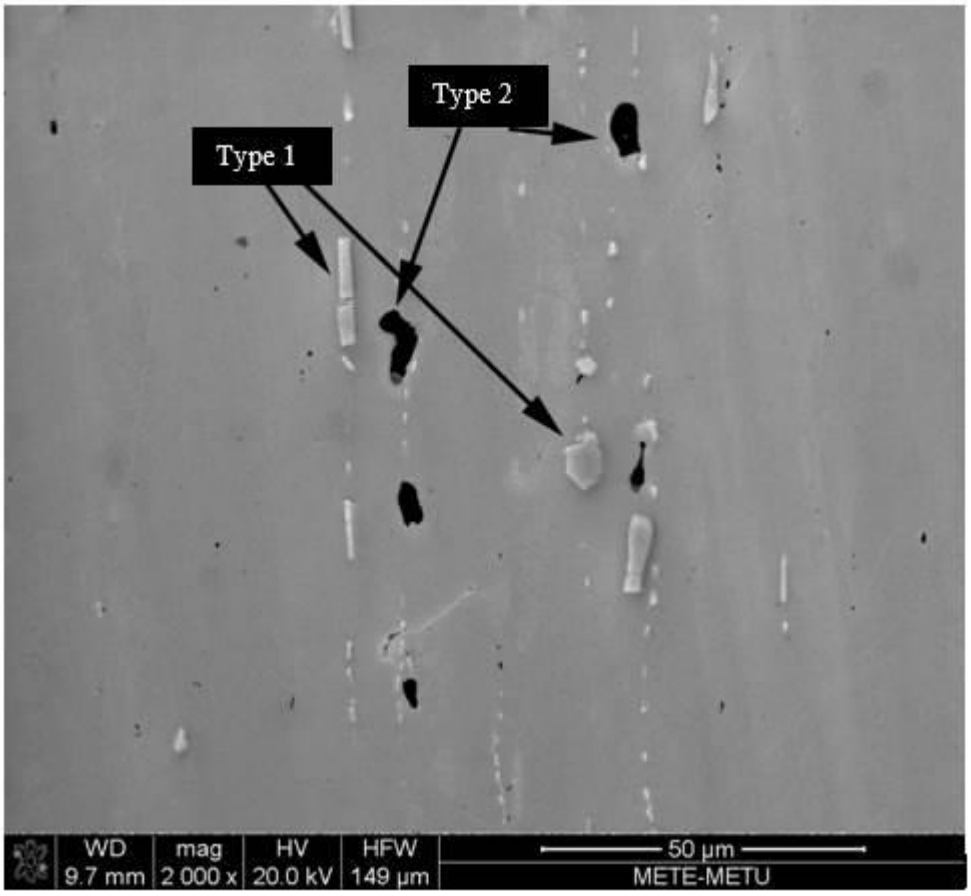

Figure 22 SEM graph of 7039 base metal showing primary phases and intermetallics

Table 18 The weight percentages of primary phases of Type 1 and Type 2

Wt %	%Al	%Si	%Cr	%Fe	%Mg	%Mn
Type 1	64,59	5,89	3,19	18,89	-	7,44
Type 2	8,53	28,62	18,30	-	44,55	-

Considering 7039 aluminum alloy, different phases can appear such as $Mg_3Zn_3Al_2$, $MgZn_2$, $(FeCr)Al_7$, Mg_2Si or even Mg_5Al_8 after welding with 5356 filler. [12] As far as the elemental distribution in Table 18 is considered, it seems that the dark primary

phases (Type 2) are of Mg_2Si type, whereas the light ones (Type 1) are of Al-Fe-Cr intermetallic such as $(Fe,Cr)_3SiAl_{12}$.

Similar with the base metal, filler metal (5356) is also subjected to EDX analysis in order to verify the composition. The average of four measurements and the comparison of these results with the nominal composition of 5356 confirm that the filler wire is of 5356 type (Table 19).

Table 19 The spectral analysis of 5356 and the comparison of the results

	%Zn	**%Mg**	**%Mn**	**%Cu**	**%Fe**	**%Si**	**%Cr**	**%Ti**	**%Al**
Literature	0.10	4.50-5.50	0.050-0.20	0.10	0.40	0.25	0.050-0.20	0.060-0.20	Bal.
5356	*	5.50	0.85	0.18	0.35	*	1.36	-	Bal.

*Zn and Si could not be observed since the peaks of some elements can be overlapped.

5.1.2. Mechanical Testing of 7039 Aluminum Alloy Plate

To compare the mechanical properties attained after welding, it is important to know the properties of the parent metal itself. Further, it is also critical to verify the aging condition of the as received 7039 plate in order to plan the post-weld heat treatment route. Therefore, preliminary tensile tests and hardness measurements were conducted to create a basis for the further studies.

The tensile test results were given in Table 20 together with the nominal values of 7039 aluminum alloy listed in ASM Handbook. [8]

Table 20 Preliminary tensile test results for 7039

	7039-T64 [8]	**7039-T61 [8]**	**Transverse direction**	**Rolling direction**
Ultimate Tensile strength (MPa)	450	400	455.0	451.8
			460.7	470.3
0.2% offset yield strength (MPa)	380	330	396.4	400.9
			408.0	418.8

As can be seen, the temper condition of as received 7039 alloy is very close to that of T64. Temper designation T64 describes the heat treatment route as: Solution heat treated and then followed by artificial aging in under aging condition that are between T6 and T61 in order to improve the formability. The ultimate tensile strength is greater than T61 condition but coherent with the T64 condition, further, yield strength also shows greater values according to the literature which may due to the environmental conditions in storage or coming from the production process itself.

Following the tensile tests in accordance with ASTM B557, hardness measurements were conducted for further hardness distribution alteration. These results would provide a comparison with that of as welded and post-weld heat treated samples. The hardness values would also give an idea about the existing mechanical condition of the as received 7039 aluminum alloy. The hardness distribution and the locations of the points can be seen in Figure 23. The measurements were taken at the plate section with the average of six measurements yielded 136.8 HV. (136±6 HV).

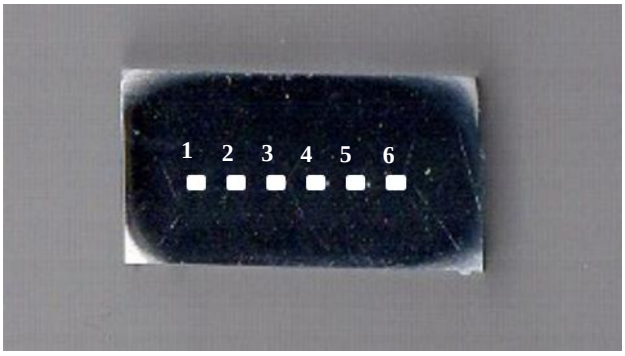

Figure 23 The representative sample of the 7039 plate and the location of the hardness measurements

Comparing the results with the theoretical values it seems that they are interpretable and significant. The 7039-T64 hardness values are around 133 HV (Table 4) which are very close to the measurements performed in this study.

Table 21 The measured values of base metal hardness

Designation Number (Figure 25)	Hardness Value (HV)
1	143
2	142
3	136
4	137
5	131
6	132

5.2. Welding Results

5.2.1. Macrostructural Examinations

In order to check the quality of the weldments, macroexaminations were performed. The welding parameters were kept constant for the first set of samples which were containing 45 and 30 degrees of V and X groove forms.

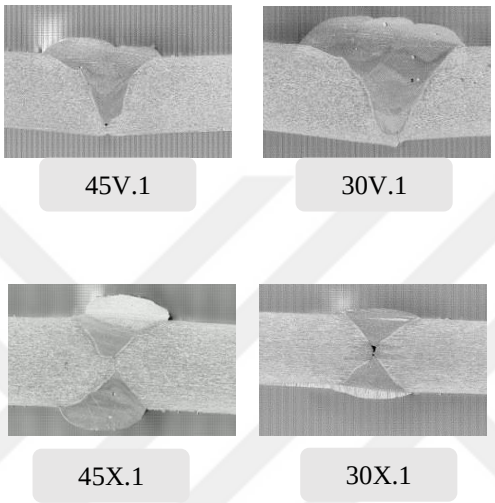

Figure 24 Macrographs of the samples

As can be seen from the macro-photos (Figure 24) of the samples after welding, lack of fusion and bonding defects can be observed in X grooved samples. Therefore, since these defects would affect the results for tensile tests, new X grooved samples with same groove angles were welded. The macro photos of the new samples, i.e. re-welded using the same parameters are given in Figure 25.

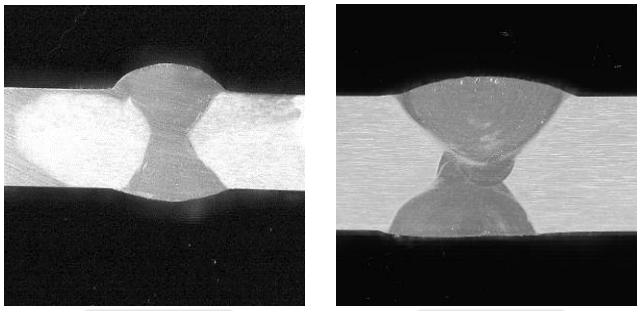

45X.2 30X.2

Figure 25 Macrographs of new (second set) welded samples

The difference between the welds can be clearly seen by comparing Figure 24 and Figure 25. The junction points are free from defects and there is not any lack of fusion.

5.2.2. Microstructural Examinations

Microstructure examinations were performed at the cross section of the samples where the weld deposit was also included. Since all the parameters were same for all samples but the weld forms were different, it resulted in samples with different heat input. The base metal, weld deposit and fusion zone can be examined for each sample particularly.

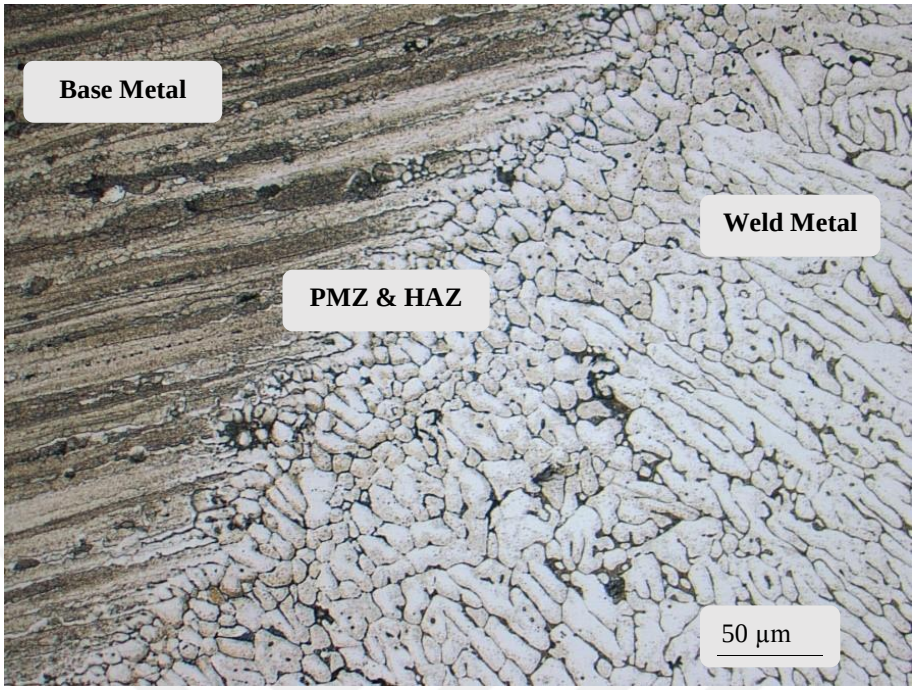

Figure 26 45V.1 weld and parent metal. Keller's reagent. (PMZ: Partially melted zone, HAZ: Heat affected zone)

For 45V.1 (Figure 26), there cannot be seen any porosity or inclusion coming from the welding in the vicinity of fusion zone or in the weld deposit. However, porosity can be seen in weld metal for sample 30V.1 (Figure 27). These might have come up with the dissolved gas trapped in the weld metal during welding.

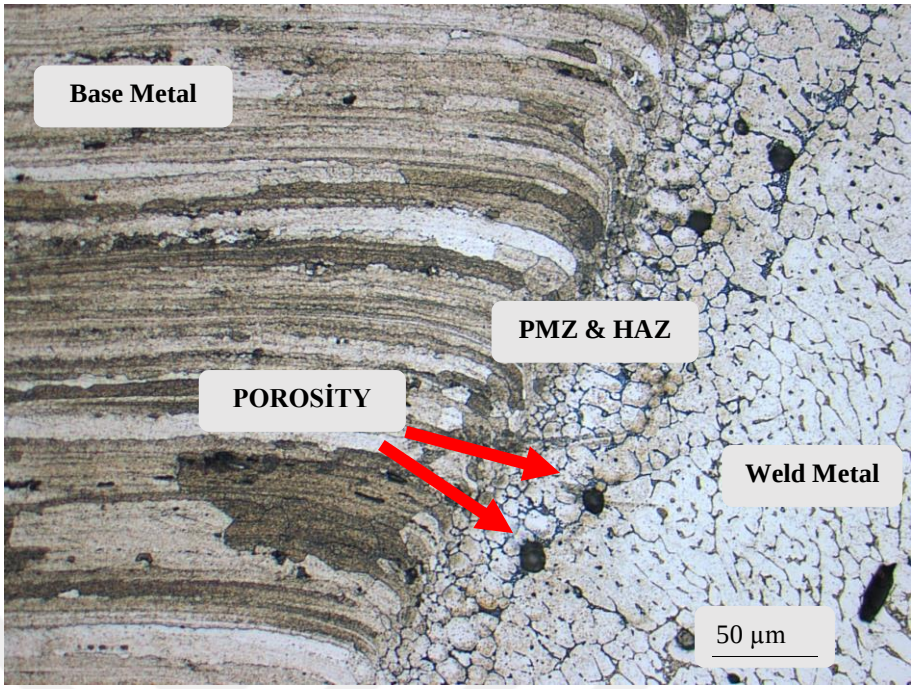

Figure 27 30V.1 weld and parent metal. Keller's reagent. **(**PMZ: Partially melted zone, HAZ: Heat affected zone)

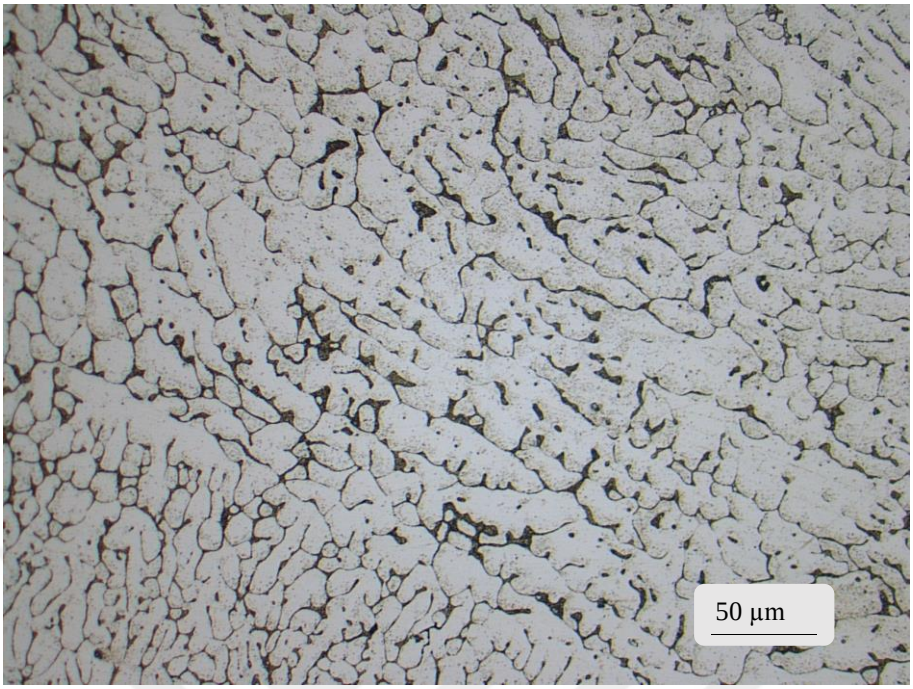

Figure 28 45V.1. The microstructure of the weld metal. Dendritic structure. Keller's reagent.

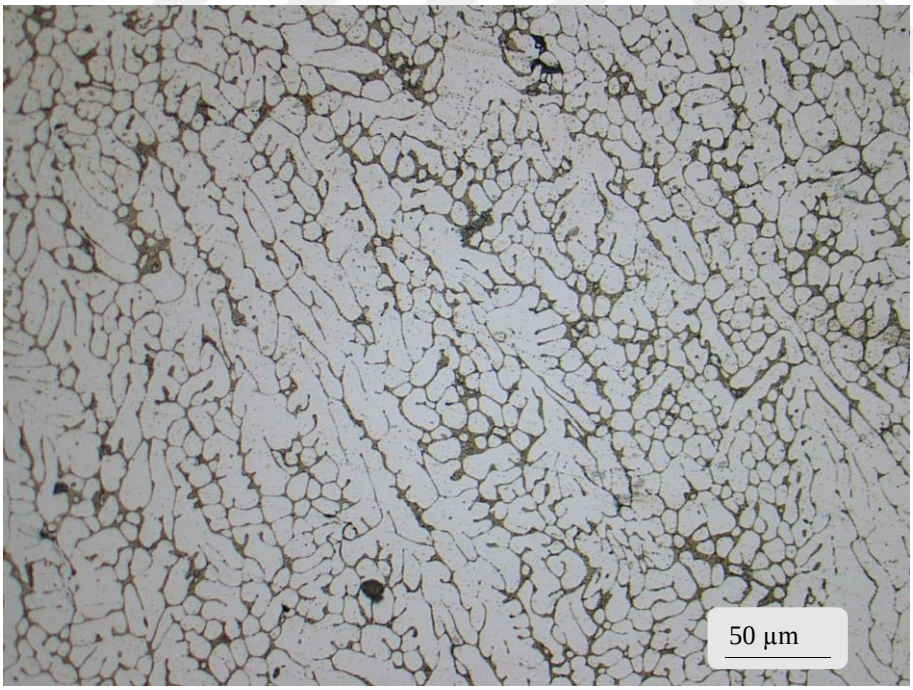

Figure 29 30V.1. The microstructure of the weld metal. Dendritic structure. Keller's reagent.

Figure 28 and Figure 29 showed that for V formed weld grooved samples, namely 45V.1 and 30V.1, the microstructures of the weld deposit were almost same and had a dendritic structure. However, different from 45V.1, in 30V.1, the dendrite arms were more directional. The base metal micrographs can be seen in Figure 30 and Figure 31.

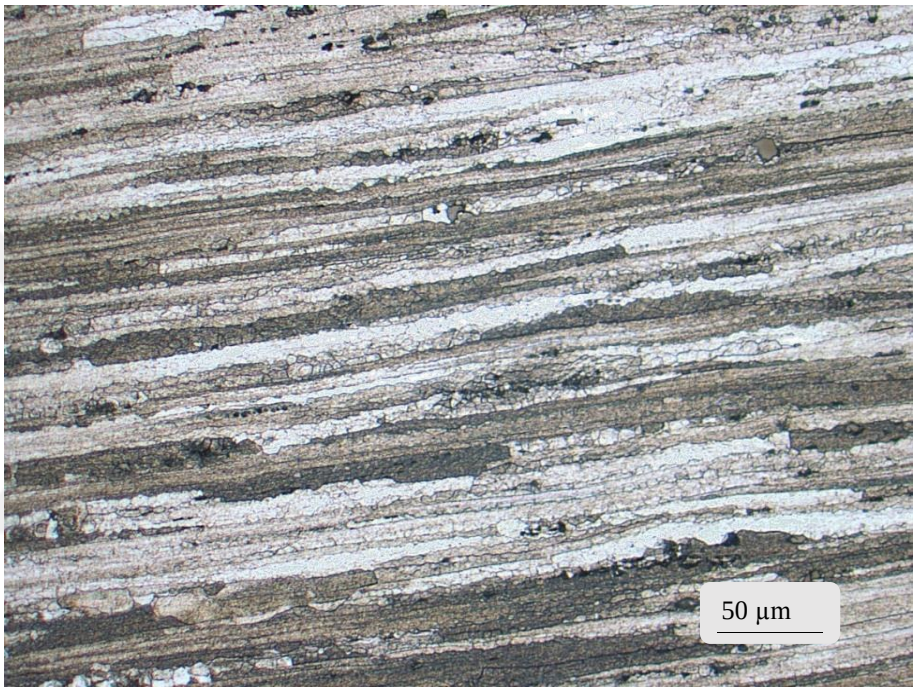

Figure 30 45V.1. The microstructure of the base metal. Keller's reagent.

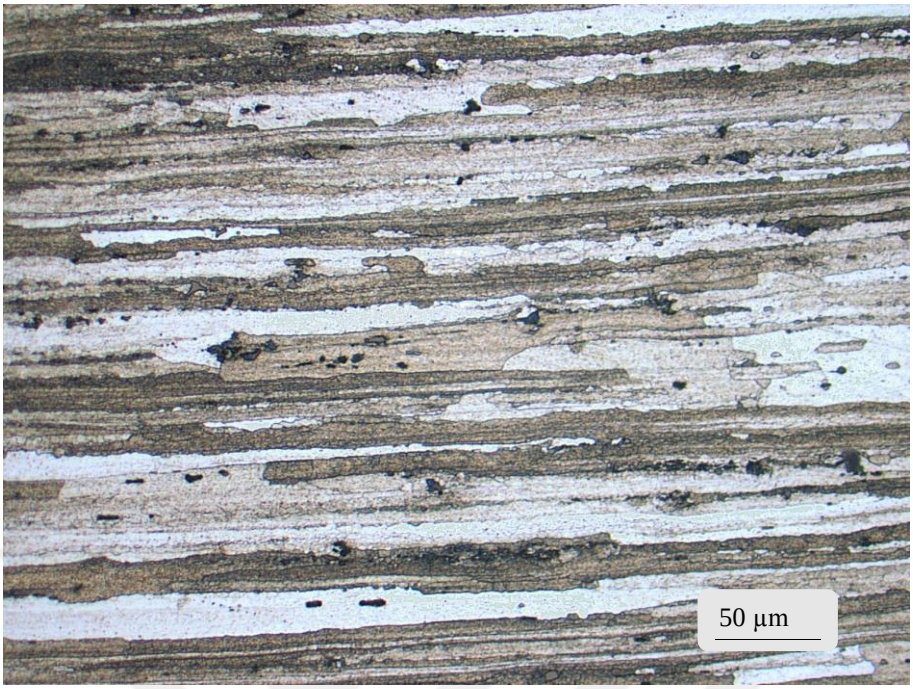

Figure 31 30V.1.The microstructure of the base metal. Keller's reagent.

In addition of optical examinations, for further understanding, Sample 45.V.1 was examined under SEM. The fusion line and HAZ regions were investigated in a different perspective (Figure 32 and Figure 33).

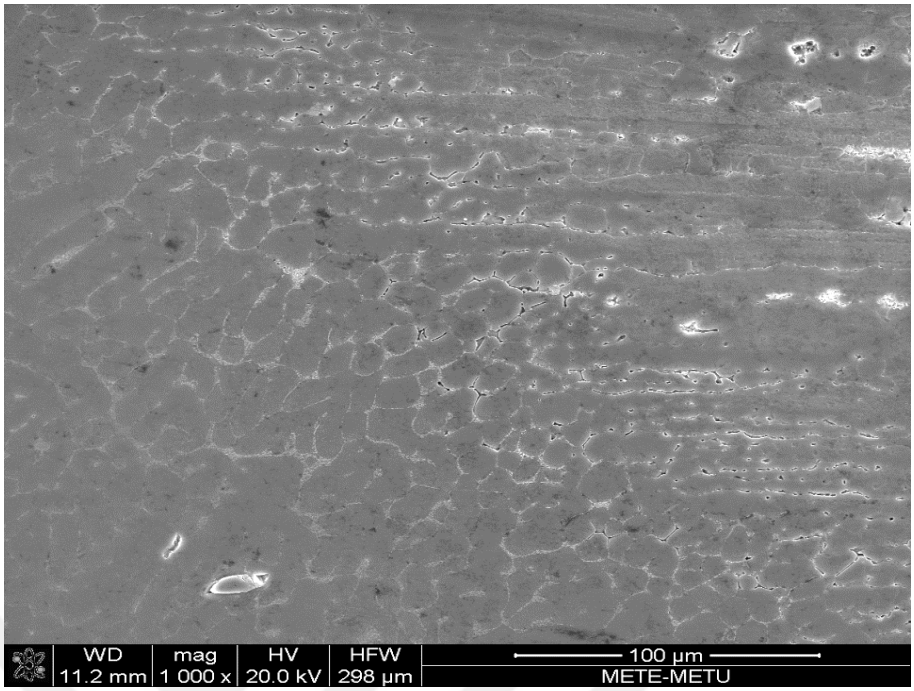

Figure 32 45V.1. The SEM image of fusion line.

Adjacent to HAZ, grainy structure can be seen easily which shows HAZ in 45V.1 after welding. Similar structures are also seen in 30V.1.

The same route was followed for X formed weld grooves. Since two sets of X formed weld grooves had been used in this study, the microexaminations were performed separately. The first set includes 45X.1 and 30X.1.

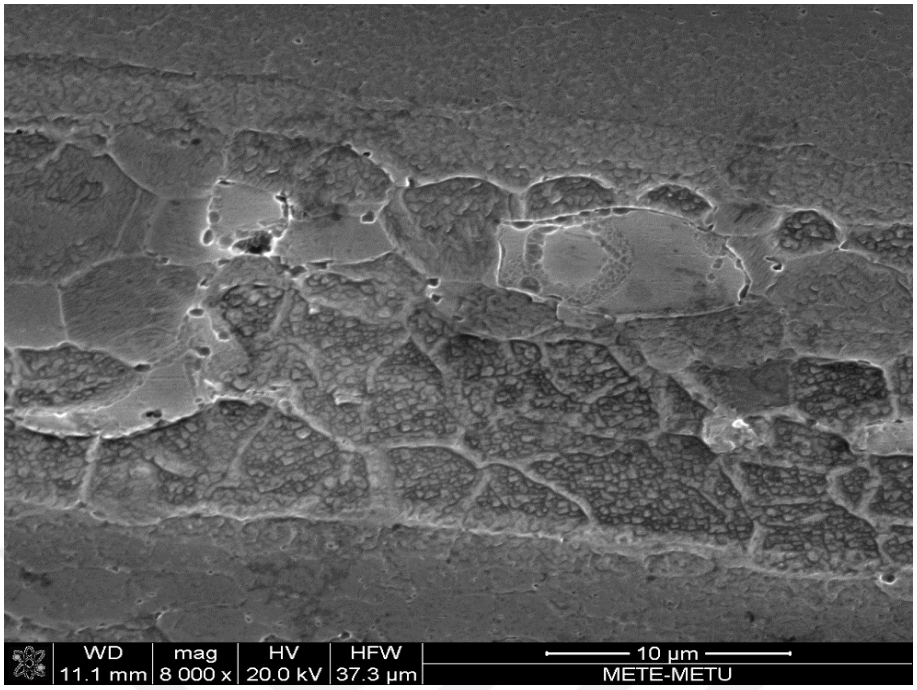

Figure 33 SEM image of HAZ, 8000x magnification, 45V.1 (45° V Weld Groove)

The weld and parent metal micrographs of the first set of X formed weld grooves can be seen in Figure 34 and Figure 35. Further the weld metal micrographs (Figure 36 and Figure 37) of the first set were also given in figures. As can be seen from the Figure 36 and Figure 37, the structures were almost same for all samples including V formed weld groove samples.

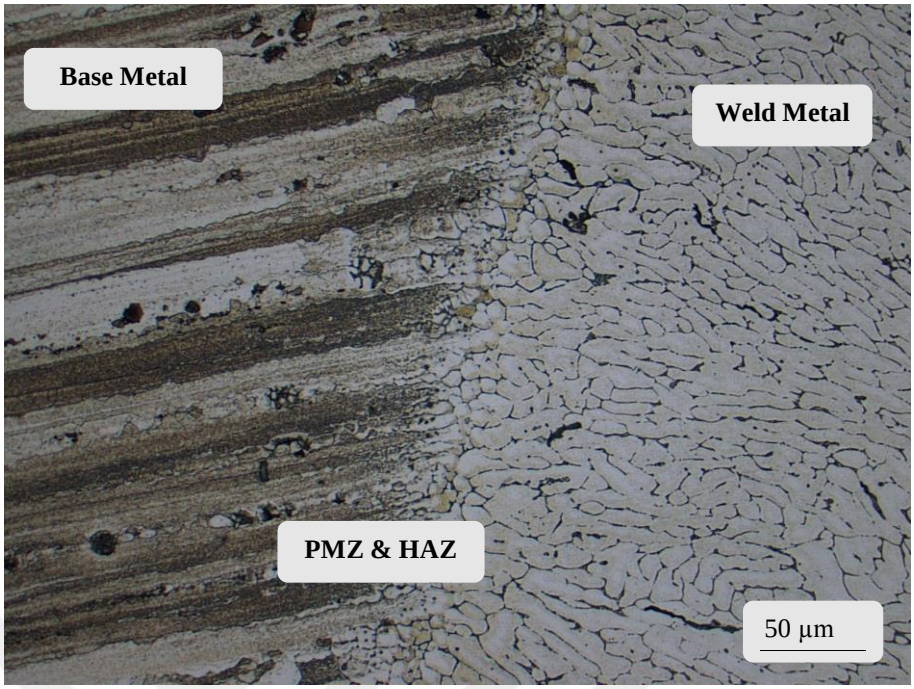

Figure 34 45X.1. The microstructure of weld and parent metal. First set. Keller's reagent. (PMZ: Partially melted zone, HAZ: Heat affected zone)

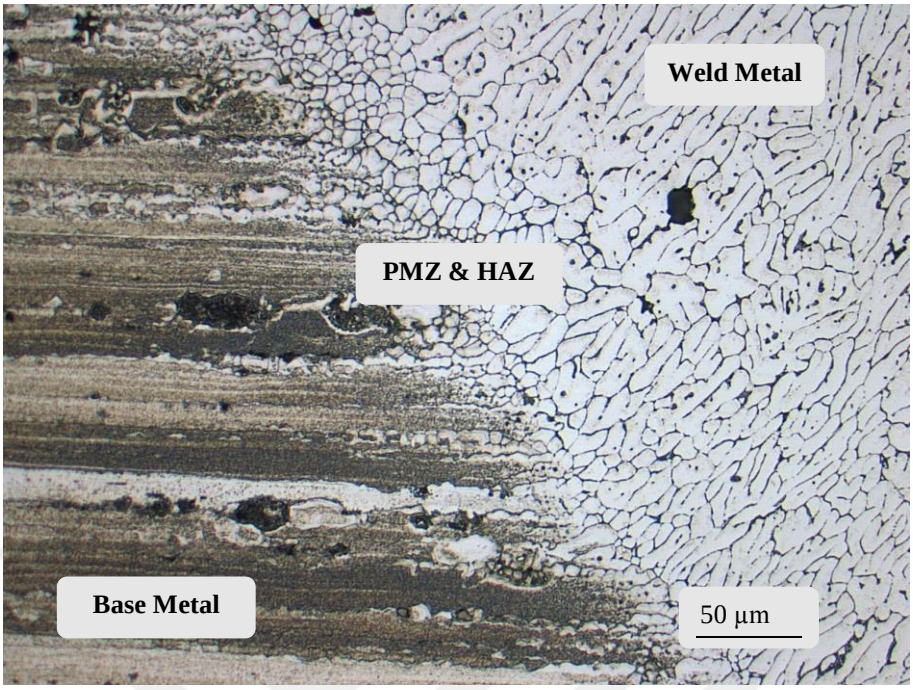

Figure 35 30X.1. The microstructure of weld and parent metal. First set. Keller's reagent. (PMZ: Partially melted zone, HAZ: Heat affected zone)

Figure 36 45X.1. The microstructure of weld metal. Dendritic structure. First set. Keller's reagent.

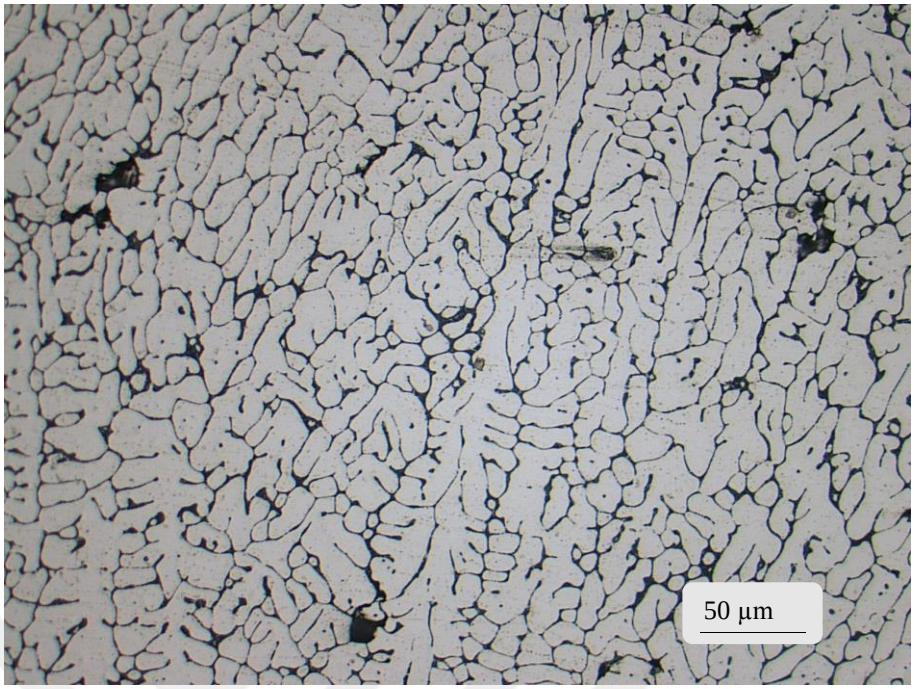

Figure 37 30X.1. The microstructure of weld metal. Dendritic structure. First set. Keller's reagent.

Further microstructural examinations were done for the second set of X formed weld grooved samples that are 45X.2 and 30X.2 (Figure 38 and Figure 39).

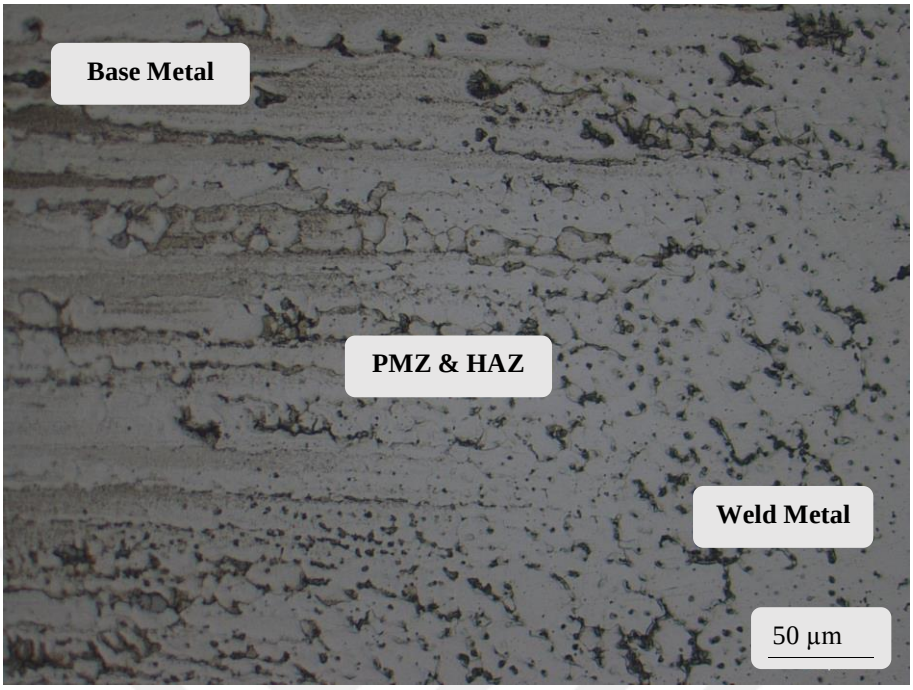

Figure 38 45X.2. The microstructure of weld and parent metal. Second set. Keller's reagent. (PMZ: Partially melted zone, HAZ: Heat affected zone)

The morphology of the weld metal was same for 45X.2 and 30X.2. Weld metal micrograph belong to 30X.2 was given in Figure 40. Similarly, the base metal morphologies were also very similar for the first and second of V formed weld grooved samples which were exhibited in Figure 30 and Figure 31.

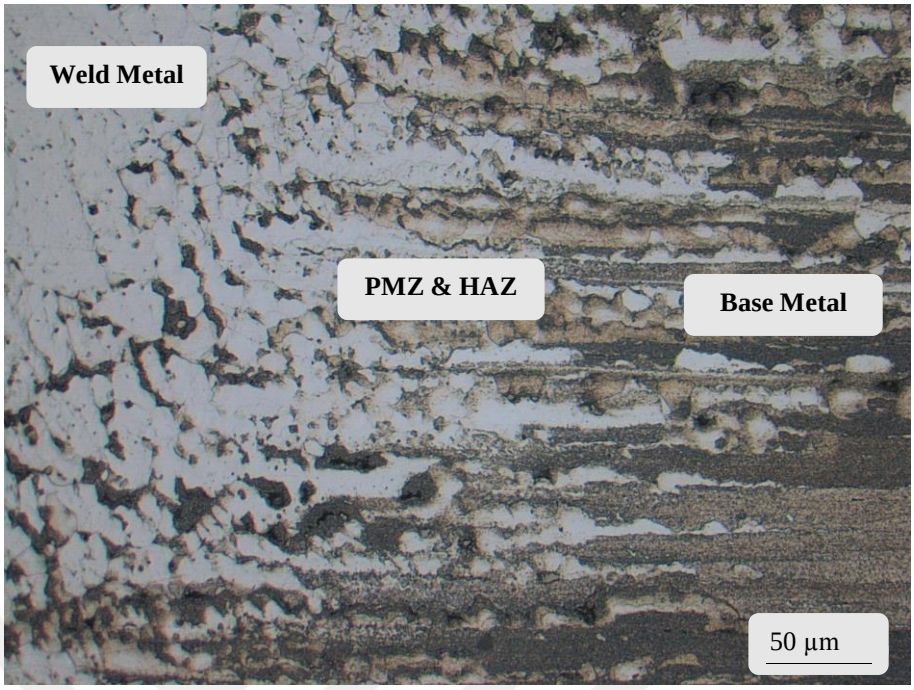

Figure 39 30X.2. The microstructure of weld and base metal. Second set. Keller's reagent. (PMZ: Partially melted zone, HAZ: Heat affected zone)

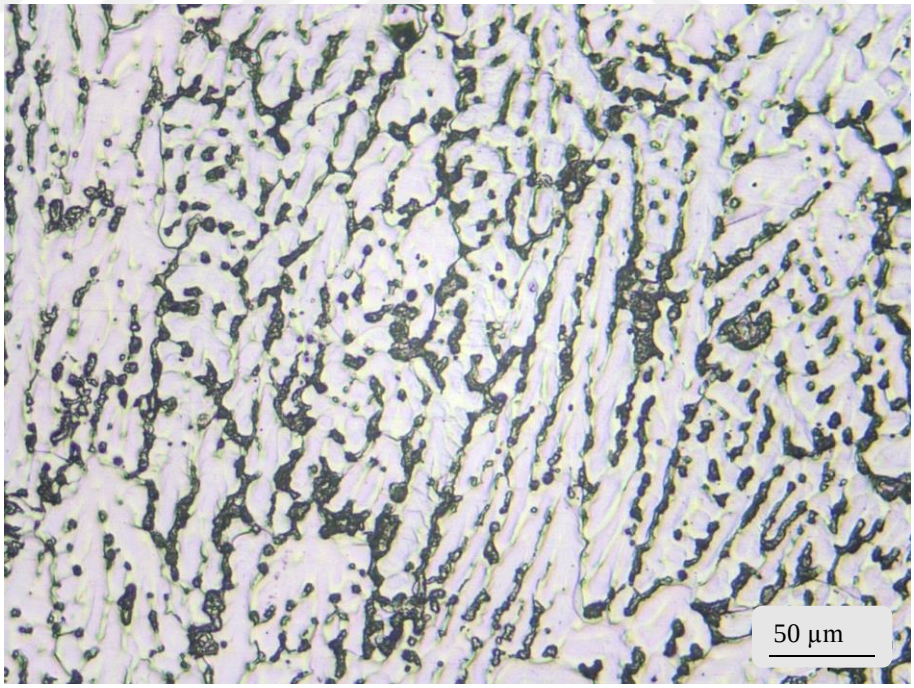

Figure 40 30X.2. The microstructure of weld metal. Second set. Keller's reagent.

5.3. Post Weld Heat Treatments

5.3.1. Hardness Measurements

Welding impairs the mechanical strength of the materials, particularly in the HAZ which is due to high temperatures attained during welding. Therefore several welded samples were heat treated in order to determine the optimum post weld heat treatment procedure. In this section only the microstructural examinations and the hardness of the samples are given. Mechanical test results are given in the following sections.

In the first step of post weld heat treatment (HT.550.4HR), a solutionizing temperature of at 550°C for 4 hours was selected. Then the parts were water quenched and then aged at 190°C for 6 hours. These parameters are proposed by Singh and his colleagues in welded samples of 7039 alloy [34]. The hardness measurements of 45V.1 proved that the post weld heat treatment was not suitable since the hardness values were decreased both in HAZ and base metal. The hardness distribution of samples after HT.550.4HR treatment throughout the section can be seen in Figure 41 and tabulated in Table 22.

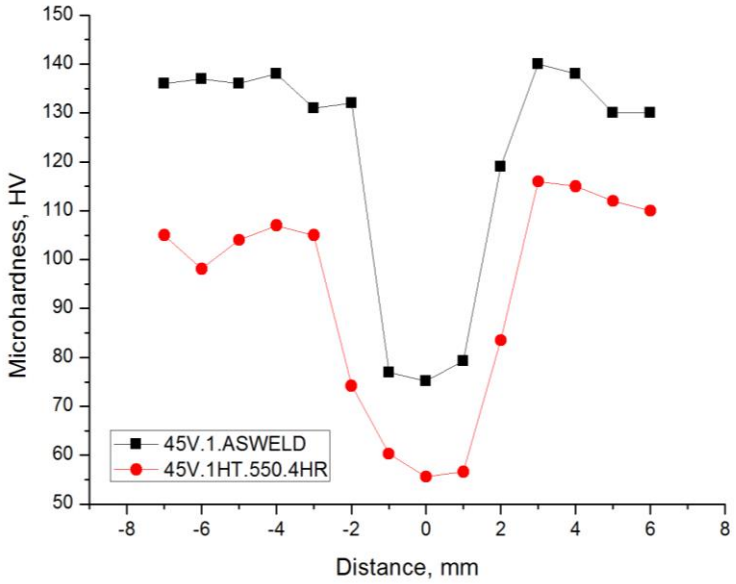

Figure 41 Hardness distribution in 45V.1 after post weld and post weld heat treatment. (HT.550.4HR).

Since HT.550.4HR post-weld heat treatment caused a decrease in all hardness values, no further microstructural examination were conducted. Following this, second step post weld heat treatments were carried out. The hardness measurement results for HT.480.2HR and HT.480.20HR can be seen in Figure 42 and tabulated in Table 23.

Table 22 Hardness values of 45V.1 in as weld and post weld heat treated (HT.550.4HR) condition

Distance, mm	Hardness, As Weld, HV	Hardness, HT.550.4HR, HV
-7	136	105
-6	137	98.1
-5	136	104
-4	138	107
-3	131	105
-2	132	74.2
-1	76.9	60.3
0	75.2	55.6
1	79.3	56.6
2	119	83.5
3	140	116
4	138	115
5	130	112
6	130	110

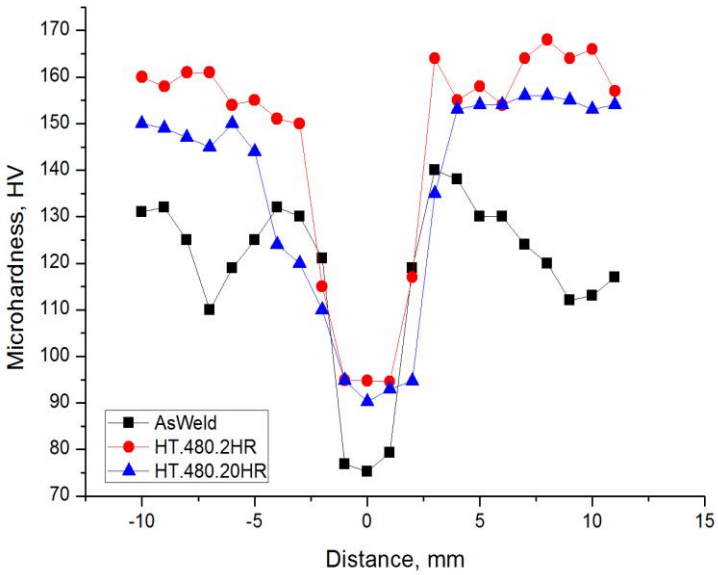

Figure 42 Changes in hardness values after HT.480.2HR and HT.480.20HR

Table 23 Hardness values of 45V.1 in as weld, HT.480.2HR and HT.480.20HR condition

Distance, mm	Hardness, As Weld, HV	Hardness, HT.480.2HR, HV	Hardness, HT.480.20HR, HV
-10	131	160	150
-9	132	158	149
-8	125	161	147
-7	110	161	145
-6	119	154	150
-5	125	155	144
-4	132	151	124
-3	130	150	120
-2	121	115	110
-1	76,9	94,9	94,8
0	75,2	94,8	90,3
1	79,3	94,6	93
2	119	117	94,7
3	140	164	135
4	138	155	153
5	130	158	154
6	130	154	154
7	124	164	156
8	120	168	156
9	112	164	155
10	113	166	153
11	117	157	154

As seen, the HT.480.2HR treatment yields the highest hardness values among other heat treatment procedures. On the other hand, the hardness distribution of HT.480.2HR samples is higher than HT.550.4HR but lower than HT.480.20HR procedures. The hardness distributions in relation to X and V grooves will be discussed in Mechanical Testing section.

5.3.2. Microstructures

An attempt was made to examine the microstructural variations in heat treatment of the samples. The microstructural alterations after HT.550.4HR, HT.480.2HR and HT.480.20HR, are compared in Figure and Figure. The secondary phase precipitates in transition zone (Parent metal – HAZ – Weld deposit) of the specimens are compared in Figure. On the other hand, the microstructural development in weld deposit is exhibited in Figure. As seen, post heat treatment changes the microstructures. Especially in HT.480.2HR, the amount of interdendritic precipitates become lower in amount, which is an indication that some of are taken into solid solution. In the case of HT.480.20HR, although the dendritic structure is destroyed, a second (dark appearing) phase precipitation is evident.

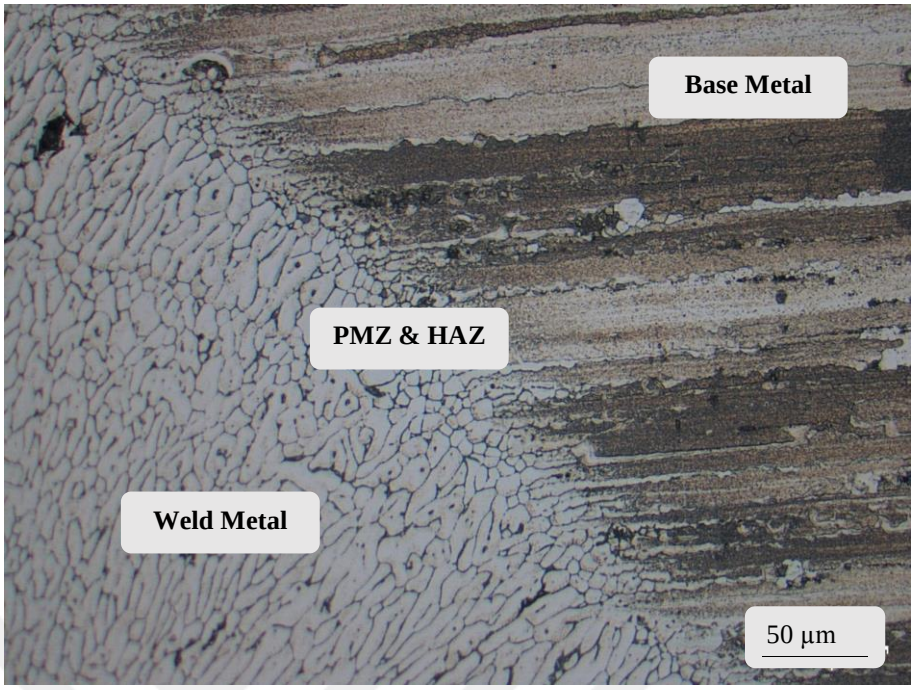

(a)

(b)

Figure 43 Comparison of microstructures (a) As weld (b) HT.480.2HR (c) HT.480.20HR. Keller's reagent.

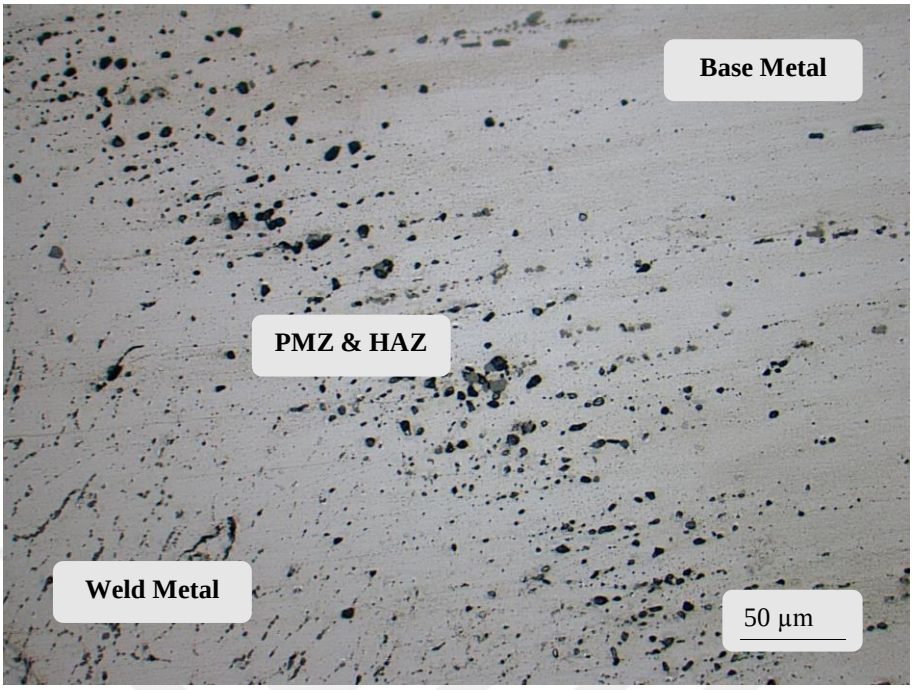

(c)

Figure 43 (cont.) Comparison of microstructures (a) As weld (b) HT.480.2HR (c) HT.480.20HR. Keller's reagent.

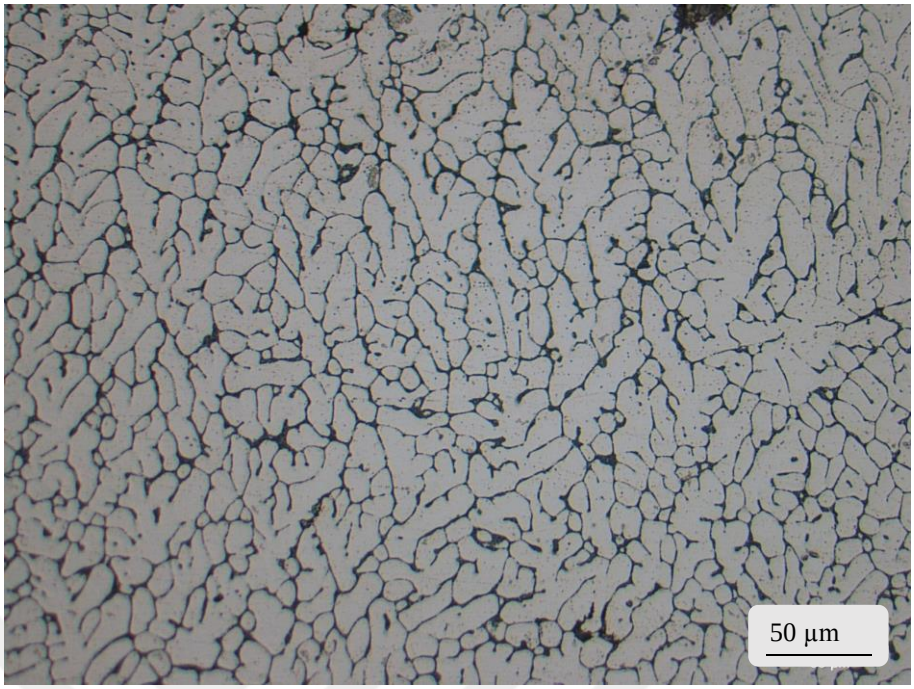

(a)

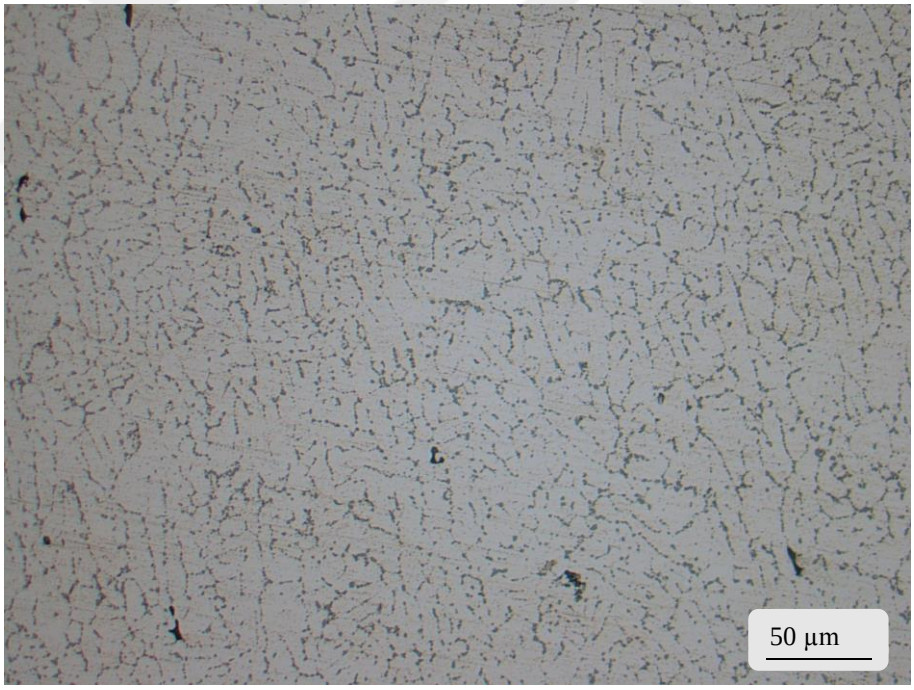

(b)

Figure 44 Comparison of weld metal microstructures (a) As weld (b) HT.480.2HR (c) HT.480.20HR. Keller's reagent.

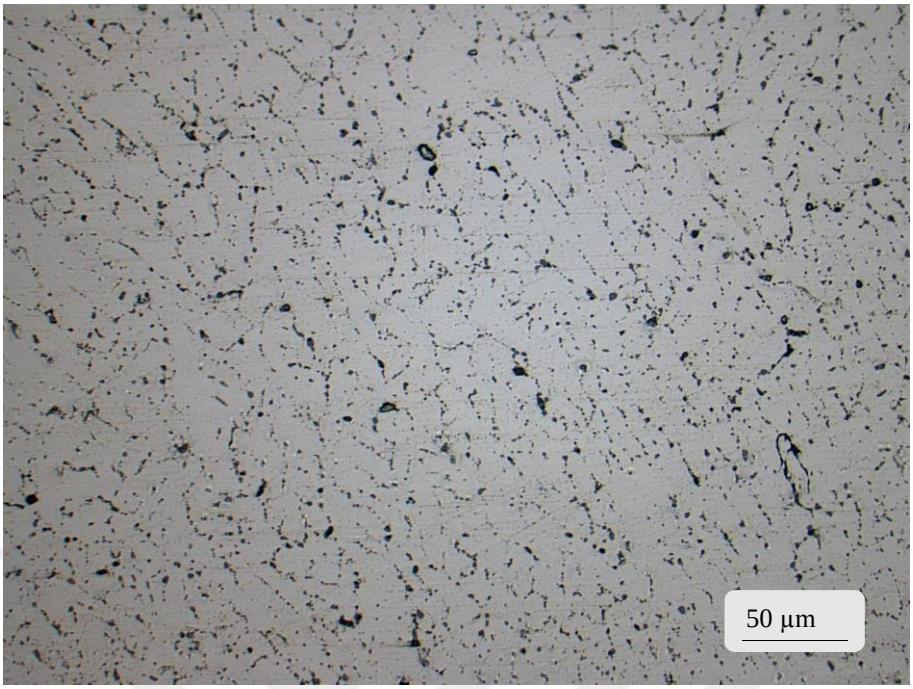

(c)

Figure 44 (cont.) Comparison of weld metal microstructures (a) As weld (b) HT.480.2HR (c) HT.480.20HR. Keller's reagent.

In Figure 45 and Figure 47, EDX analyses were performed in order to characterize the elemental distribution of these precipitates after post weld heat treatments. In Figure 45, the EDX point analysis of the chosen precipitates and in Figure 46 elemental mapping can be seen for HT.480.2HR treatment.

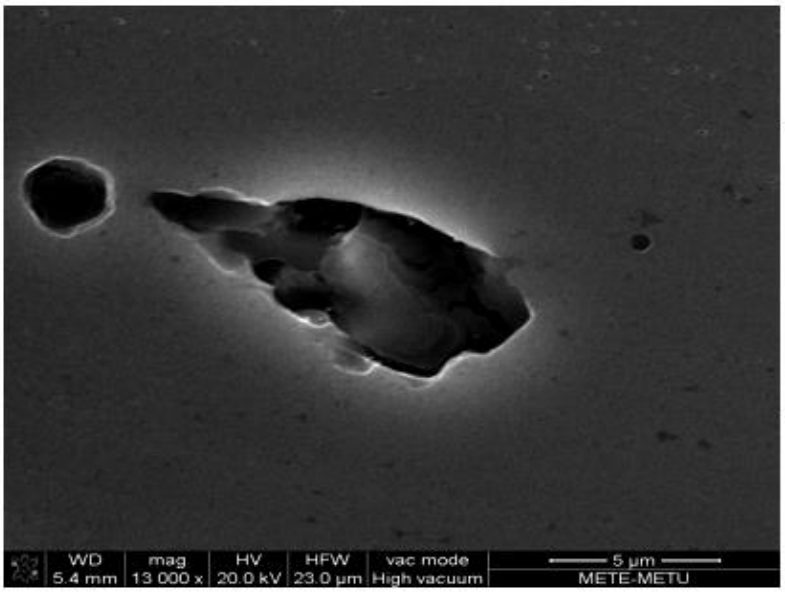

Element	Wt%	At%
Cr	32.51	20.21
Mg	8.88	11.80
Al	34.36	41.17
Si	22.60	26.01
Zn	1.65	0.82

(a)

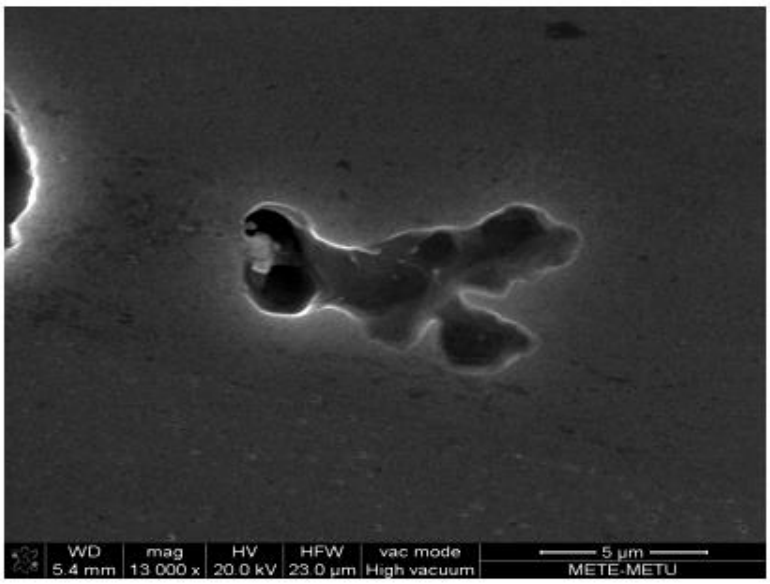

Element	Wt%	At%
Cr	0	0
Mg	2.87	3.26
Al	92.74	94.84
Si	0.09	0.09
Zn	4.30	1.81

(b)

Figure 45 EDX analysis of precipitates in HT.480.2HR heat treated sample, fusion zone and HAZ

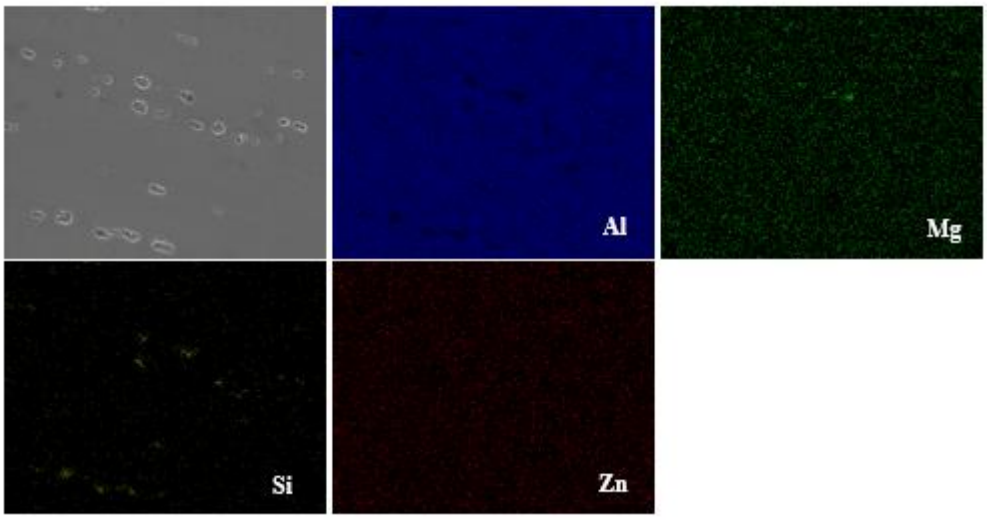

Figure 46 SEM. Elemental mapping of HT.480.2HR

Same analyses were conducted for HT.480.20HR and the elemental distribution can be seen in Figure 47 and Figure 48. In Figure 48, the precipitates located in fusion line and just near the HAZ.

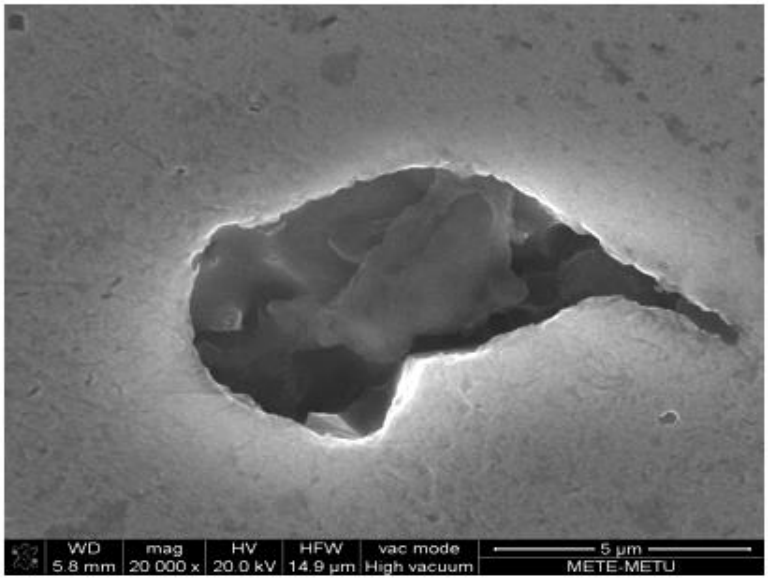

Element	Wt%	At%
Cr	8.84	4.87
Mg	1.32	1.55
Al	83.30	88.41
Si	3.95	4.03
Zn	2.60	1.14

(a)

Figure 47 EDX analysis of precipitates in HT.480.20HR heat treated sample, fusion zone and HAZ

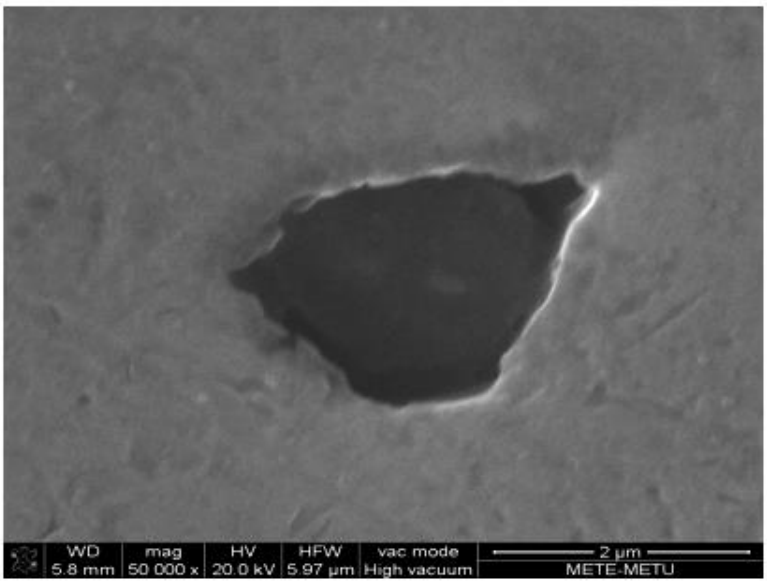

Element	Wt%	At%
Cr	8.60	4.64
Mg	14.90	17.19
Al	59.63	61.99
Si	15.70	15.68
Zn	1.17	0.50

(b)

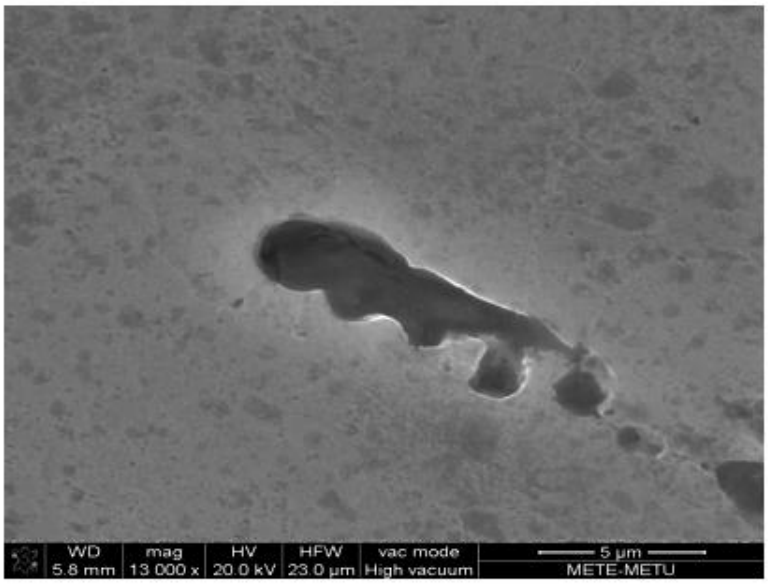

Element	Wt%	At%
Cr	8.51	4.70
Mg	6.91	8.15
Al	73.09	77.74
Si	7.48	7.64
Zn	4.01	1.76

(c)

Figure 47 (cont.) EDX analysis of precipitates in HT.480.20HR heat treated sample, fusion zone and HAZ

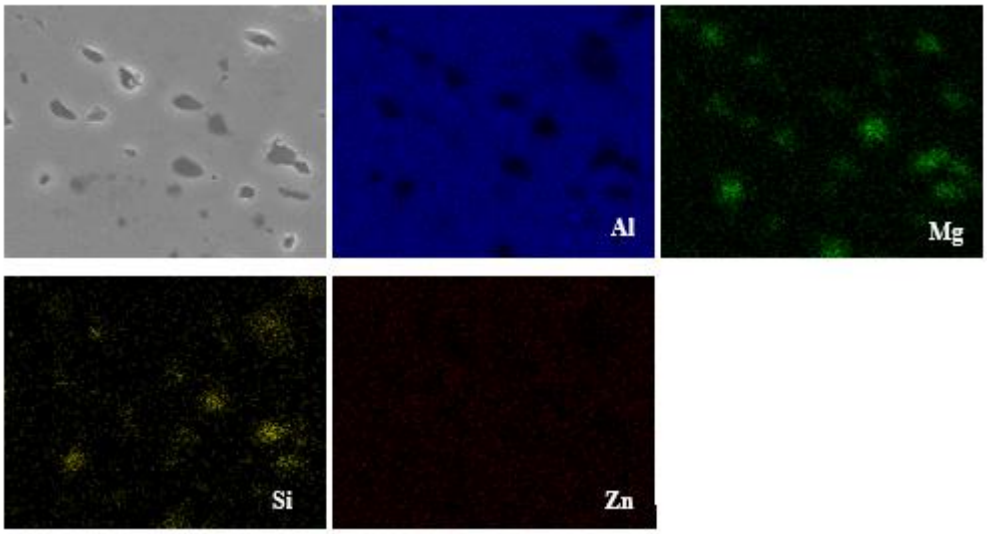

Figure 48 SEM. Elemental mapping of HT.480.20HR

As shown in Figure 43 and Figure 44, HT.480.2HR treatment, which is solutionized at 480°C for 2 hours and water quenched, then aged at 120°C for 20 hours, is more effective in destroying the dendritic structure. As far as the X and V grooved specimens are concerned, HT.480.2HR treatment yields similar results such that in both type of grooves: the amount of precipitates are minimized (Figure 49, Figure 50, Figure 51 and Figure 52) This is most probably due to that the second phase particles are taken into solution.

As far as EDX analyses in Figure 45 and Figure 47 are concerned they are most probably Al-Cr and Mg_2Si based particles. However, as etchant attacks the second phase particles preferentially, it becomes difficult to identify them after etching.

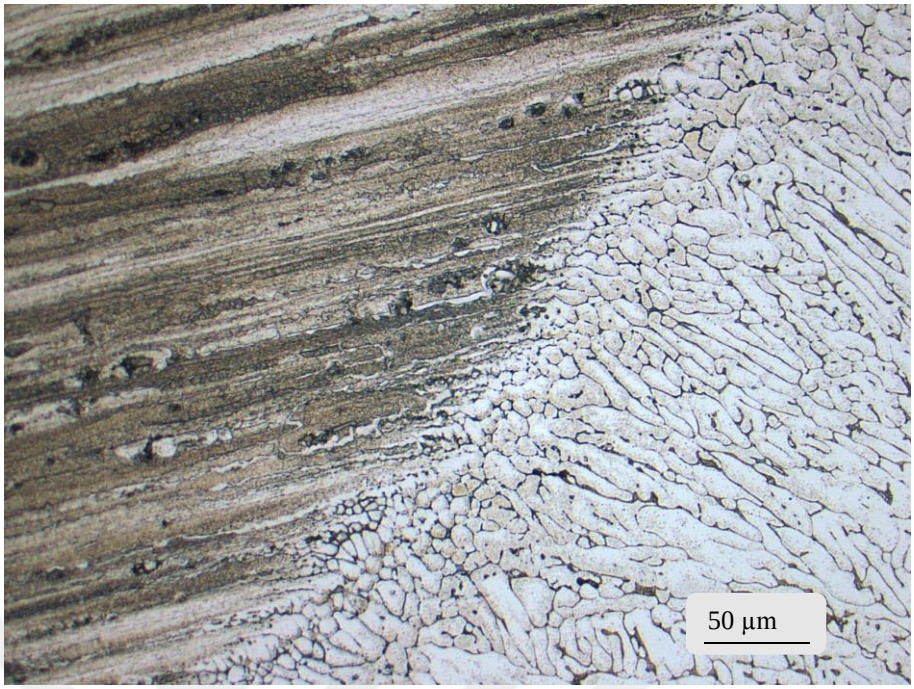

(a)

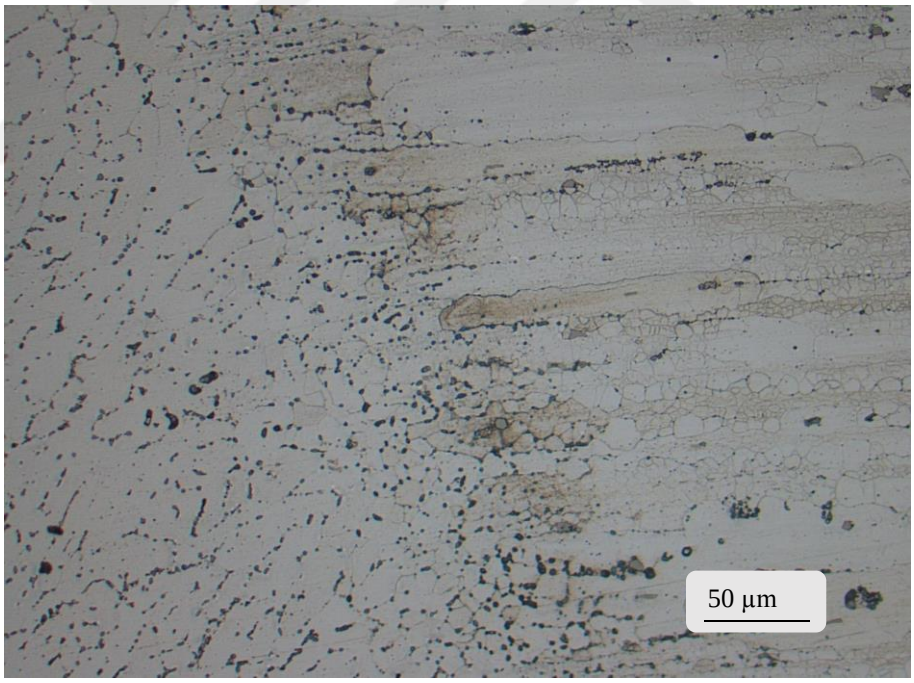

(b)

Figure 49 45V.1. Comparison of microstructures (a) As weld (b) HT.480.2HR. Keller's reagent.

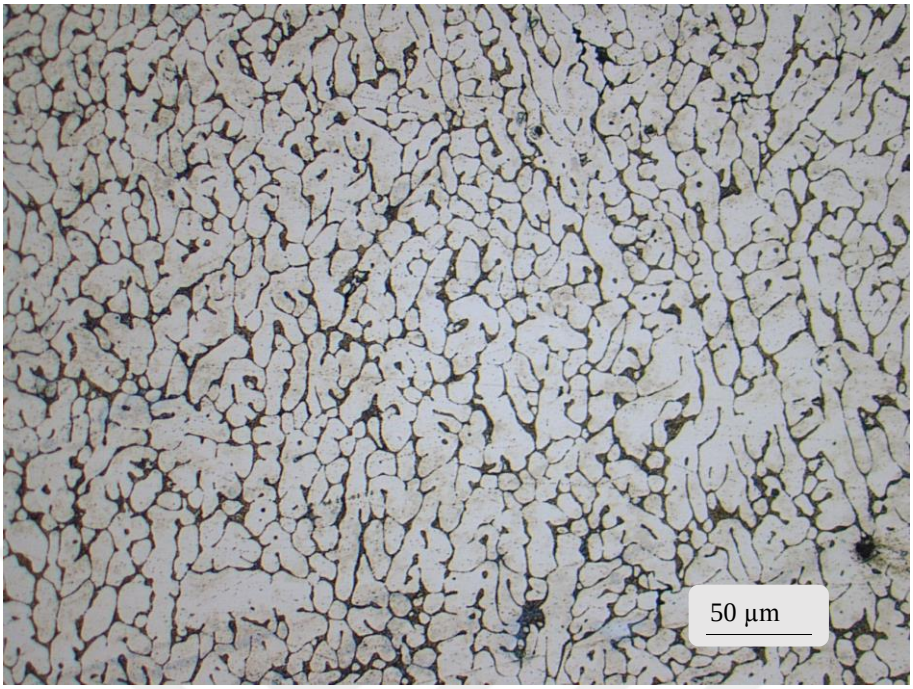

(a)

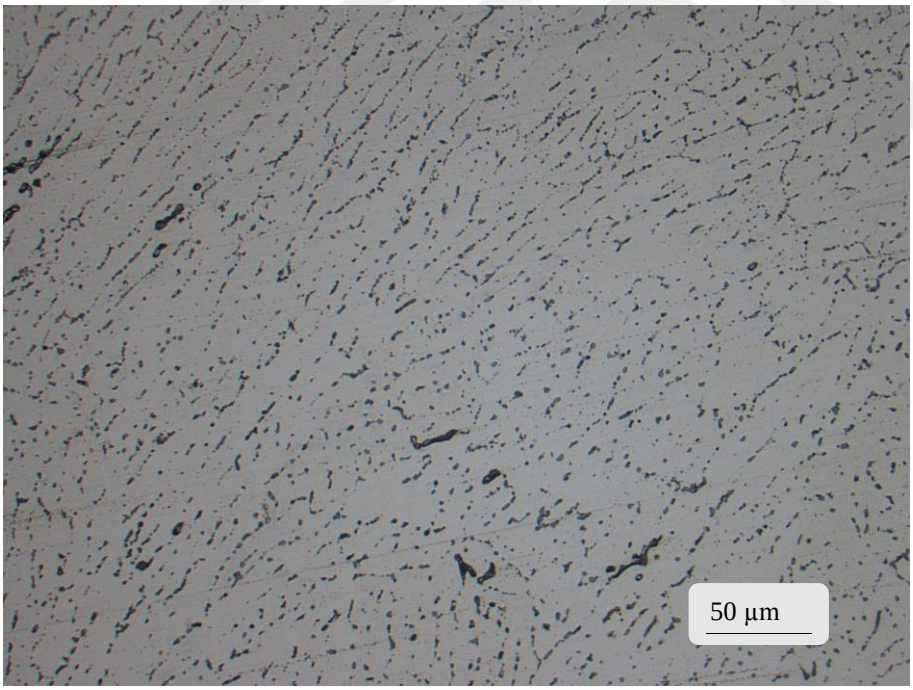

(b)

Figure 50 45V.1. Comparison of weld metal microstructures (a) As weld (b) HT.480.2HR. Keller's reagent.

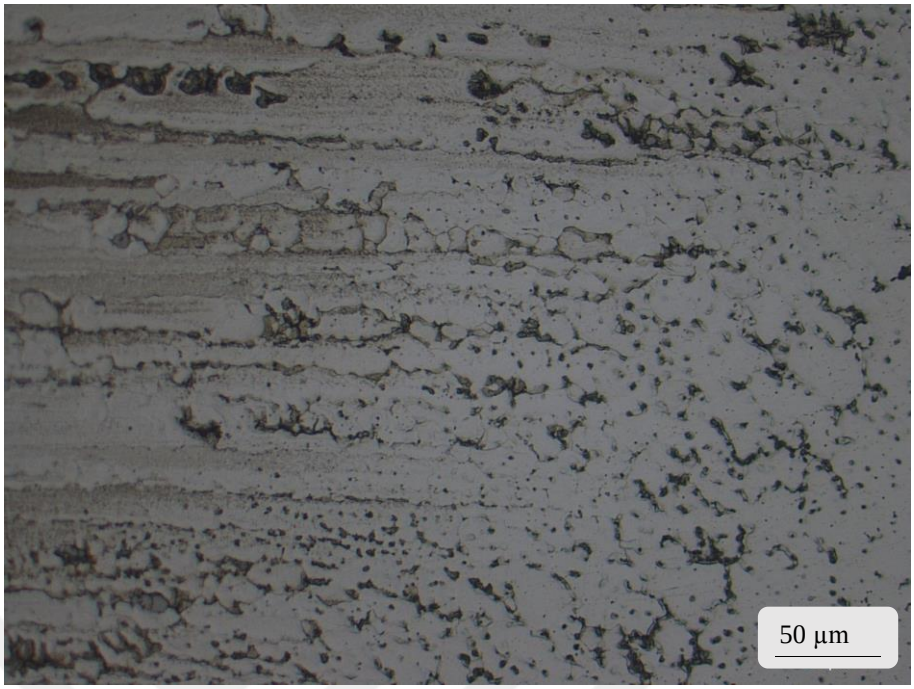

(a)

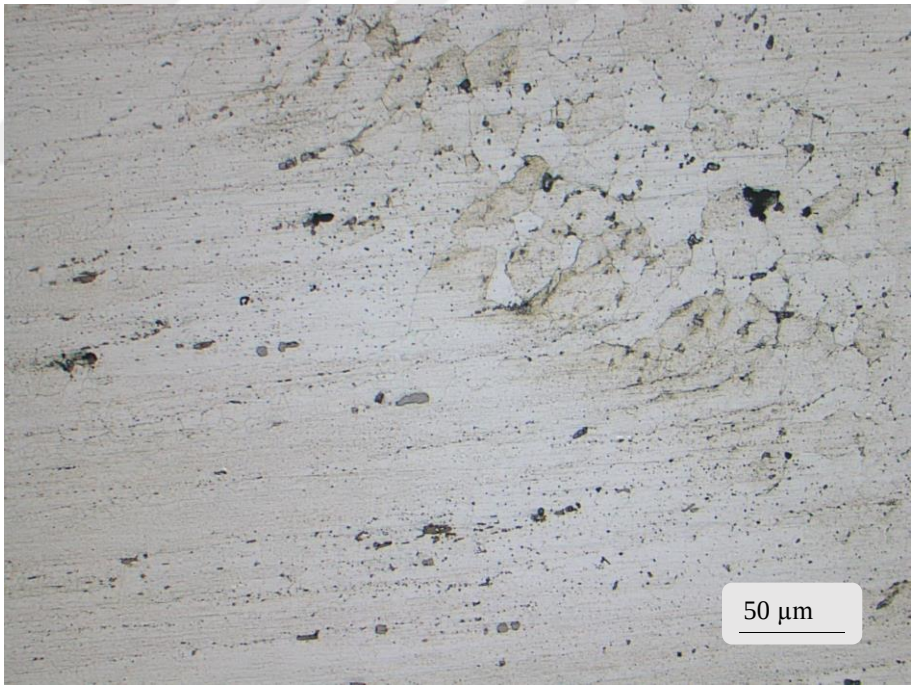

(b)

Figure 51 45X.2. Comparison of microstructures (a) As weld (b) HT.480.2HR. Keller's reagent.

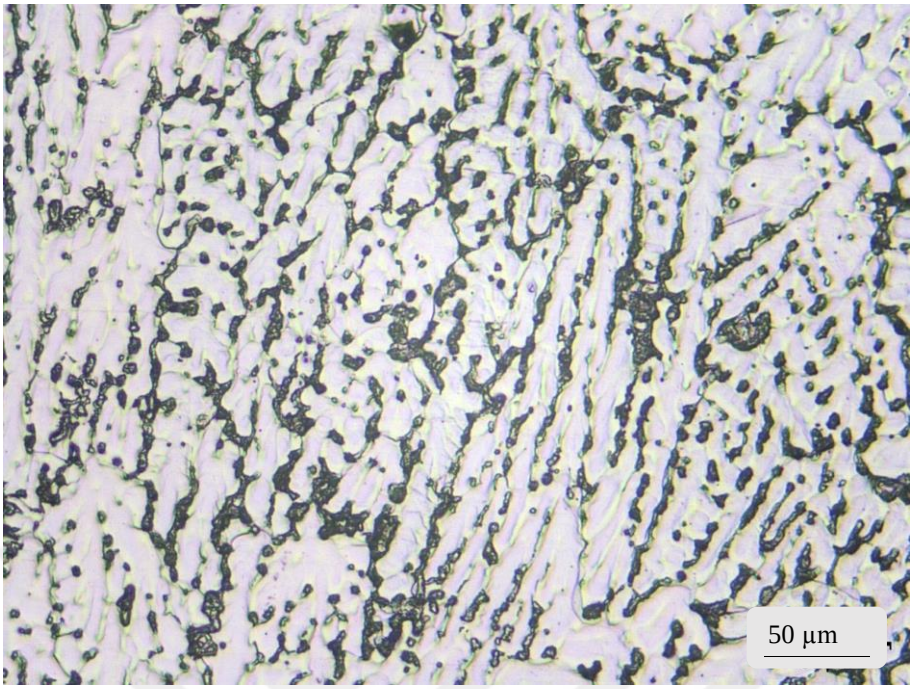

(a)

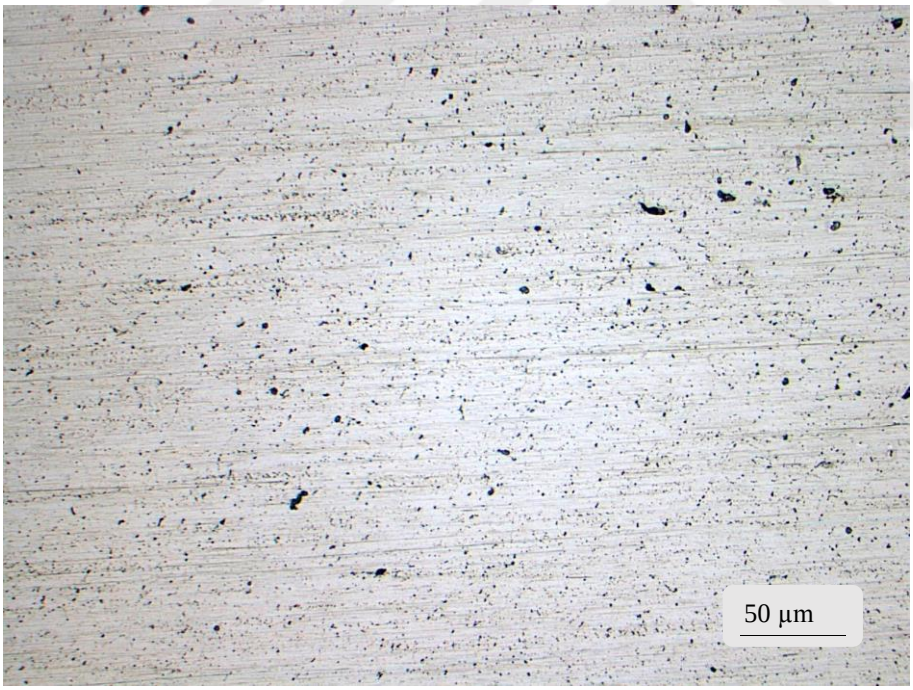

(b)

Figure 52 45X.2. Comparison of weld metal microstructures (a) As weld (b) HT.480.2HR. Keller's reagent.

5.4. Mechanical Tests

Mechanical tests were done in order to prove the effectiveness of the heat treatments. In the scope of this study, a specific increase in HAZ is expected. In this part of the study, the effectiveness of the post weld heat treatments were investigated.

5.4.1. Hardness Measurements

The hardness measurements were only performed on X (45X.2 and 30X.2) and V (45V.1 and 30V.1) grooved samples both in as-welded and welded and post heat treated condition. The hardness distributions can be seen in Figure 53.

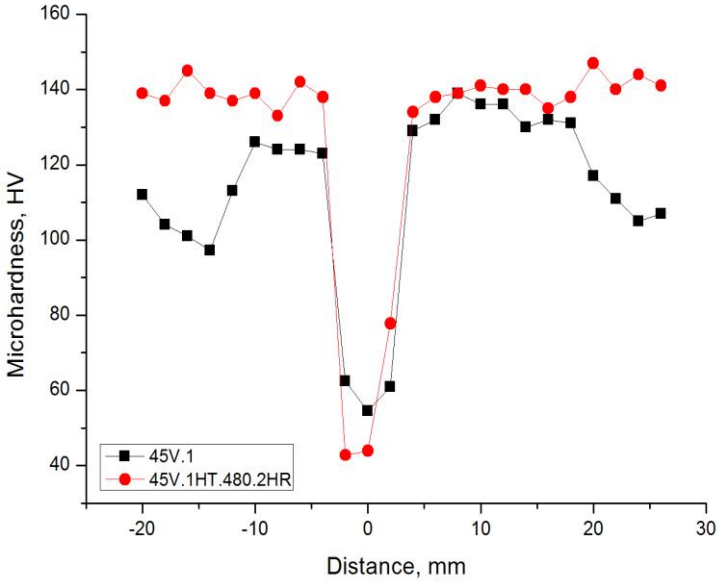

Figure 53 Comparison of the hardness distributions of V-formed and X-formed weld grooved samples in as weld and post weld heat treated (HT.480.2HR) conditions.

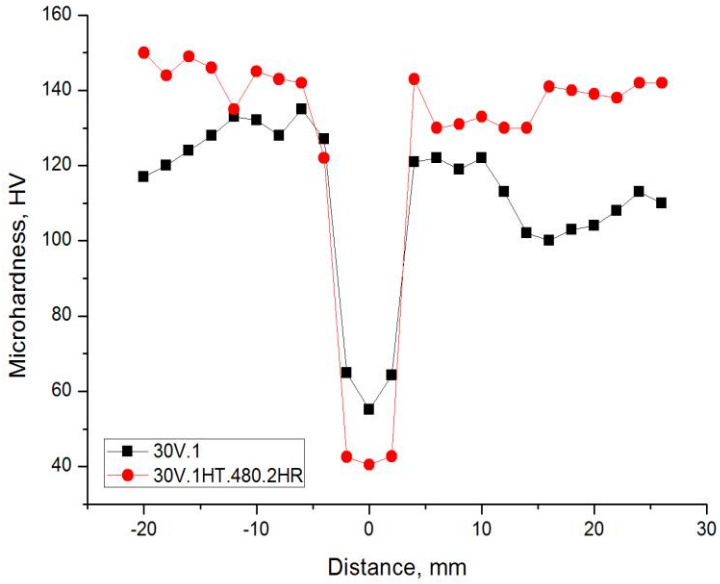

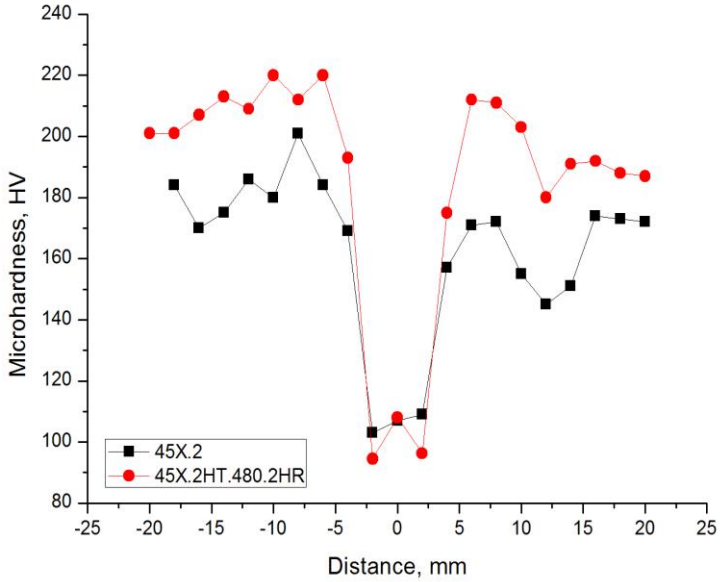

Figure 53 (cont.) Comparison of the hardness distributions of V-formed and X-formed weld grooved samples in as weld and post weld heat treated (HT.480.2HR) conditions.

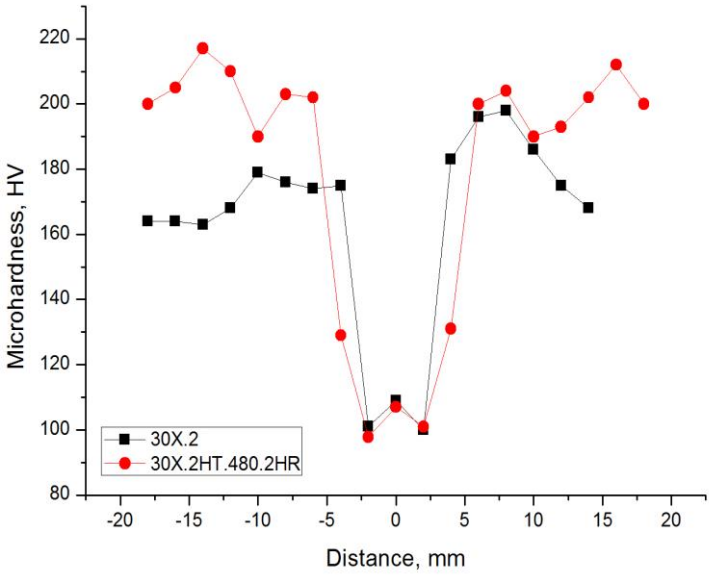

Figure 53 (cont.) Comparison of the hardness distributions of V-formed and X-formed weld grooved samples in as weld and post weld heat treated (HT.480.2HR) conditions.

As can be seen from Figure 53, post weld heat treatment increased the hardness values in HAZ for all grooved samples. Weld deposit was not affected as much as HAZ which was proven with the graphs given.

The increase of hardness in HAZ in HT.480.2HR was higher. The comparison of hardness values of the as welded samples and post weld heat treated samples can also be seen in Figure 54 and Figure 55. As seen, the hardness distribution of X grooved are higher than V grooved specimens.

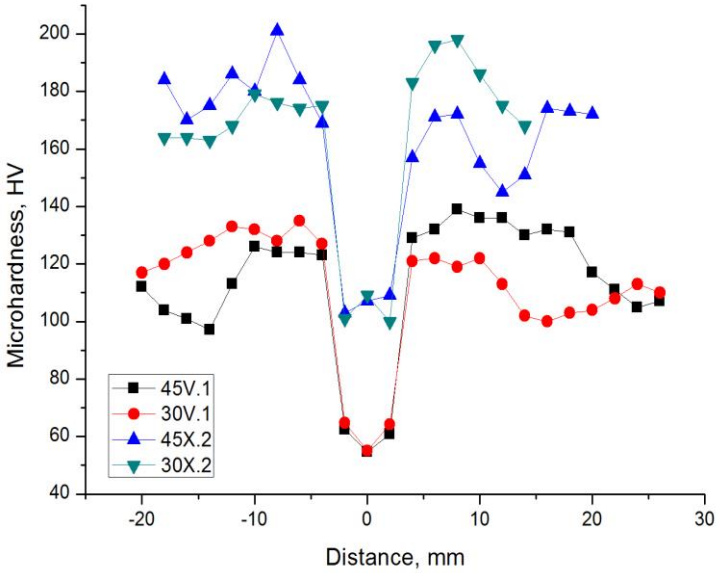

Figure 54 Comparison of the hardness distributions of V-formed and X-formed weld grooved samples in as weld conditions.

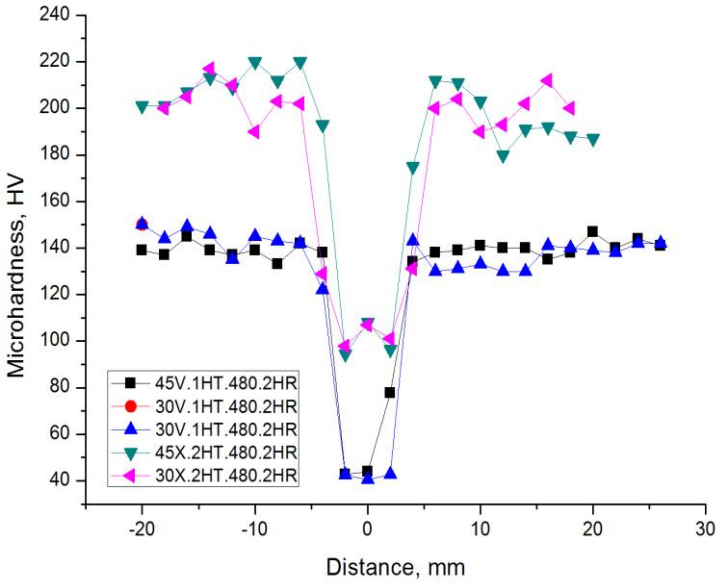

Figure 55 Comparison of the hardness distributions of V-formed and X-formed weld grooved samples in heat treated (HT.480.2HR) conditions.

5.4.2. Tensile Tests

The summary of the mechanical testing results can be seen in Table 24. In macroexaminations, several discontinuities were discovered therefore, these discontinuities would be kept in mind while tensile tests were performing.

Table 24 Mechanical property summary of samples

MATERIALS	YIELD STRENGTH (0.2%OFFSET) (MPA)	ULTIMATE TENSILE STRENGTH (MPA)
Literature 7039-T64	380	450
Experimental Base Metal (7039)-LRD-1	400.9	451.8
Experimental Base Metal (7039)-LRD [2] -1	418.8	470.3
Experimental Base Metal (7039)-TRD [1] -1	396.4	455.0
Experimental Base Metal (7039)-TRD-2	408.0	460.7
45V.1-1-AW [3] (45°V)	177.5	200.1
45V.1-2-AW (45°V)	189.3	219.1
45V.1-3-AW (45°V)	187.3	187.6
45V.1-1-HT [4] (45°V)	106.3	106.7
45V.1-2-HT (45°V)	143.0	156.1
30V.1-1-AW(30°V)	183.6	185.2
30V.1-2-AW(30°V)	195.8	196.4
30V.1-3-AW(30°V)	-	150.0
30V.1-1-HT (30°V)	101.2	111.7
30V.1-2-HT (30°V)	138.0	180.1
45X.2-1-1-HT (45°X)	179.3	284.1
45X.2-1-2-HT (45°X)	177.9	285.9
45X.2-1-3-HT (45°X)	185.6	285.4
45X.2-2-1-AW (45°X)	180.7	282.2
45X.2-2-2-AW (45°X)	182.8	287.4
45X.2-2-3-AW (45°X)	179.8	278.6
30X.2-1-1-AW (30°X)	186.0	256.9
30X.2-1-2-AW (30°X)	191.5	258.5
30X.2-1-3-AW (30°X)	190.4	246.3
30X.2-2-1-HT (30°X)	135.3	208.3
30X.2-2-2-HT (30°X)	164.7	243.8
30X.2-2-3-HT (30°X)	154.7	212.3

[1]: Transverse Rolling Direction [2]: Longitudinal Rolling Direction [3]: As Weld [4]: Heat Treated

In order to compare the results more clearly, the test data is also plotted in bar chart form (Figure 56). Maximum UTS was seen in 45X.2 after welding process. On the contrary, maximum yield strength was seen in 30V.1 after welding.

By applying post weld heat treatment, the highest UTS and yield strength values were obtained in 45X.2.

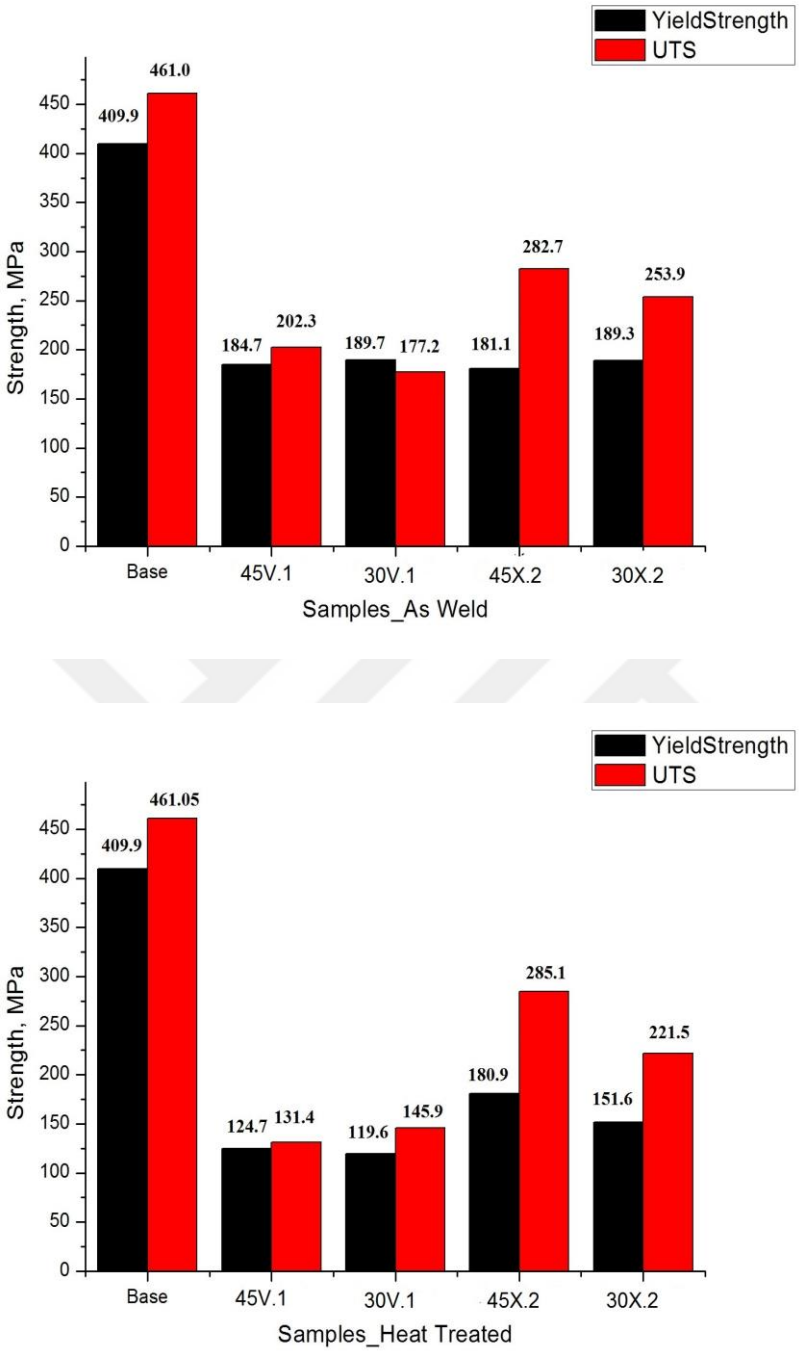

Figure 56 The comparison of average yield strength and UTS of samples in as weld and heat treated conditions

5.5. Results of Software Calculations

As mentioned previously, the weight fraction of the phases and other calculations can be seen in figures below by using JMat Pro and ThermoCalc softwares.

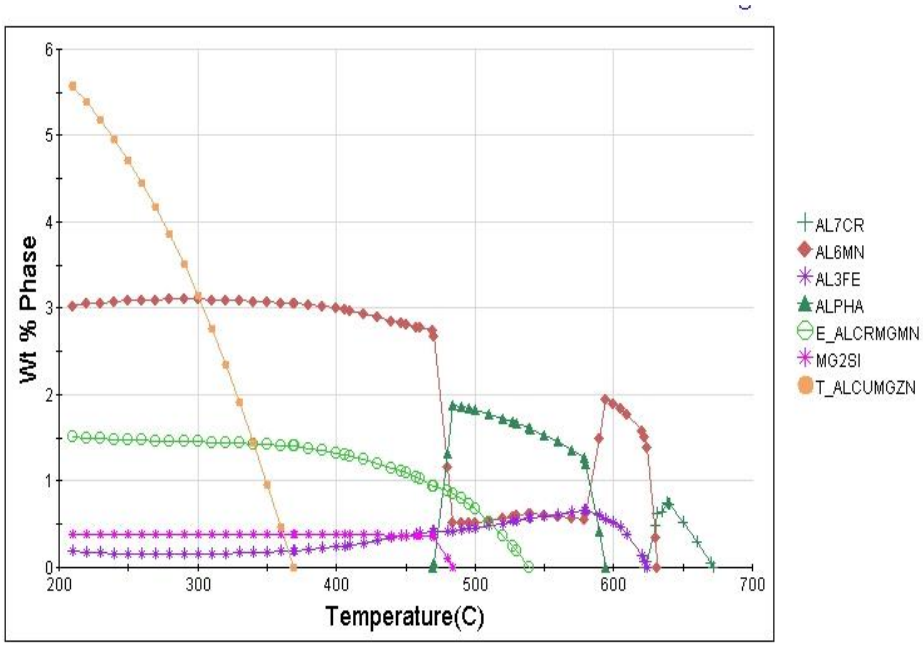

Figure 57 Weight fraction of the phases for 7039 aluminum alloy with respect to temperature. JMat Pro.

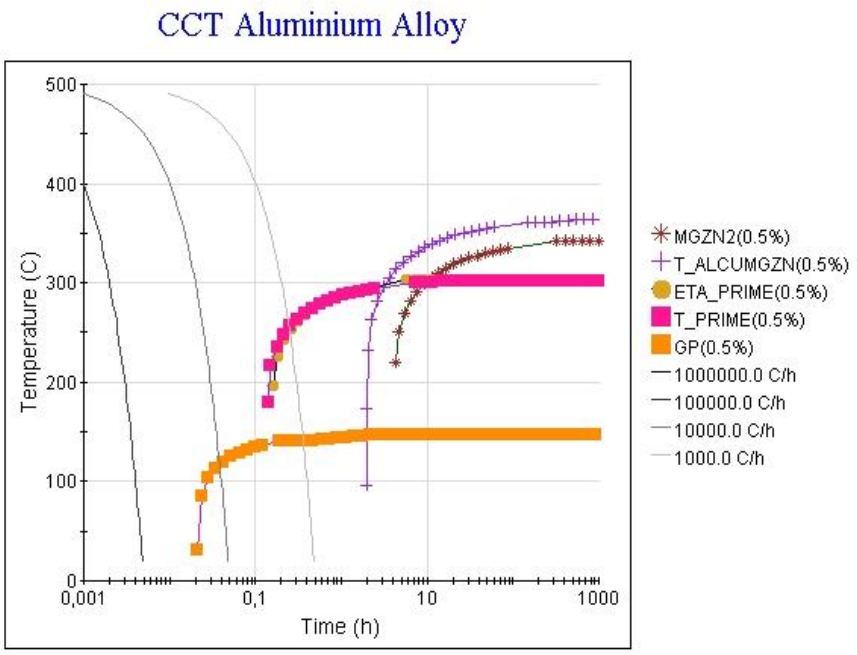

Figure 58 CCT diagram for 7039 aluminum alloy. JMat Pro.

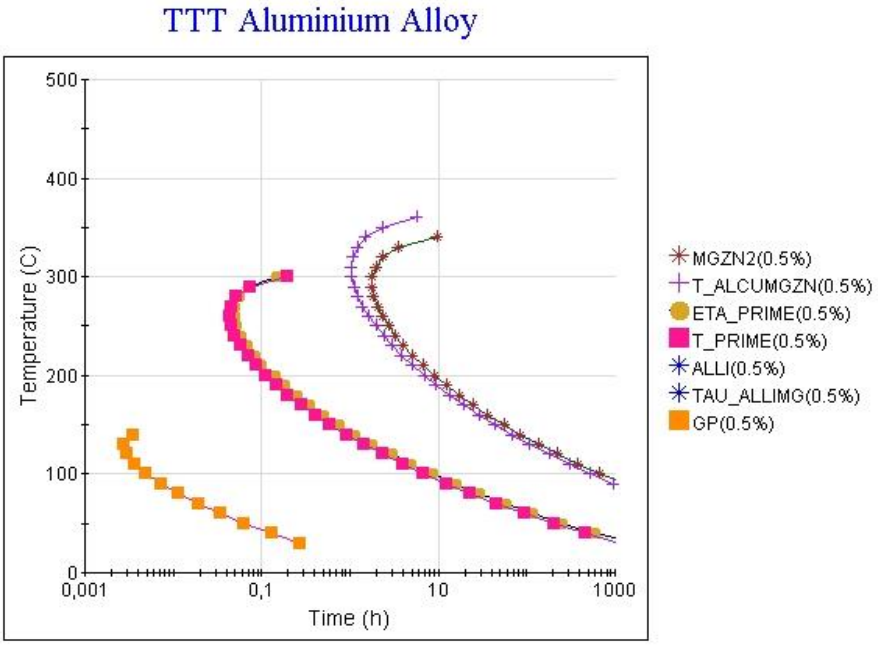

Figure 59 TTT diagram for 7039 aluminum alloy. JMat Pro.

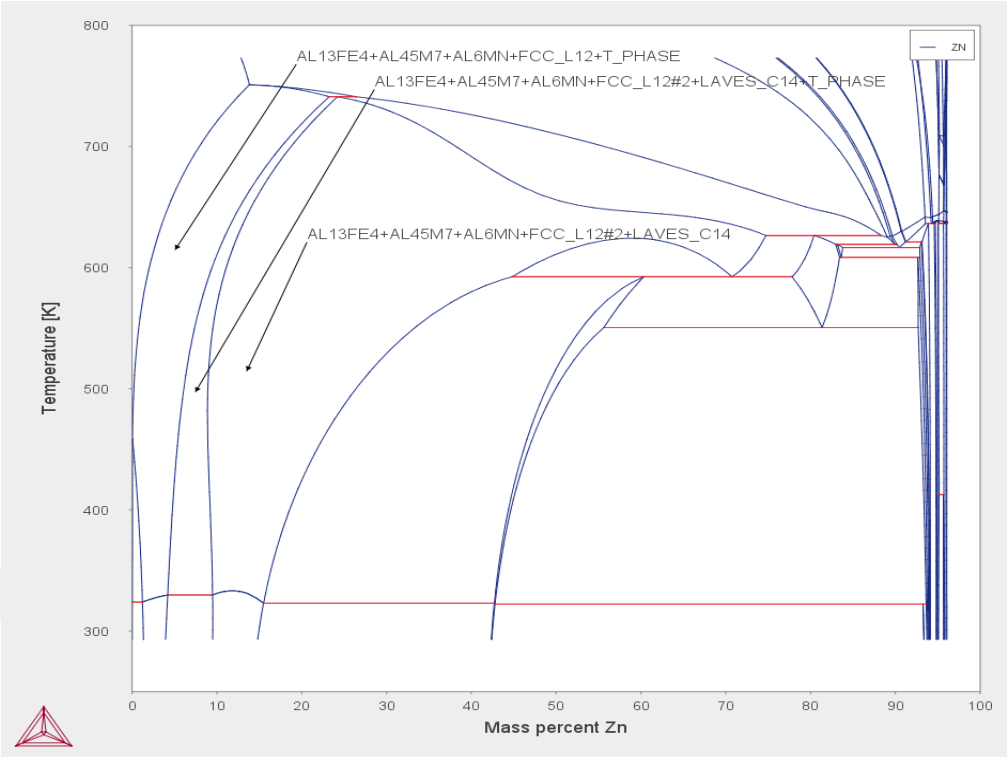

Figure 60 Phase diagram for Al-Zn aluminum alloy. ThermoCalc.

5.6. Fracture Surface Morphologies

Fracture surfaces of the tensile test specimens would give the idea about the fracture mechanism and the region where the fracture occurred. Therefore, after tensile tests, the fractures surfaces of welded samples were examined and given in figures Figure 61, Figure 62, Figure 63 and Figure 64. It is found that the fracture surface morphologies had a similar appearance in all samples. The fracture type was in ductile morphology and fracture occurred throughout the fusion line in V and X grooves. Dimples could be seen throughout the fracture surface. Gas porosities were also seen in all samples.

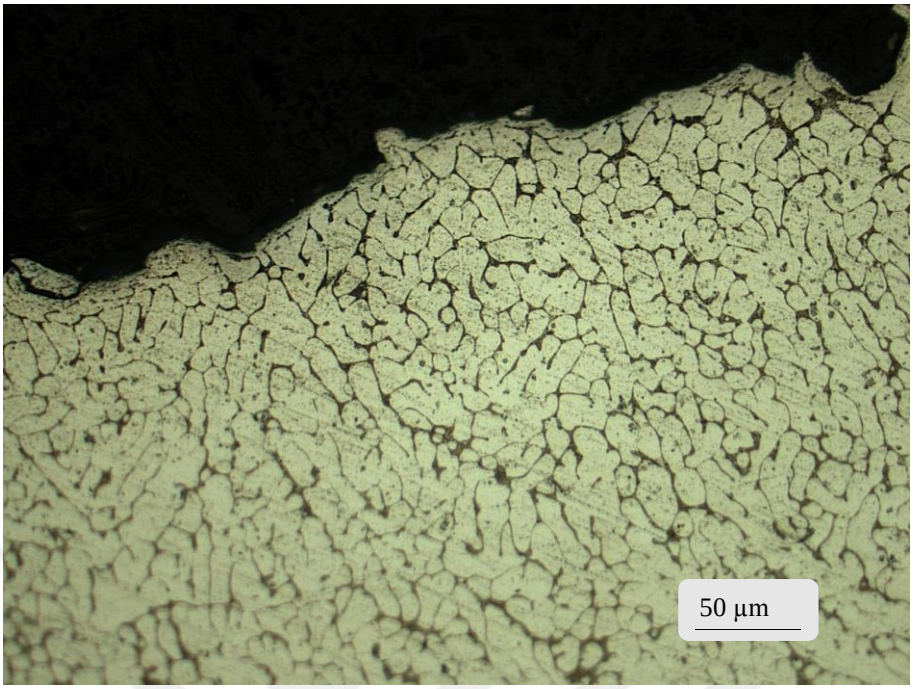

Figure 61 45V.1. The section for weld metal from fracture surface. Keller's reagent.

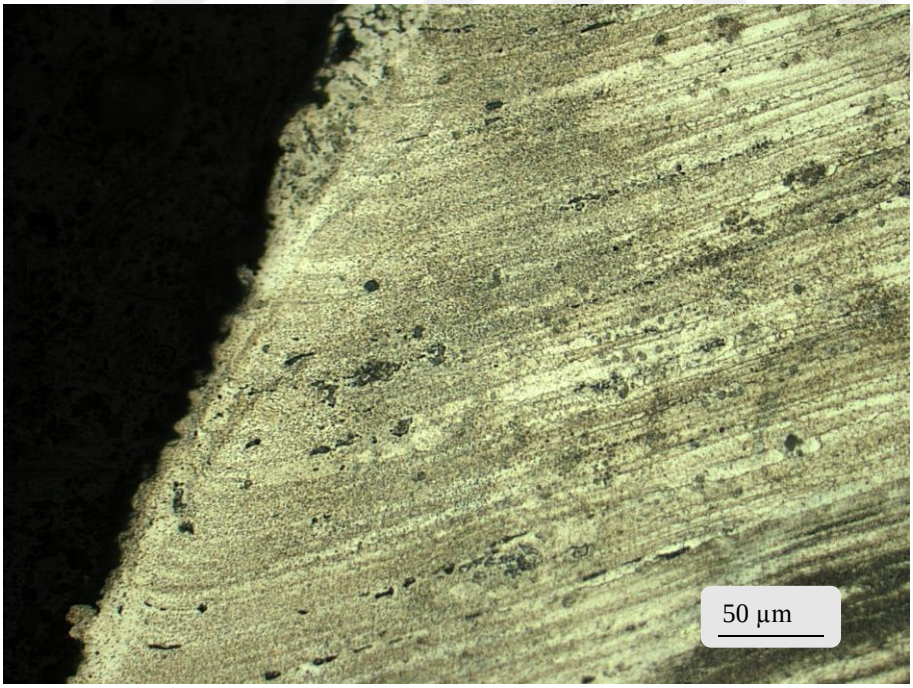

Figure 62 45V.1. The section from the fracture surface (edge-fusion line). Keller's reagent.

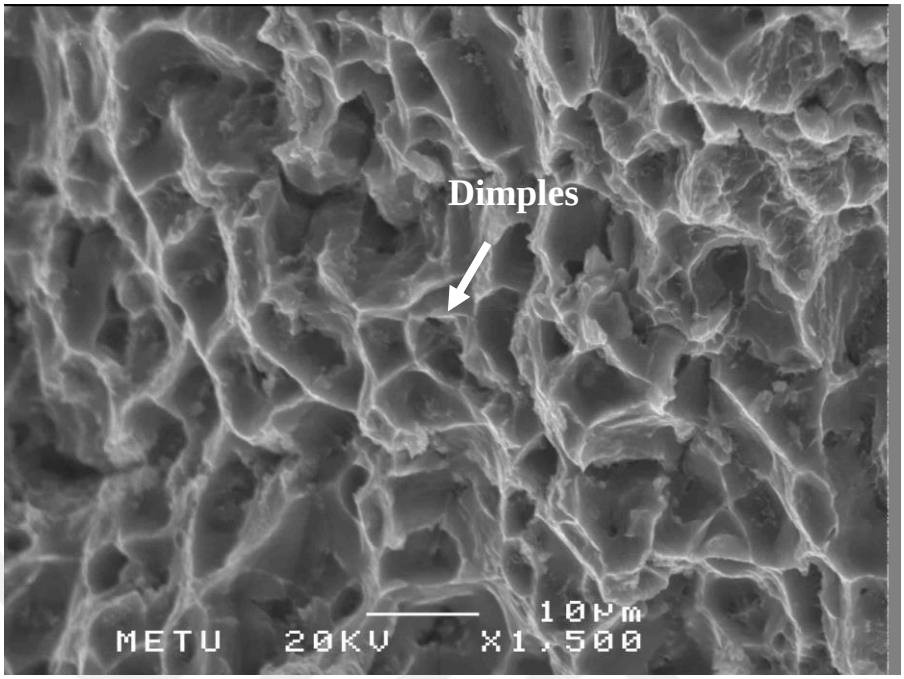

Figure 63 45V.1. The image of fracture surface under SEM.

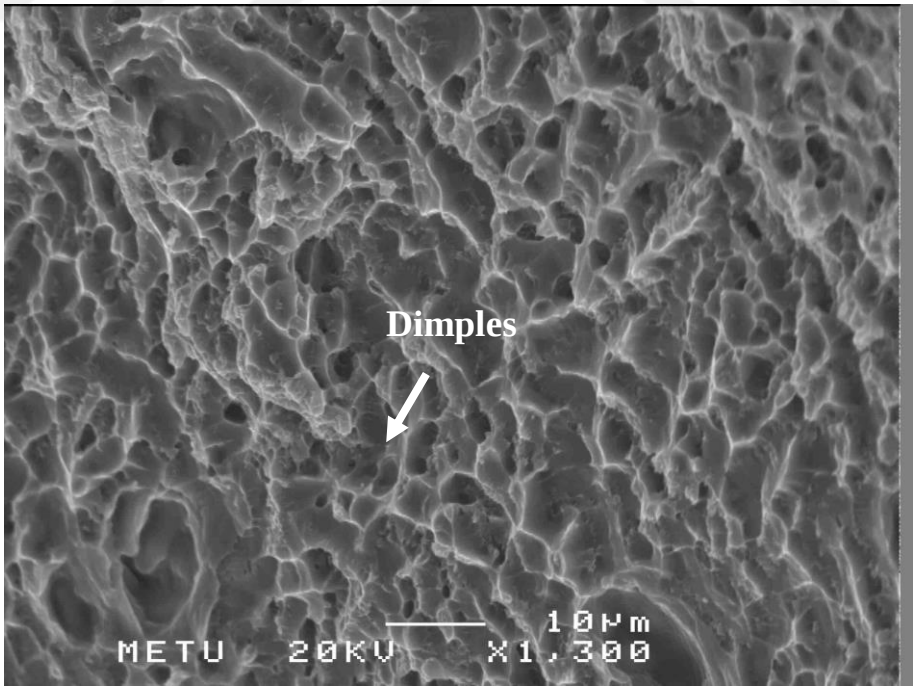

Figure 64 30V.1. The image of fracture surface under SEM.

CHAPTER 6

DISCUSSION

Discussion part aims to investigate issues, such as the relations between the heat input (line energy) that changes with the weld groove forms and the mechanical properties, the recovery of the mechanical properties, particularly hardness and tensile strength, by performing post weld heat treatments for each weld groove. Further, the microstructure alterations are discussed after welding and post weld heat treatments for each different weld grooves.

6.1.Heat Input Examinations for Different Weld Grooves in As Weld Condition

Line energy, i.e. heat input per unit length, or heat input according to ASME IX, is a parameter that can be modified by changing the weld parameters in welding process. According to Table 13, in order to have good welding quality, the parameters must be calculated before starting the welding process. After deciding the suitable parameters and trials performed the welding process must be done. The heat input and other measurements were calculated according to EN 1011-1:1998 and it is found that, 45V.1 (45°V Groove) has the highest heat input as a result of wider butt welding area. Also number of passes play an important role for heat input since, 45V.1 has more number of passes among of all. Comparing the X welds between

each other, for the first set, 45X.1 (45°X Groove) has higher heat input than 30X.1 (30°X Groove). The main reason for this comes from the differences in number of passes and the area subjected to heat is higher which is 90° for 45X.1 and 60° for 30X.1. However heat input remains same for the second set of X welds since the number of passes was same. For further understanding, comparing the first set and second set of X welds with each other, when voltage is kept constant, and current is increased, the heat input will increase as expected. This can be seen from the results of 30X.1 and 30X.2, which had same number of passes but different heat inputs. When current, I, was increased, arc energy and heat input was increased and as can be seen from Table 13, 30X.2, was subjected to a heat input more than 30X.1.

6.2.Microstructure Examinations for Different Weld Grooves in As Weld Condition Subjected to Different Heat Input

Heat input coming from the welding process results with changes in microstructure as a result of solidification mode and microstructure size. As mentioned previously, solidification mode is mainly affected by heat input, welding speed and therefore, an increase in heat input by keeping welding speed constant results with decrease in temperature gradient, thus the microstructure transforms from cellular to dendritic structure as can be seen from Figure 5 theoretically. Moreover, increasing heat input results in a coarser microstructure. In heat treatable welds, generally four microstructural zones can be seen, and by changing the weld parameters the width of these zones may change. In weld deposit, the structure has a mixture of melted base plate and the filler metal in as cast dendritic cell structure. Since intergranular melting and subsequent cooling exists in FZ (fusion zone) between liquidus and solidus, as cast columnar/dendritic grain structure can be seen. In HAZ, since the temperature is not enough to reach liquidus the morphology is same as with the base metal but varies from fine precipitates associated with grain boundaries to coarse precipitates dispersed throughout the grain matrix.

In the light of this knowledge, samples with different groove shapes were compared, for V weld grooved 45V.1 and 30V.1. The specimen 45V.1 has higher heat input than 30V.1 as mentioned. This argument was supported by the microstructure of 45V.1. The grains in fusion line (mushy zone) were coarser in 45V.1 with respect to 30V.1. (Figure 26 and Figure 27) The same situation can also be seen in the weld deposits of the samples. 30V.1 had a dendritic structure, however, as a result of higher heat input, the structure in 45V.1 seemed to be more like cellular, but still in some regions dendritic structure could be seen. Further, discussing the X weld grooved samples, in the first set, 45X.1 has higher heat input than 30X.1. Considering all micrographs of this set, grain growth in some regions were seen in 45X.1 compared with 30X.1 (Figure 34 and Figure 35). The cellular structure in 45X.1 was also more evident than 30X.1. For the second set of X weld grooved samples, same heat input were calculated, and when the micrographs were examined, almost same microstructure were seen in both fusion zones and weld deposits which were as cast grains.

Weld pool shape is another consideration which is also affected by welding parameters. Low welding speeds and low heat input results more elliptical weld pool whereas high welding speeds and high heat input results tear dropped shape weld pool. The macrographs gave the idea about the weld pool shape depending on the weld parameters. Since the weld speed was constant for V grooves and the first set of X grooves, higher heat inputs results with more tear dropped weld pool shapes. For instance, 45V.1 had sharper V shape weld pool than 30V.1 which had smooth and elliptical in horizontal shaped weld pool. Similarly, for the second set of X weld grooves, they had lower welding speeds resulted with softer elliptical weld pool shapes compared with the first set of X grooves which had higher welding speed.

6.3. Compositional Changes in As Weld Samples in Weld Deposits

Since 7039 is susceptible to hot cracking during welding, filler materials are commonly used to increase the strength of the weld metal. Together with increasing the strength of the weld, it is known that alloying elements have considerable effects on the properties of the alloys. Since welding is a process that melts the metal, therefore elemental changes can be seen and additionally, using filler material during the process, there may be compositional mixture of the melted filler material with the parent metal. These changes may also have an effect on the mechanical properties together with microstructure.

Especially, Mg and Mn play important roles for the solidification range of 7039 alloy. For example, Mg increases the solidification range, therefore, mushy zone becomes larger. On the other hand, Mn controls the recrystallized grain size and decreases size of the mushy zone.

6.4.Effect of Different Weld Grooves on Mechanical Properties in As Weld Condition

Arc welding, as mentioned previously reduces the mechanical strength of the materials. Therefore, the regions subjected to heat coming from the welding process has a considerable effect on mechanical properties. As can be seen from Table 24, the yield strength and UTS of the welded plate is nearly half of the one-piece, raw plate. Welding reduced the UTS value to nearly half. The lowest yield and tensile strength was seen in 30V.1 although it was subjected less heat input than 45V.1. This may stem from the internal weld defects seen in 30V.1. In Figure 24, several gas porosity can be seen in 30V.1 which may affect the tensile strength negatively together with welding process itself. In X grooves, for the first set, the yield strength and UTS data’s are not trustable, since there were welding defects which most

probably affect the results adversely. For this reason these results were not taken into consideration. The weld quality was much better in the second X groove set, as can be seen in Table 24. The specimen 30X.2 showed lower UTS but higher yield strength although the heat input were same for this group. Lower UTS values of the 30X.2 specimen can be attributed to lack of fusion problems which were discovered on the fracture surface of all test samples.

6.5. Post Weld Heat Treatment and Its Effect on the Microstructure and Mechanical Properties

Three different post weld heat treatments were applied to recover the mechanical strength and hardness in HAZ. These heat treatments changed the microstructures after heat treatment as expected. The main idea was to achieve a heat treatment process so that, the alloy precipitates in weld and HAZ zone of 7039 are taken into solution and by aging subsequently could restore the mechanical properties.

For HT.550.4HR, the solutionizing and aging temperatures were higher, so that the re-solution of the precipitates were rapid compared to the others. According to the study of Kelsey [30] and Sara et. al. [37], in welding the temperatures reach up to 315.6°C or above and results in partial or complete solution of fine precipitates. The evenly distributed precipitates were redissolved therefore impaired the strength. Further, 7039 begins to overage at temperatures above 160°C and as a result, precipitates agglomerates and coarsens. This coarsening causes a reduction in mechanical properties coming from the loss of the coherency between the precipitate and its matrix. In this study, a dramatic decrease in hardness observed in HT.550.4HR, compared to HT.480.2HR and HT.480.2HR could be due to this reason.

Further, the main difference between HT.480.2HR and HT.480.20HR was the solutionizing time. As can be seen from the micrographs given in Figure 43 and

Figure 44, increasing solutionizing time resulted in disappearance of the dendritic structure and dissolving of several precipitates.

According to Figure 57 and Figure 60, the dissolution temperatures can be seen, such as, at temperatures near to 500°C, Mg_2Si is dissolved and at temperatures which means for HT.480.2HR and HT.480.20HR the complete dissolution of Mg_2Si is not possible. In Figure 58, it can be said that during welding, it is not possible to see precipitation while solidification. However, the software calculations were conducted for the base metal composition, therefore elemental alterations in filler would affect the diagrams.

After post weld heat treatment, several precipitates were subjected to EDX analysis. According to results (Figure 47), after HT.480.20HR, approximately two or three different possible types of precipitates were detected. One of them was identified as Mg_2Si (Figure 47b) and the other as an Al-Fe-Cr intermetallic. The EDX mapping of HT.480.20HR indicated the presence of mainly $MgSi_2$ type precipitates. Why coarsening is seen in Mg and Si rich phases is not known at the moment and further examinations are needed to characterize the precipitates.

However, the hardness values were almost same after HT.480.2HR and HT.480.20HR and yet, increasing solutionizing times resulted in decrease in hardness. This decrease in hardness may be due to coarsening.

Another point is the changes in the yield and UTS values of the samples after post weld heat treatments. According to the hardness measurements, the most effective post weld heat treatment was HT.480.2HR, and all different angled grooved samples showed almost same increase in hardness after post weld heat treatment.

This indicates that, by performing suitable post weld treatment local recovery of strength loss can be possible.

The hardness increase in HAZ was distinguishably more than hardness increase in weld deposits for all grooves. In Figure 56, however, comparing the UTS and yield

strength of welded specimens with that of base metal, welding causes a decrease in strength. Although an increase was expected after heat treatment, as a result of the mentioned overaging problems, particular decreases were seen in each sample. Together with the microstructural transformations, welding defects most probably play an important role.

CHAPTER 7

CONCLUSION

In view of the results obtained in this study, the following conclusions can be drawn:

1. The heat input coming from the welding process itself deteriorates the strength of the 7039 aluminum alloy plate. Also, changing the groove angle of the welds results in different heat inputs and therefore different mechanical responses, which are different amounts of decrease in strength, are seen.

2. After welding of all samples, very similar microstructures are seen. However, differences occur on the width of the mushy zones, grains structures in HAZ and fusion line. 45V.1 has coarser grains in mushy zone than 30V.1. Similar behavior is seen in 45X.1 and 30X.1.

3. After welding, by performing suitable post weld heat treatments, strength was increased in HAZ most probably due to disappearance of the dendritic structure and dissolving of several precipitates. The hardness values in HAZ were increased from approximately 125HV to 160HV. However, the hardness's of the weld deposit did not change considerably, which were in the range 75 to 95 HV.

4. The strength of the welded specimens was much lower than 7039 plate. The UTS of 7039 plate was found approximately as 460MPa. However, after

welding the highest strength attained was only 285MPa with post weld heat treated 45X.2 specimen. However, a comparison of X and V weld grooves indicate that X-weld grooved welding method is more successful.

5. Weld defects play an important role for tensile tests. It is shown that in tensile testing failure initiates from weld defects such as lack of fusion. In most cases, most of the fracture is seen from the fusion line which is the weakest point due to the presence of mushy structure.

REFERENCES

1. Mindivan, H., et al., *Wear behaviour of 7039 aluminum alloy.* Materials Characterization, 2005. 54(3): p. 263-269.
2. *Aluminum*, in *Britannica*.
3. Wöhler, F., *Űber das Aluminium.* Annalen der Physik und Chemie, 1827. 11: p. 15.
4. Mandal, N.R., *Aluminum Welding*. 2 ed. 2005, Kharagpur, India: Narosa Publishing House. 1-20.
5. *Alüminyum ve Alüminyum Alaşımları I* G.-S. TR, Editor. p. 7.
6. Singh, R., *Applied Welding Engineering. Processes, Codes and Standards*. 2012, Oxford, UK: ELSEVIER.
7. Hall-Heroult Process [Digital image]. (n.d.). Retrieved September 06, 2016, from http://www.balcoindia.com/operation/reduction.aspx
8. *Specialty Handbook Aluminum and Aluminum Alloys*, in *Properties of Wrought Aluminum Alloys*, J.R. Davis, Editor., ASM INTERNATIONAL. p. 2.
9. CASSADA, W., J. LIU, and J. STANLEY, *Aluminum alloys for aircraft structures* Advanced Materials and Processes 2002(12): p. 3.
10. HIRSCH, J., K.F. KAHAUSEN, and L. LOHTE. *Advances in industrial aluminum research and development* in *Mater Sci Forum*. 2002.
11. ROMETSCH, P.A., Y. ZHANG, and S. KNIGHT, *Heat treatment of 7xxx series aluminum alloys-Some recent developments.* Transactions of Nonferrous Metals Society of China, 2014. 24: p. 15.
12. Mondolfo, L.F., *Aluminum Alloys: Structure and Properties*. 1976, Boston, MA: Butterworth & Co Ltd. 842-882.
13. Nowill, C., *Investigation of the Quench and Heating Rate Sensitivities of Selected 7000 Series Aluminum Alloys*, in *Materials Science and Engineering*. 2007, WORCESTER POLYTECHNIC INSTITUTE: United States.

14. Sharma, C., V. Upadhyay, and A. Tripathi, *Effect of Welding Processes on Tensile Behavior of Aluminum Alloy Joints.* International Journal of Mechanical, Aerospace, Industrial, Mechatronic and Manufacturing Engineering, 2015. 9(12): p. 1932-1935.

15. *ARMOR PLATE, ALUMINUM ALLOY, 7039*, in *MIL-DTL-46063H*. 1998.

16. *Wrought Aluminum and Aluminum Allloys*, in *Heat Treaters Guide, Practices and Procedures for Nonferrous Alloys*, H. Chandler, Editor. 1996, ASM International.

17. Kou, S., *WELDING METALLURGY*. 2 ed. 2003, Canada: A JOHN WILEY & SONS, INC., PUBLICATION.

18. E, G.F., Weld J. , 1980. 59(23).

19. AKKUS, M., *Effect of Welding Parameters on the Hot Cracking Behavior of 7039 Aluminum-Zinc Alloy* in *Metallurgical and Materials Engineering*. 2010, Middle East Technical University: Ankara p. 101.

20. TIRKES, S., *HOT CRACKING SUSCEPTIBILITY OF TWIN ROLL CAST Al – Mg ALLOYS*, in *METALLURGICAL AND MATERIALS ENGINEERING*. 2009, MIDDLE EAST TECHNICAL UNIVERSITY: ANKARA. p. 108.

21. Kou, S. and H. C, *Liquation cracking in full-penetration Al-Cu welds.* Welding Journal, 2004. 83(2): p. 50-58.

22. S, K. and H. C, *Liquation mechanisms in multicomponent aluminum alloys during welding.* Welding Journal, 2002. 81(10): p. 211-222.

23. Pepe, J.J. and W.F. Savage, 1970, 1970. 49: p. 545.

24. Mathers, G., *The welding of aluminium and its alloys* ed. C. Press. 2002, Cambridge, England: Woodhead Publishing Ltd. .

25. KOTAN, G., *Investigation of Microstructural Homogenity and Thermal Stability of Equal Channel Angular Pressed and Aged 2024 Al Alloy*, in *Metallurgical and Materials Engineering*. 2014, Middle East Technical University: Ankara p. 203.

26. Committee, A.H., *Heat Treating of Aluminum Alloys*. Heat Treating. Vol. 4. 1991: ASM International.

27. MACAR, M., *Investigation of Dynamic Behavior of Aluminum Alloy Armor Materials* in *Mechanical Engineering*. 2014, Middle East Technical University: Ankara. p. 152.

28. in *Principles and Technology of the Fusion Welding of Metals*. 1981, Mechanical Engineering Publishing Co.: Peking, China.

29. Mizuno, M., T. Takada, and S.J. Katoh, Japanese Welding Society, 1967. 3: p. 74–81.

30. Kelsey, R.A., Weld. J.,, 1971. 50.

31. KOU, S. and L. Y. 1982, Carnegie-Mellon University: Pittsburg, PA.

32. Sharma, C., D.K. Dwivedi, and P. Kumar, *Effect of welding parameters on microstructure and mechanical properties of friction stir welded joints of AA7039 aluminum alloy.* Materials and Design, 2012. 36(2012): p. 379–390.

33. Kumar, P., A.C. A, and S. Kumar, *Study of Heat Input for GTA Welded Aluminium Alloy 7039.* International Journal of Engineering Science and Innovative Technology (IJESIT), 2013. 2(5).

34. Singh, R.K.R., et al., *The microstructure and mechanical properties of friction stir welded Al–Zn–Mg alloy in as welded and heat treated conditions.* Materials and Design, 2011. 32: p. 682-687.

35. Sharma, C., D.K. Dwivedi, and P. Kumar, *Effect of post weld heat treatments on microstructure and mechanical properties of friction stir welded joints of Al–Zn–Mg alloy AA7039.* Materials and Design, 2013. 43: p. 134-143.

36. *ALLOY 5356 WELD DATA SHEET*. AlcoTec Wire Corporation: USA.

37. Pérez-Bergquist, S.J., et al., *The dynamic and quasi-static mechanical response of three aluminum armor alloys: 5059, 5083 and 7039.* Materials Science and Engineering: A, 2011. 528(29–30): p. 8733-8741.